RAPID SCREENING OF REACTIONS OF RARE-EARTH METAL COMPLEXES THROUGH MALDI-TOF MASS SPECTROMETRY

NDUKA IKPO

Rapid Screening of Reactions of Rare-Earth Metal Complexes Through MALDI-TOF Mass Spectrometry

By

Nduka Ikpo

A thesis submitted to the School of Graduate Studies

in partial fulfillment for the degree of

Master of Science

Department of Chemistry

Memorial University of Newfoundland

August 2008

St. John's, Newfoundland and Labrador, Canada

Abstract

This thesis describes investigations into the applicability of inert atmosphere matrix-assisted laser desorption ionization time-of-flight mass spectrometry (MALDI-TOF MS) technique for rapid screening of reactions. Complexation reactions of lanthanide amide reagents $Ln\{N(SiMe_3)_2\}_3$ (where Ln = Sm, Gd, Ho, Yb, Y or La) with amine-bis(phenol) ligands ($[O_2N_2^{t\text{-}Bu,Me}]H_2$, $[O_2N_2^{t\text{-}Bu}]H_2$, $[O_2NN'^{t\text{-}Bu}]H_2$ and $[O_2NN'^{t\text{-}Am}]H_2$) were probed using anthracene as the matrix. This technique rapidly confirmed ligand coordination by showing excellent agreement between the experimental and theoretical isotope patterns. Spectra of isolated lanthanide amine-bis(phenolate) amido complexes are similar to those seen from small scale parallel reactions of metal amides and protonated ligands. Although in all cases molecular ion peaks were not observed, peaks for lanthanide arene complexes, $[M + arene]^{+\cdot}$, formed *in situ*, were seen. The absence of these molecular ion peaks was due to difficulties in ionizing Ln^{3+} complexes by charge-transfer, and the low coordination number of the lanthanide ions led to laser-assisted arene complex formation. The mechanism of ionization in this study is proposed to involve adduct formation.

The screening of the hydroamination-cyclization reaction of 5-phenyl-4-pentyne-1-amine potentially catalyzed by various lanthanide amine bis(phenolate) complexes was also studied. Characterization of the reaction mixtures from *in situ* hydroamination reactions showed changes in mass spectral patterns from the starting materials. Also, significant differences in the spectra of the mixtures containing lanthanide $[O_2N_2]$ and $[O_2NN]$ complexes were observed. The aminoalkyne substrate is proposed to coordinate

to the metal center of the lanthanide bearing $[O_2N_2]$ complexes indicating potential precatalysts for hydroamination of aminoalkynes. These results demonstrate the utility of MALDI-TOF MS as a potential technique for rapid screening of reactions of paramagnetic and extremely moisture-sensitive metal complexes. Aspects of this work have been accepted for publication: Nduka Ikpo, Samantha M. Butt, Kayla L. Collins and Francesca M. Kerton*, *Organometallics*, om 2008-00453b, accepted for publication August 2008.

Acknowledgements

First, I would like to thank my supervisor Dr. Fran Kerton, for giving me the opportunity to join her research group, where she has been very patient with me as well as guiding, directing and producing valuable advice and encouragement during these two years.

I would like to express my appreciation to my supervisory committee: Dr. Chris Kozak and Dr. Sunil Pansare for their helpful discussion as it related to my research. My appreciation especially goes to Dr. Kozak, who was always available to offer advice and support. I am grateful to Linda Windsor, Julie Collins and Celine Schneider for their help with MALDI-TOF MS and NMR instruments.

I would like to thank NSERC (Dr. Kerton's Discovery Grant), and the Chemistry Department of MUN for their financial support. All of the faculty and staff of the Chemistry Department are acknowledged for the help they provided to me.

To my colleagues in the Green Chemistry and Catalysis group "The best group to work with", I wish to thank Rebecca, Hassan, Kamarul, Hu and Uttam for making the lab a great place to work in and also to the numerous undergraduates.

I wish to thank my wife Uzoamaka Happiness. Words cannot express my gratitude for the patience, prayers, encouragement and love she has shown me, which keeps me going. She is truly a God-given wife. My heartfelt appreciation goes to my beloved mother, my siblings and my friend Nkeiru for their prayers and encouragement. I love you all.

I thank my God, without whose mercy I don't believe I would be at this point of my life.

In loving memory of my father

Table of Contents

List of Tables

List of Figures

List of Schemes

List of Abbreviations

δ	Chemical shift (in NMR)
CID	collision induced dissociation
DMF	*N,N*-dimethylformamide
ee	enantiomeric excess
ESI-MS	electrospray ionization mass spectrometry
Et	ethyl
Et_2O	diethyl ether
g	gram
GC	gas chromatography
h	hour
HPDO3A	10-(2-hydroxypropyl)-1,4,7,10-tetraazacyclododecane-1,4,7-triacetic acid
HPLC	high performance liquid chromatography
HTM	high-throughput method
Hz	Hertz
^{i}Pr	isopropyl
IR	infrared
Ln	lanthanide
M	molar
m/z	mass-to-charge ratio

MALDI-TOF MS	matrix assisted laser desorption ionization time-of-flight mass spectrometry
Me	methyl
MeOH	methanol
mg	milligram
mL	millilitre
MS	mass spectrometry
NLO	nonlinear optical
NMR	nuclear magnetic resonance
p	pentet (in NMR)
Ph	phenyl
q	quartet (in NMR)
rt	room temperature
s	singlet (in NMR)
t	triplet (in NMR)
t-Am	tertiary pentyl or amyl
t-Bu	tertiary butyl
THAP	2,4,6-trihydroxyacetophenone
THF	tetrahydrofuran

Chapter 1

Organolanthanide Complexes in Catalysis

1.1 Historical Background of Rare-Earth Metals

The lanthanides constitute the series of elements with 4*f* valence orbitals within the periodic table, spanning from lanthanum through lutetium, and they have in common, a xenon core configuration and occupied 6*s* orbitals.[1] The lanthanide elements and Group 3 metals of the periodic system (scandium and yttrium) are collectively known as rare-earth elements. The name "rare-earth" implies that the metals are terrestrially scarce, and expensive. However, many lanthanides are cheap and more plentiful than some transition metals. The rare-earth name came about due to their late discovery.[2] Yttrium is classified alongside the lanthanides as a result of the characteristic "lanthanide contraction". This phenomenon is attributed to poor shielding of the 4*f* electrons caused by the progressive decrease in the radius of the metals with increasing atomic number (effective nuclear charge) across the lanthanide series from lanthanum to lutetium. On this basis, the ionic radius of 0.88 Å for Y^{3+} falls between that of Ho^{3+} and Er^{3+} in the lanthanide series, consequently the properties of Y^{3+} are similar to Ho^{3+}, as shown in **Figure 1.1**. Although Sc^{3+} is substantially smaller than the lanthanides, it was classified as a rare earth metal due to the fact that scandium complexes have similar properties to those of yttrium and lanthanum. Such complexes present an inert gas core electronic configuration and predominantly a +3 oxidation state.[3]

References for Chapter 1 begin on page 37

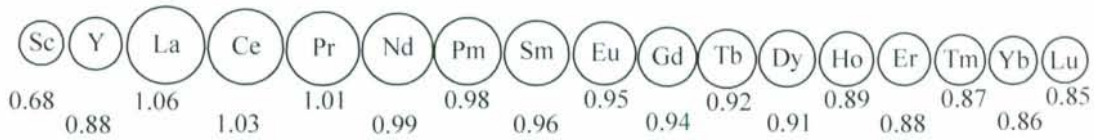

Figure 1.1 Ionic radii of lanthanide(III) ions (Å, 6-coordinate).[3]

1.2 Development of Organometallic Chemistry of Lanthanides

The organometallic chemistry of the lanthanides began with the pioneering work of Wilkinson and Birmingham. In 1954, they synthesized the first organolanthanide complexes, the tris(cyclopentadienyl) derivatives (**1.1**), as shown in **Figure 1.2**.[4] Despite this initial discovery, advancement in the field of organolanthanide chemistry was impeded by the perception that these compounds were remarkably sensitive to oxygen and water. They were also considered to be highly ionic, representing trivalent versions of the alkali and alkaline earth metal organometallic compounds, and therefore, it was thought that exciting organometallic chemistry could not be achieved with f-block species, unlike the d-block elements. This was because it was assumed that the lanthanide elements lacked the proper orbital interactions to enable interesting reaction chemistry to occur.

However, further progress in the area of lanthanide chemistry commenced as a result of the availability of more sophisticated preparative and analytical techniques in the 1970s and 1980s. The organolanthanide chemistry of the rare earth metals gained a significant awakening in 1974 as a result of the preparation of a series of alkyl, aryl and alkynyl bis(cyclopentadienyl) derivatives (**1.2**) (**Figure 1.2**), by Tsutsui and Ely.[5] This

References for Chapter 1 begin on page 37

achievement overturned an early, common assumption that organolanthanide chemistry is limited to ionic π-bonded organometallic ligands.

1.1

1.2

Figure 1.2 Tris(cyclopentadienyl) (**1.1**) and bis(cyclopentadienyl) derivatives (**1.2**).

1.3 General Properties of The Rare-Earth Metals

The lanthanides possess the general electronic configuration $[Xe]4f^n5d^16s^2$ (where n = 0 to 14) and provide reactivity unprecedented in main group and *d*-block chemistry. The $4f^n$ orbitals, which become filled in the lanthanide series, have limited radial extension and are shielded from the valence shell by the filled 5*s* and 5*p* orbtals.[3] This effect leads to highly ionic lanthanide-ligand interactions that are dominated by electrostatic and steric factors. A stable 3+ oxidation state dominates lanthanide chemistry, although a few other oxidation states are available, such as Sm(II), Yb(II), Eu(II) and Ce(IV), which have exceptional use in organometallic and organic reactions as reducing and oxidizing agents.[2]

In contrast to the transition metals, there is an absence of oxidative addition/reductive elimination processes due to, in most cases, the availability of a single

References for Chapter 1 begin on page 37

oxidation state. Furthermore, in the presence of limited covalent bonding, the lanthanides exhibit reactivity that is not governed by the requirement of compatible orbital symmetries as observed for *d*-block metals. Therefore, a series of lanthanide complexes will have similar chemical properties and differences will most often originate from the change in central ion size. This can sometimes be observed in the resulting co-ordination number, geometry and reactivity of the lanthanide complexes. The slight variation in the cationic size offers the opportunity to fine-tune reactivity by changing the lanthanide and consequently, the radius of the central metal. In addition, since lanthanide-ligand interaction is controlled by steric factors rather than orbital interactions, the reaction site can be manipulated by changing the ligand size.[1b]

The lanthanides have large ionic radii giving preference towards high coordination numbers in the range of 8-12. This offers the potential for the lanthanides to be compatible with sterically-demanding ligands in order to obtain highly reactive monomeric compounds. However, due to their size, oligomeric structures or "ate" complexes (incorporating alkali metal ions in the structure) can sometimes be obtained even with sterically-demanding ligands due to persistent Lewis base complexation.

The highly electrophilic nature of the lanthanides gives rise to their hard acidic properties and consequently their suitability for "hard" donors. This property explains why most of the rare-earth metal complexes are stabilized by oxygen and nitrogen donor ligands.[1,6,7] The aforementioned properties contributed significantly to the novel organometallic and coordination chemistry observed with the lanthanides today.

References for Chapter 1 begin on page 37

1.4 Organo Rare-Earth Metal Complexes in Catalysis

Over the past four decades, there has been increasing effort to design the most active and most selective catalysts for various chemical transformations.[8] This is spurred by the quest to replace multi-step, expensive and environmentally harmful processes with single-step, solvent-free benign alternative routes.[9] Organolanthanide complexes have merit in providing simpler and less expensive ways of achieving chemical transformations. Early studies of organolanthanide complexes with cyclopentadienyl ligands revealed that lanthanide species can effectively catalyze olefin polymerization.[10] As a result, organolanthanides attracted considerable attention and highly active catalysts were discovered for other beneficial olefin transformations such as hydroamination,[11] polymerization,[12] hydrogenation,[13] and hydrosilylation.[14] These reactions are all highly atom-efficient addition processes (**Scheme 1.1**).

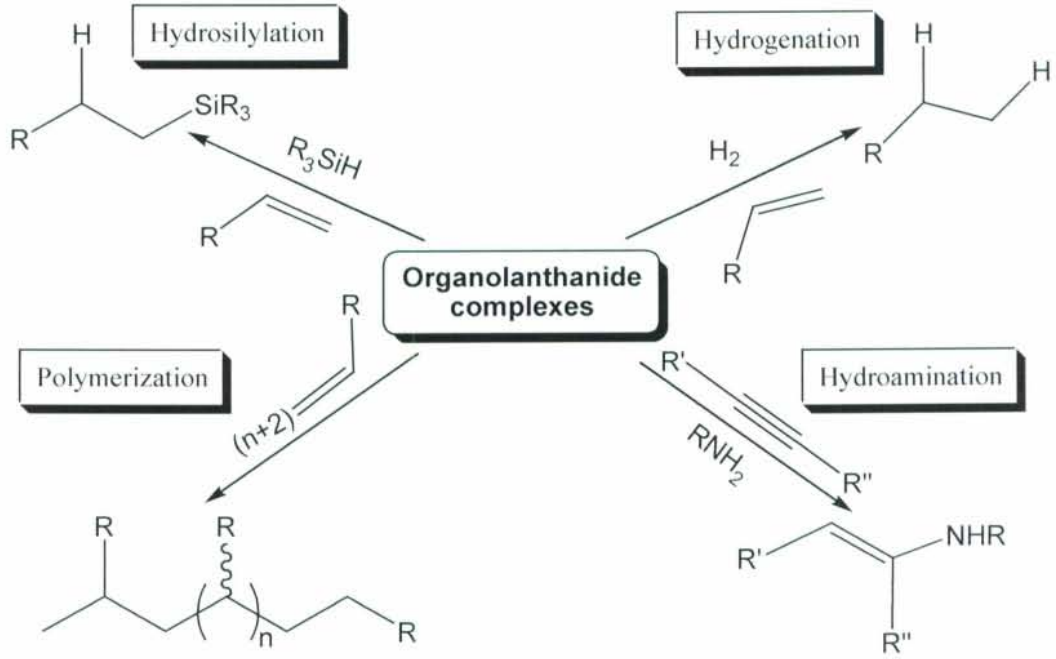

Scheme 1.1 Examples of organolanthanide-catalyzed reactions.

References for Chapter 1 begin on page 37

1.4.1 Organo-lanthanocene Complexes in Catalysis

Cyclopentadienyl ligands are suited to the rare earth metals, as they are capable of ionic bonding thereby offering stability and solubility to their metal complexes. They have been widely used to produce an abundance of compounds and have dominated the organometallic chemistry of the lanthanides and the early transition metals for a long time. Lanthanocene species that have been prepared include bis(pentamethylcyclopentadienyl) $Cp^*_2LnCH(SiMe_3)_2$ (**1.8**), *ansa*-lanthanocenes $Me_2SiCp'_2LnCH(SiMe_3)_2$ (**1.5**) (in which a bridging group connects the Cp rings) and half lanthanocenes (**1.6**) as shown in **Figure 1.3**. Where $Cp' = \eta^5$- C_5Me_4, $Cp^* = \eta^5$- C_5Me_5, Ln = Lu, La, Y, Sm, Nd.

Unsubstituted cyclopentadienyl ligands produce lanthanide compounds that are thermally unstable and insoluble in hydrocarbon solvents resulting in low catalytic activity. On the other hand, substituted cyclopentadienyl complexes are relatively stable, soluble and exhibit high catalytic activity.[15] However, the inherent difficulties associated with the synthesis of modified cyclopentadienyl ligands have led to an extensive search for non-cyclopentadienyl tunable ligands. These include dianionic, monoanionic and neutral donor environments that permit the synthesis of mono-, bis- and tris(alkyl) complexes, respectively. The alkyls were common features of the early catalysts, however, in recent years hard donor ligands such as oxygen and nitrogen have also been complexed to the lanthanide metals to yield catalysts.

References for Chapter 1 begin on page 37

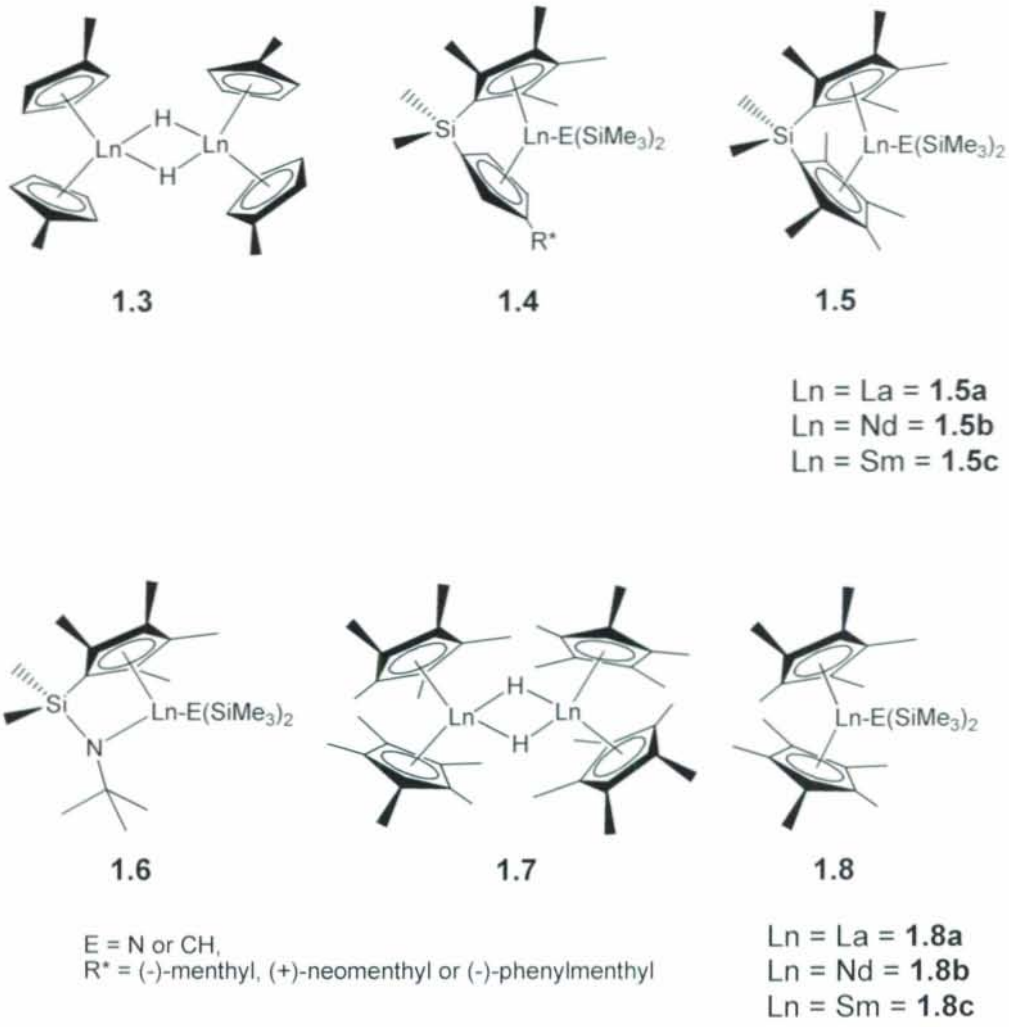

Figure 1.3 Examples of cyclopentadienyl rare-earth metal complexes.[16]

1.4.2 Non-Metallocene Complexes in Catalysis

In the search for alternative non-cyclopentadienyl ligands for lanthanides and early transition metals, the most important donor atoms are nitrogen and oxygen. This is attributed to their "hard" basic nature, which makes them well-suited for the "hard" acidic

nature of lanthanide and early transition metals ions. New non-cyclopentadienyl ligands containing these donors provide the opportunity for flexible tuning of steric and electronic demands. The chemical properties and rate of catalysis of organolanthanide complexes are greatly controlled by the steric nature of the ancillary ligand coordinated to the metal. Therefore, these "hard" basic ligands have greatly affected homogeneous catalyst discovery in this field.[17] A wide range of nitrogen-based and mixed nitrogen-oxygen donor ligands have been synthesized and studied including amidinates,[18] guanidinates,[19] β-diketiminates,[20] bis(phenolates),[21] and bis(silylamides).[22] Lanthanide metals have been shown to coordinate with some of these ligands which have then been used to catalyze a wide range of chemical transformation processes.

β-Diketiminato ligands bear only one negative charge, a characteristic feature that makes them suitable to complex with Group 3 metals for production of dialkyl derivatives. Utilizing this property, Piers and co-workers reported the first structurally characterized cationic organoscandium compound (**Figure 1.4**).[20] They found that under $B(C_6F_5)_3$ activation that the sterically bulky complex (**1.9a**) with tertiary-butyl substituents at the backbone, mediated effective polymerization of ethylene at 50 °C. On the other hand, the less bulky complex (**1.9b**) of the dibenzyl derivative showed no reactivity toward alkenes under the same experimental conditions. Interestingly, the activity of the catalyst generated from **1.9a** approached those observed for metallocene and Group 4 element-based catalysts.

References for Chapter 1 begin on page 37

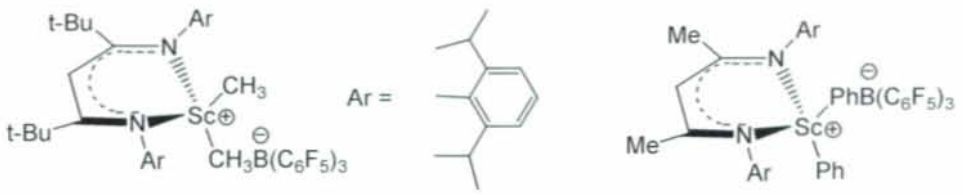

1.9a **1.9b**

Figure 1.4 Scandium β-diketiminato complexes for ethylene polymerization.

In 1992, Schauverien and co-workers communicated the preparation of mononuclear organolanthanum complexes of bis(phenolate) ligands.[23] The complexes were synthesized by mild protonolysis of $[La\{CH(SiMe_3)_2\}_3]$ with a chiral bis(phenol) and yielded tris-THF species. The lanthanium bis(phenolate) complex **1.10** is shown in **Figure 1.5**. However, catalytic activity of these complexes has not been reported.[15]

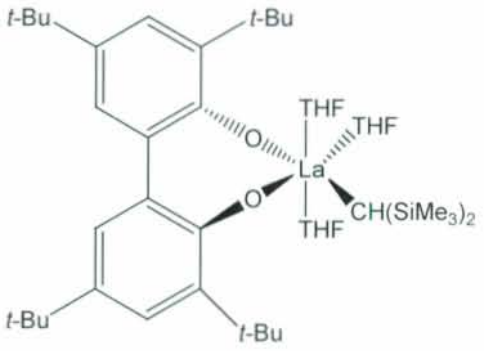

1.10

Figure 1.5 Lanthanum bis(phenolate) complex.

References for Chapter 1 begin on page 37

In 2007, Shen and co-workers published the synthesis of methylene bridge-linked bis(phenolate) lanthanide amido complexes by a salt metathesis reaction.[21] The neodymium complex **1.16** is shown in **Figure 1.6**. The complexes were prepared by reaction of one equivalent of bis-phenoxide ligand, to two equivalents of $[Ln\{CH(SiMe_3)_2\}_2(\mu\text{-}Cl)(THF)]_2$. The resulting product was a precursor for the synthesis of other methylene bridge-linked bis(phenolate) lanthanide complexes. Shen and co-workers reported that the complexes mediated polymerization of ε-caprolactone. Observations showed that the introduction of donor atom(s) on the linker of the complexes enhanced the catalytic activity for the polymerization, though it reduced the control of stereochemistry in the polymerization process.

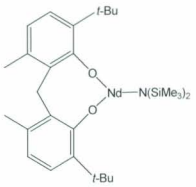

1.16

Figure 1.6 Neodymium bis(phenolate) complex.

When exploring bidentate anionic *N,O* mixed donor ligand systems, Teuben *et al.*[24] used an (alkoxysilyl) amido ligand in order to stabilize an yttrium metal center in a

bis(*N,O*-(*tert*-butyl))(alkoxydimethylsilylamido) yttrium species **1.11a** (**Figure 1.7**). These complexes are also isoelectronic with bis(benzaminato)yttrium systems (**1.11b**). Investigations into the catalytic activities of the two complexes revealed different end results. Unlike the bis(benzaminato)yttrium complexes, the negative charge for the (alkoxysilyl) amido ligands is localized on the amide nitrogen making them more acidic and reactive. Thus, the ligands are not suitable as spectator ligands due to their labile and reactive nature, which allows them to be transferred easily to other metal centers.

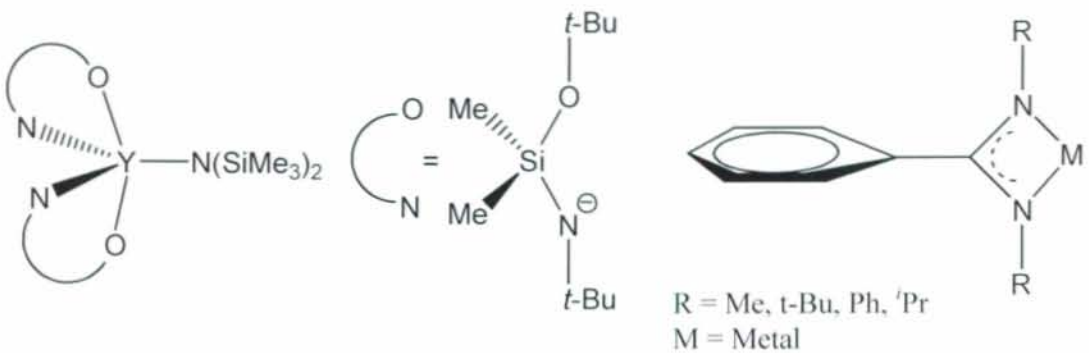

1.11a **1.11b**

Figure 1.7 Yttrium (alkoxsilyl) amido complex (**1.11a**), (alkoxsilyl) amido ligand and benzaminato ligand (**1.11b**).

Amine bis(phenol) ligands shown in **Figure 1.8** (**1.12a**) and (**1.12b**), can be synthesized in an accelerated and benign manner from readily and widely available starting materials.[25] The modular nature of their preparation allows for systematic variation of the R substituents. This enables control over electronic and steric properties

that influence catalytic activity. Exploring the versatility of such amine bis(phenol) ligands, Kerton *et al.*[26] incorporated tetradentate chelating ligands with lanthanide metals. The group demonstrated that gadolinium amine bis(phenolate) complexes **1.13** (**Figure 1.9**) generated *in situ,* were active initiators for controlled ring-opening polymerization (ROP) of ε-caprolactone. Interestingly, the addition of sterically-bulky groups such as *tert*-pentyl at the R substitutent sites increased the catalytic activity, while less sterically-demanding groups exhibited poor reactivity.

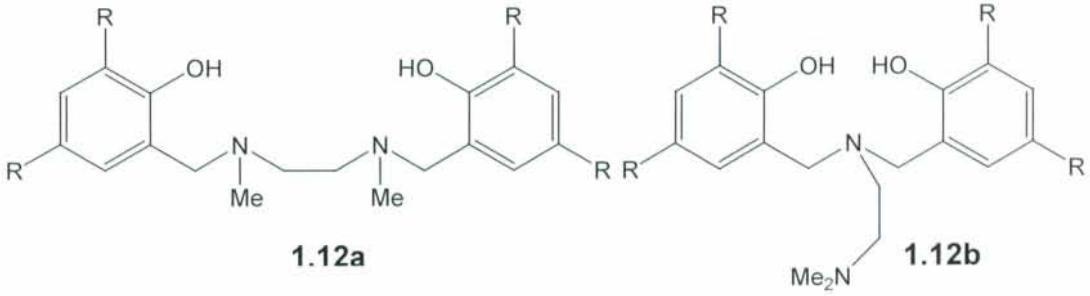

Figure 1.8 Amine bis(phenol) ligand precursors.

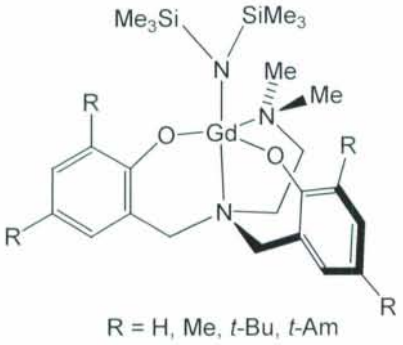

1.13

Figure 1.9 Gadolinium amine bis(phenolate) complex for ring opening polymerization of ε-caprolactone.

References for Chapter 1 begin on page 37

In regard to the successful ring-opening polymerization reactions by these ligand-containing sets, work on organolanthanides and their use in catalysis was inspired, resulting in this thesis. As a test, an atom-efficient addition reaction, namely, an intramolecular hydroamination was chosen.

1.5 Hydroamination Reactions

Nitrogen-carbon bond formation using alkenes and alkynes as reagents are very important chemical transformations in organic chemistry.[27] The addition of amines to multiple carbon-carbon bonds is a process that has been highly sought-after but poses some difficulties.[28] The direct catalytic addition of an amine functional group to carbon-carbon double, or triple bonds, known as hydroamination, generates compounds such as amines, enamines and imines. These compounds are useful due to their involvment as building blocks in basic research, the chemical industry, agriculture and pharmaceuticals.[29] The traditional approach for the production of various organo-nitrogen molecules involves nucleophilic substitution of alcohols with ammonia in the presence of a catalyst.[30] From an economic and environmental point of view, among all the different methods for generating amines and their derivatives, hydroamination is the most amiable path to the synthesis of nitrogen containing molecules. The advantage of this process over others is that the process proceeds with 100% atom economy. In addition, the desired products can be synthesized from inexpensive, readily accessible starting materials.

While the hydroamination of alkenes produces amines directly (**Scheme 1.2**), hydroamination with alkynes gives enamines and imines. The latter can be subsequently

References for Chapter 1 begin on page 37

reduced to obtain amines (**Scheme 1.3**), although enamines and imines themselves are useful building blocks.[27,31]

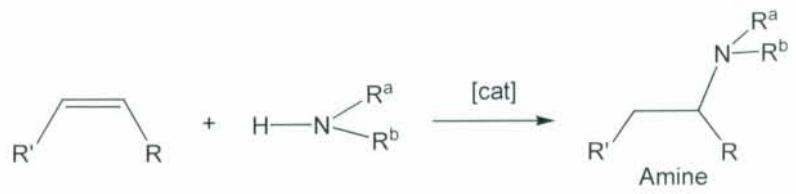

Scheme 1.2 Hydroamination of alkenes.

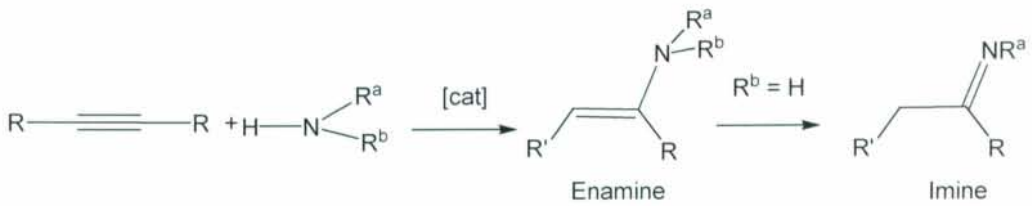

Scheme 1.3 Hydroamination of alkynes.

Thermodynamically, intermolecular hydroamination of alkenes poses more challenges when compared to that of alkynes.[28] Intermolecular hydroamination of alkenes is slightly exothermic, and the free energy ΔG^0 for the addition of an amine to a carbon-carbon double bond is estimated to be -17 KJ/mol.[28b] The reaction is hindered as a result of a high energy barrier for the approach of the π carbon-carbon double bond and the σ nitrogen-hydrogen bond, due to electrostatic repulsion of electrons. A [2 + 2] cycloaddition of N-H to the alkene would result in an orbital symmetry-forbidden process, which is unfavourable. Furthermore, due to the highly negative reaction entropy at higher temperatures, equilibrium is shifted towards the reactants. Alkenes and alkynes undergo nucleophilic attack by amines in the absence of a catalyst if the double or triple

bond is activated by neighbouring electron-withdrawing functionalities such as ketones, esters, nitriles and sulfones. However, the reaction can be accelerated by catalysts.[32]

1.5.1 Catalytic Hydroamination of Alkenes and Alkynes

Alkali metal ions, transition metals or lanthanide complexes can catalyze hydroamination of alkenes and alkynes. In general, these metals each employ a different mechanism for the hydroamination reaction. Carbon-carbon multiple bonds are susceptible to nucleophilic attack, and their activation can be achieved by π-coordination using late-transition metal centers, such as Pd(II) and Pt(II).[32] This renders the olefin more receptive towards nucleophilic attack by the amine. Alternatively, an N-H bond can be activated by deprotonation to the more nucleophilic amide of lanthanides and alkali metals.[28b] Another mechanism proceeds through oxidative addition of the N-H bond to a coordinatively unsaturated late-transition metal in a low oxidation state, for instance Rh(I) and Ir(I). This then permits insertion of the olefin into the resulting M-N or M-H bond. [28b]

Late-transition metals offer the advantage of greater polar functional group tolerance with a variety of substrates. However, their use as hydroamination catalysts has been limited by their short catalyst lifetime, slow reaction rates, moderate selectivity and limited scope.[16] Therefore, early transition-metal and lanthanide-based catalysts have an important role to play in this field.

The generally accepted catalytic pathway proposed for hydroamination/cyclization of various aminoalkynes catalyzed by organolanthanide complexes involves the activation of the amine substrate by the precatalyst to generate

References for Chapter 1 begin on page 37

lanthanide amido species, which are presumably the catalytically active species. This is followed by the lanthanide amide species undergoing irreversible and thermoneutral olefin insertion through four-centered transition states. The resulting lanthanide alkyl species undergo exothermic protonolysis by excess of amine substrate, thereby releasing and regenerating the catalyst **(Scheme 1.4)**.[33]

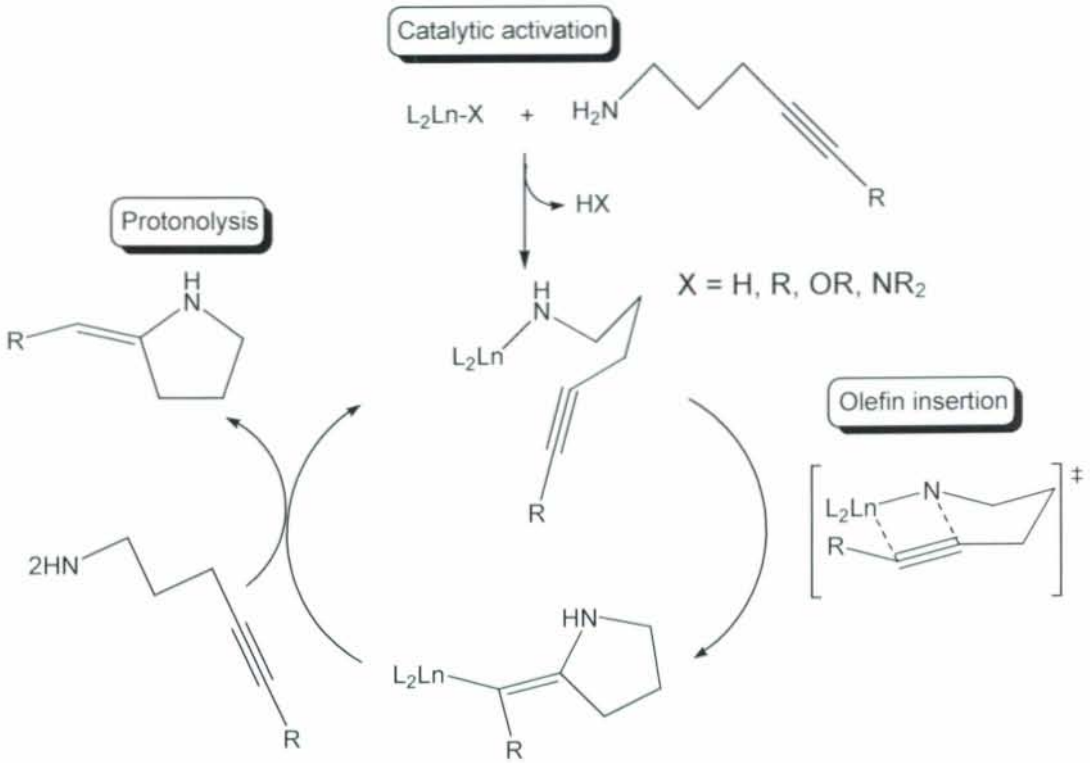

Scheme 1.4 Catalytic cycle for organolanthanide catalyzed hydroamination/cyclization of aminoalkynes.

References for Chapter 1 begin on page 37

1.5.2 Lanthanocene Hydroamination Catalysts

In 1996, Marks *et al.*[11] pioneered the hydroamination-cyclization reactions of aminoalkenes and aminoalkynes to produce corresponding five-, six- and seven-membered nitrogen containing heterocycles (pyrrolidines and piperidines). Exploring the reaction scope of the lanthanocene (**1.8**) with regard to ring size, regio- and diastereoselectivity for the cyclization of 2,2-dimethylaminopent-4-ene-1-amine (**1.14a**). Marks observed that increasing the lanthanide (III) ion radius and increasing access for the substrate at the metal center by using *ansa* ancillary ligands raised the turnover frequencies. The relative catalyst activity is in the order of (**1.5**) > (**1.8**) (**Figure 1.10**).

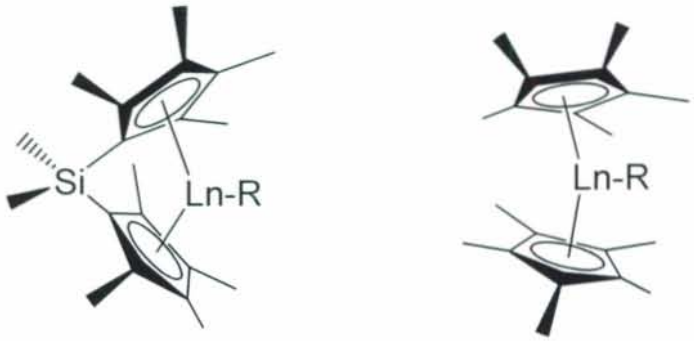

1.5 **1.8**

R = $N(SiMe_3)_2$ or $CH(SiMe_3)_2$

Figure 1.10 Comparison of ansa-bridged lanthanocene (**1.5**) and non-bridged lanthanocene (**1.8**).

References for Chapter 1 begin on page 37

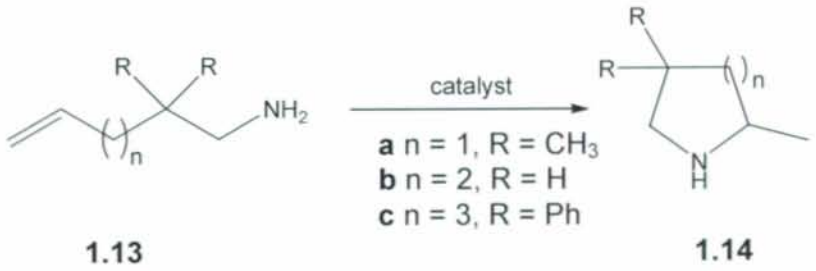

1.13 **1.14**

Scheme 1.5 Intramolecular hydroamination/cyclization of aminoalkenes.

Organo rare earth metals have shown efficiency in activation not only of carbon-carbon multiple bonds of alkenes and alkynes but also of allene substrates (**1.15**). This can be achieved in a highly regioselective and stereoselective manner using a samarium cyclopentadienyl complex (**Scheme 1.6**).[16,34]

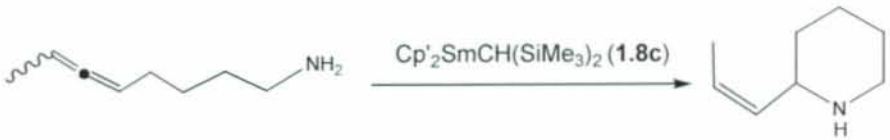

1.15 **1.16**

Scheme 1.6 Intramolecular hydroamination/cyclization of allenes. [34]

The same group of Marks demonstrated that intermolecular hydroamination can be coupled with successive intramolecular hydroamination/cyclization to allow formation of C-N or C-C bonds, generating polycyclic compounds.[35] Pentahydrodimethyl-dipyrrolopyrazine (**1.18**) was synthesized in one step from *N*-allylpropargylamine (**1.17**) by a succession of four C-N and C-C bond-forming reactions catalyzed by an organosamarium complex (**1.8c**) in 93% yield (**Scheme 1.7**). This was an amazing achievement in this field.

References for Chapter 1 begin on page 37

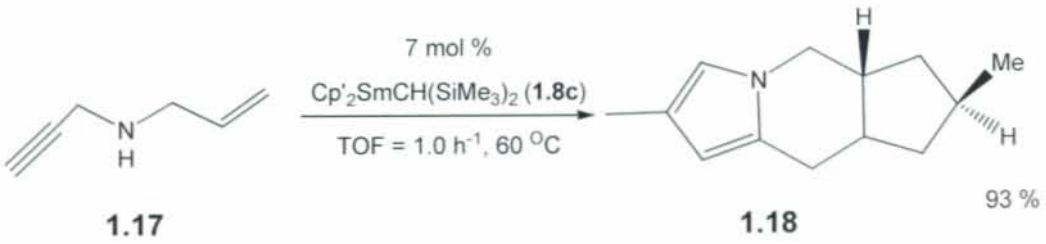

1.17 **1.18**

Scheme 1.7 Intramolecular tandem hydroamination/tricyclization.

1.5.3 Organolanthanocene Asymmetric Hydroamination Catalyst

Marks and co-workers reported the first enantioselctive catalyst for hydroamination-cyclization of aminoalkenes using C_1-symmetric chiral *ansa*-lanthanocene complexes (**1.4**).[34] The chiral group was incorporated on one of the cyclopentadienyl rings as a (-)-menthyl or (+)-neomenthyl or (-)-phenyl menthyl group, as shown in **Figure 1.11**. The precatalysts exhibited the same catalytic activity and enantioselectivity as their achiral analogues and demonstrated increases in activity with increasing ionic radii. Also, an increase in the enantiomeric excess (74%) was obtained at lower temperature (– 30 °C) for the formation of five-membered rings. Enantiomeric excess dropped dramatically in the formation of homologous six-membered rings (15-17%). The asymmetric induction and value of enantiomeric excess depended on the nature of the chiral substituents R* on the Cp ring, and not on the purity of the precatalyst.

References for Chapter 1 begin on page 37

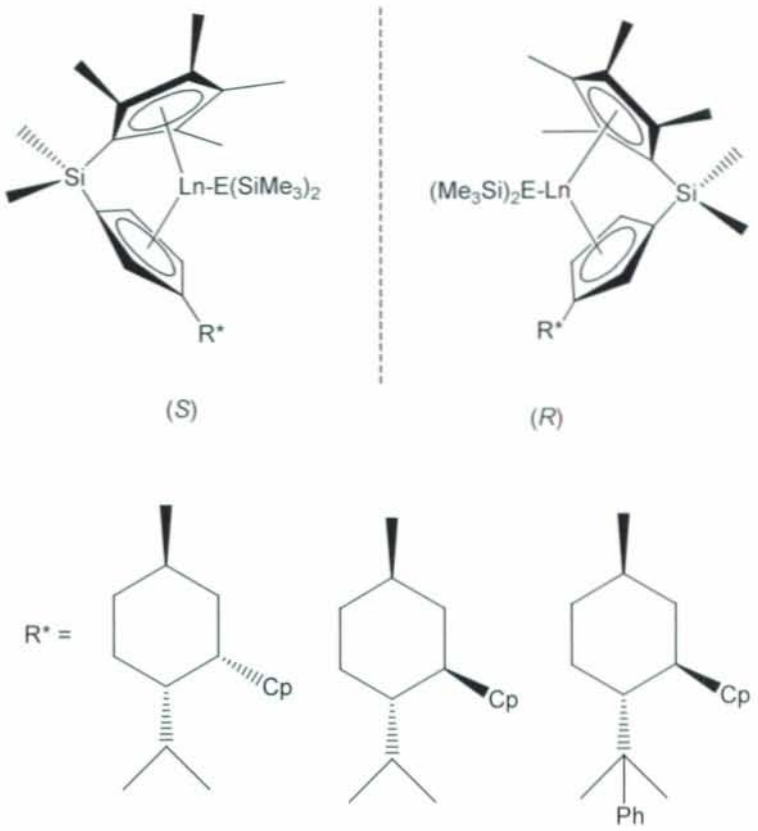

Figure 1.11 Chiral lanthanocene hydroamination catalyst.

1.5.4 Non-Lanthanocene Hydroamination Chiral Catalysts

Recently, catalytic intramolecular hydroamination of olefins has attracted huge interest as an invaluable path for the synthesis of nitrogen heterocycles. This, coupled

with the shift from cyclopentadienyl to non-cyclopentadienyl ancillary ligands, has prompted researchers to investigate numerous classes of ligands. Some of the early work in this area was performed by Livinghouse.[36] In 2001, his group communicated the intramolecular hydroamination-cyclization of aminopentenes into pyrrolidines, mediated by a neodymium tris-silylamide complex, $[Nd\{N(SiMe_3)_2\}_3]$. This work initiated the synthesis and use of non-cyclopentadienyl complexes for the intramolecular hydroamination of olefins. Livinghouse and co-workers subsequently developed a series of bidentate and tetradentate non-cyclopentadienyl containing ligands, and isolated their lanthanide-amido complexes (**1.19, 1.20** and **1.21**) as shown in **Figure 1.12**. These species demonstrated an improved reaction rate and diastereoselectivity for this reaction.[37,38]

Livinghouse's group generated the axially-chiral bis(thiolate) complexes of yttrium(III) (**1.19**) *in situ* by heating $[Y\{N(SiMe_3)_2\}_3]$ with an equimolar amount of proligand in the presence of two equivalents of thiophene as an auxillary ligand.[37] The yttrium complexes catalyzed highly stereospecific intramolecular hydroamination-cyclization of different aminoalkene substrates. The catalysts showed good activity and enantiomeric excess (up to 60-87%) for the cyclization of various aminopentene species at 60 ^{0}C. Livinghouse *et al.* explained these results by considering the steric factors at play in his complexes. The enantioselectivity was found to be dependent on the bulkiness of the R substituent adjacent to the metal binding aperture. This was demonstrated with an increase in the enantioselectivity by an increase of the steric bulk in the silyl substituent of the thiolate group.

References for Chapter 1 begin on page 37

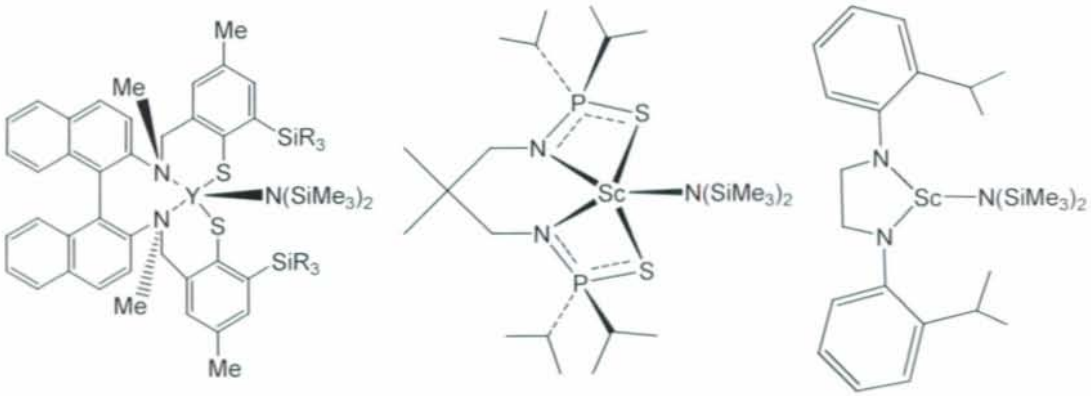

1.19 **1.20** **1.21**

19a = R = Me
19b = R = Et
19c = R = Me_2Ph

Figure 1.12 Yttrium bis(thiolato), Sc- bis(thiophosphinic)-amidate and Sc(III)-chelated diamide complexes.

Thiophosphinic amidate complexes of the Group 3 and 4 metals have also exhibited excellent catalytic activities for olefin hydroamination.[38] Thus, Livinghouse *et al.*[39] synthesized scandium thiophosphinic amidate complex (**1.20**) from an amine elimination reaction between scandium amide $[Sc\{N(SiMe_3)_2\}_3]$ and the free ligand. However, the organoscandium complex showed no catalytic activity towards aminoalkenes. This led to the preparation of the scandium-chelated diamide complex (**1.21**). It was thought that this would be more active and as anticipated, the complex

References for Chapter 1 begin on page 37

efficiently catalyzed the cyclization of 2,2-dimethylpent-4ene-1amine in good yield and rate.

In 2003, Marks and co-workers investigated the use of C_2-symmetric bis(oxazolinato)lanthanide complexes (**Figure 1.13** (**1.22**)) as hydroamination catalysts.[40] Complexes were generated *in situ* by reaction of $[Ln\{N(SiMe_3)_2\}_3]$, (Ln = La, Nd, Sm, Y, Lu) with a commercially available oxazoline ligand. They used the complexes to achieve enantioselective intramolecular hydroamination/cyclization of various aminoalkenes and aminodienes. The catalysts were active at room temperature, with the highest enatiomeric excess (67%) being observed in the cyclization of 2,2-dimethylpent-4-en-1-amine (**1.13a**). Improvement in rate and enantioselectivity were observed to correlate with increases in metal ionic radius. Marks *et al.*[40] compared these results with those obtained for C_1-symmetric metallocene precatalysts under various reaction conditions and found greater enantioselectivity for the organolanthanide oxazoline complexes. A screening study of the oxazoline ligands revealed that aryl stereodirecting groups at the oxazoline ring 4 positions and additional substitution (geminal dimethyl or aryl) in position 5 of the bisoxazoline ligand (**1.31**) was responsible for good enantioselectivities and high catalytic activity.

1.22

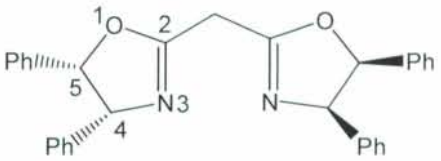

1.23

Figure1.13 Lanthanide bis(oxazolinato) complexes and bis(oxazoline) ligand used as catalyst for intramolecular hydroamination.

References for Chapter 1 begin on page 37

In related studies, Hultzsch and co-workers[41] described the synthesis of chiral yttrium binaphtholate complexes by arene elimination from the reaction between [Y(*o*-$C_6H_4CH_2NMe_2)_3$] and 3,3'-bis(tris(aryl)silyl)-substituted binaphtholate ligands (**Figure 1.14**). The complexes mediated the hydroamination/cyclization of a series of substrates at room temperature. As expected, increase in the steric bulk at the methyl groups on the aromatic substituents of silicon improved the rate and enantioselectvity of the catalytic hydroamination/cyclization of some substrates. Higher enantioselectivity was observed when the sterically-bulky complex (**1.24b**) was used. This generated 2-methyl-4,4-diphenyl-pyrrolidines based on **1.14c** with up to 95% *ee*, using scandium as the metal. The enantioselectivity decreased with bulky substrates such as methylpent-4-enylamine, which was cyclized at 60 °C with up to 53% *ee*. However, with the less-bulky complex (**1.24a**), an increase in enantioselectivity was observed for this substrate. Hultzsch *et al.*[41] attributed the difference in reactivity and selectivity between the complexes to steric factors. He explained that the methyl groups attached to the aromatic substituents sites boosted the performance of binaphtholate ligand in its chiral induction toward the substrates.

References for Chapter 1 begin on page 37

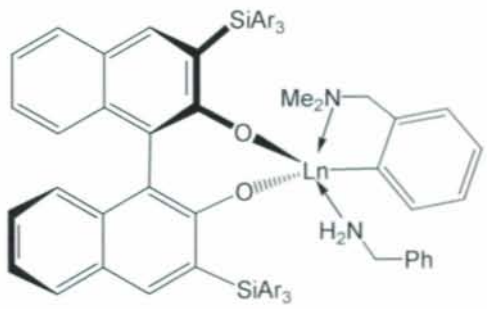

1.24a Ar = Ph
1.24b Ar = 3,5-$Me_2C_6H_3$ **Ln = Sc, Y, Lu**

Figure 1.14 Yttrium binaphtholate complex.

Despite the intense efforts of the aforementioned research groups and numerous others, a general hydroamination/cyclization catalyst system suitable for a variety of substrates has never been obtained.[27,42]

1.6 MALDI-TOF Mass Spectrometry of Metal Complexes

Researchers worldwide are investigating anionic ligands containing "hard" nitrogen and oxygen donor atoms as a replacement to cyclopentadienyl ligands in early-transition metal and lanthanide chemistry.[43,44] In most cases the catalytically-active complexes are synthesized *in situ* and are not easily isolated but can be analyzed in solution by ^{1}H and ^{13}C NMR spectroscopies. However, this method is not as useful when applied to most lanthanide compounds due to the fact that the majority of the rare-earth complexes [except those of Y^{3+}, La^{3+}, Yb^{2+}, and Lu^{3+}] are paramagnetic (Sm^{3+} f^5, Ga^{3+} f^7,

References for Chapter 1 begin on page 37

Ho^{3+} f^{10}, Yb^{3+} f^{13}). Many non-cyclopentadienyl complexes are also highly fluxional, further complicating NMR studies. The characterization of such lanthanide metal complexes depends on growth of single crystals and X-ray crystallographic determination. Thus, NMR technique is not as useful when applied to paramagnetic lanthanide compounds. [45] Therefore, there is the need for alternative sensitive methods that can provide insight into the composition of the actual catalytic species synthesized. To remedy this situation, in this thesis, a characterization method which has recently been applied to neutral organometallic complexes, namely matrix assisted laser desorption ionization time-of-flight mass spectrometry (MALDI-TOF MS),[46] was used for organolanthanide chemistry.

As new methods of mass spectrometry are developed, they are becoming useful techniques for inorganic and catalysis chemists to use in analyzing samples.[47] These techniques can provide accurate molecular mass data from mass-to-charge ratios (m/z) and isotope patterns and therefore, they can be used in the analysis of complexes uncharacterizable by routine NMR spectroscopy. Alternative mass spectrometric techniques include electrospray ionization mass spectrometry (ESI-MS), which can be used to analyze organometallics.[48a] Chen and co-workers reported the use of electrospray ionization tandem mass spectrometry (ESI-MS/MS) for rapid screening of Brookhart-type Pd(II) olefin polymerization catalysts and mechanistic studies of olefin metathesis by ruthenium carbene complexes.[48b] However, many extremely air- and moisture sensitive organolanthanide complexes may be hard to manipulate using this method since the sample is delivered as a solution, which may result in decomposition of the complex. This

References for Chapter 1 begin on page 37

can be overcome by incorporating the injector manifold inside a glove box, but this would come at a costly price.

1.6.1 MALDI-TOF Mass Spectrometry Instrumentation

MALDI-TOF MS is a laser-based "soft" ionization technique which gained widespread acceptance and recognition for the analysis of various classes of macromolecules such as biopolymers and oligomers.[49] The technique is an invaluable tool and because of its sensitivity, accuracy and the mildness of ion production, the spectra exhibit mostly singularly charged intact species.[50] A schematic diagram for a MALDI-TOF mass spectrometer (**Figure 1.15**) shows the essential features. The spectrometer fundamentally functions by irradiating a pulsed laser beam on the matrix cocrystallized with the analyte. The absorption of the photonic energy of each laser pulse results in desorption and partial ionization of the matrix which carries the analyte with it and indirectly causes the analyte molecules to be ionized by charge transfer. The resulting ions are accelerated into a mass analyzer, usually TOF where they are separated, detected and analyzed, based on time characteristic of their masses (mass-to-charge ratio).[51] The importance of the MALDI technique was recognised in 2002 by the award of the Nobel Prize to Koichi Tanaka for his contribution toward the development of soft desorption/ionization methods for mass spectrometric analyses of biological macromolecules.[52] This significant achievement opened the way for effective structural and molecular mass determination in different fields of science.

References for Chapter 1 begin on page 37

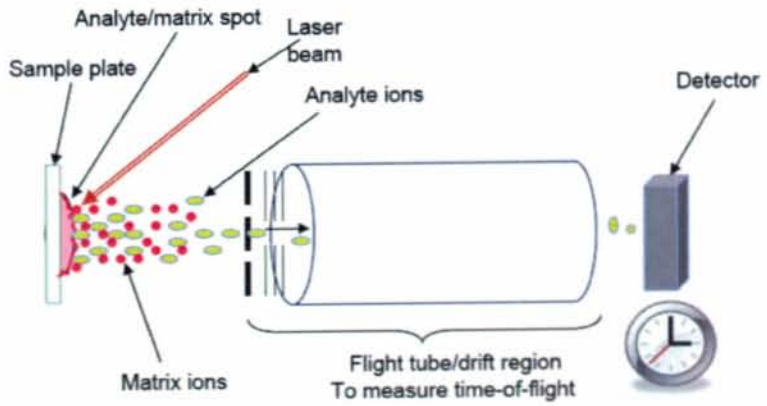

Figure 1.15 Schematic representation of the modified MALDI-TOF mass spectrometer.[51]

In 2003, Abell and co-workers described the use of MALDI-TOF mass spectrometry to rapidly probe the binding affinity of small molecules at the active sites of aspartate decarboxylase enzyme.[53] Abell selected a set of 55 compounds bearing a primary amine functional group (**Figure 1.16**) for the binding screen, and the MALDI-TOF mass spectra analysis of the screen results was very informative.

Noticing the resemblances of these compounds to oxygen-nitrogen mixed donor ligand systems and recent application of this technique to transition metal organometallics, we envisioned that the MALDI-TOF technique might be extended to rapidly probe the complexation of amine bis(phenol) ligands to lanthanide metals.

References for Chapter 1 begin on page 37

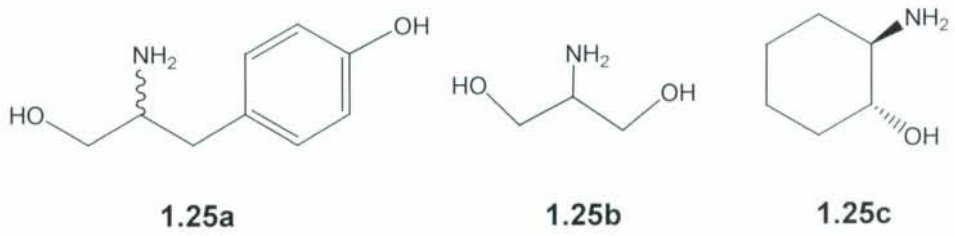

1.25a **1.25b** **1.25c**

Figure 1.16 Compounds used to assay for binding affinity using MALDI-TOF MS.

1.6.2 Previous Lanthanide and Transition Metal Studies Using MALDI-TOF MS

In 1999, Mineo *et al.*[54] reported the structural characterization of copolymers containing second-order nonlinear optically (NLO) active transition metals (**Scheme 1.8**) by MALDI-TOF MS. This group successfully characterized the copolymer product (**1.26c**) generated from the reaction of transition metal Schiff base complexes (**1.26a**) with bisphenol A (**1.26b**) using a MALDI-TOF MS technique.

References for Chapter 1 begin on page 37

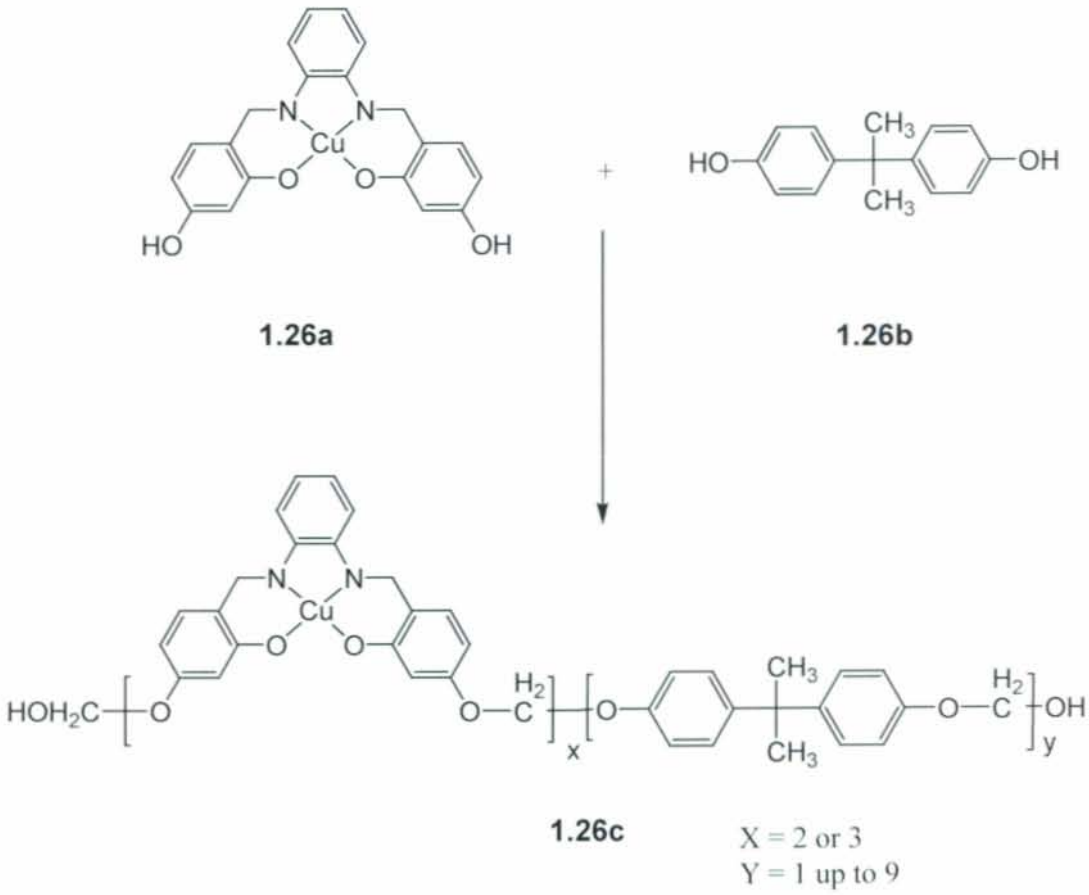

Scheme 1.8 Structural characterizations of copolymers by MALDI-TOF MS

Exploring the potential use of lanthanide complexes as magnetic resonance imaging (MRI) contrast agents, Corpillo and co-workers demonstrated the potential of MALDI-TOF MS for quantification of moisture-stable gadolinium complexes in cell lysates.[55] The complexes of ytterbium (III) and gadolinium (III) were synthesized using a solution of the ligand HPDO3A (10-(2-hydroxypropyl)-1,4,7,10-tetraazacyclododecane-1,4,7-triacetic acid) shown in **Figure 1.17** (**1.27b**), which wraps around the metal center and hinders further reactivity. The metal complexes were analyzed using the matrix 2,4,6-

trihydroxyacetophenone (THAP) (**1.27b**) which contains -OH functionalities that would react with moisture sensitive compounds.

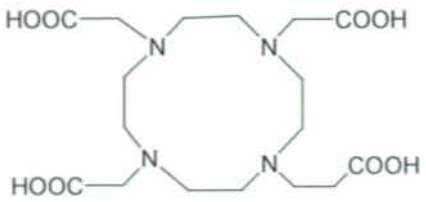

1.27a

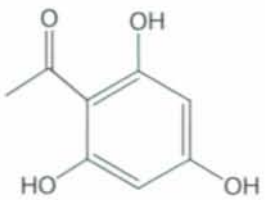

1.27b

Figure 1.17 HPDO3A ligand (**1.26a**) and THAP matrix (**1.26b**) for MALDI-TOF analysis of lanthanide complexes in cell lysates.

Fogg and co-workers applied inert atmosphere MALDI-TOF mass spectrometry (MALDI-TOF mass spectrometer interfaced to a glovebox) to study several reactions of catalytically-active metal centers, including Piers metathesis catalysts, and Grubbs first generation catalyst.[46] The Fogg group also studied the synthesis of azabis(oxazoline)-copper complexes from the reaction between oxazoline ligands and copper (II) triflate $[Cu(OTf)_2]$.

Although a few organometallic compounds and moisture-stable organolanthanides have been studied by MALDI-TOF mass spectrometry, the technique has not been widely used to study metallo-organic lanthanide complexes (with catalytic potential) that are extremely air- and moisture-sensitive. Therefore, the aim of this thesis was to apply this technique in the study of complexation of lanthanide metals, and in hydroamination reactions in order to assess its potential for high-throughput screening.

References for Chapter 1 begin on page 37

1.7 High-throughput Methods in Homogenous Catalyst Discovery

Homogeneous catalyst discovery is motivated by the desire for higher efficiency and selectivity. In many cases, no good predictive models are available for homogeneous catalysts due to highly variable structure-activity relationships.[56] Hence, to obtain the desired efficiency and selectivity for a catalytic reaction, the catalyst must be prepared, tested, adjusted and optimized. Traditionally, a new potential homogeneous initiator or catalyst is prepared, purified and assayed separately, which is time consuming. However, high-throughput methodology in homogeneous catalyst discovery offers the opportunity to accelerate the rate at which new catalysts are discovered and optimized.[57]

The development and the accomplishment of parallel synthesis and rapid screening techniques in combinatorial chemistry brought about the use of the high-throughput method (HTM) in homogeneous catalyst discovery.[58] This approach involves different stages: the parallel synthesis of a library of many ligands of related structure, the parallel synthesis of a wide range of catalysts, and the rapid screening of these catalysts for a desired property; and the identification of the catalyst, called 'hits' which show the best desired property. Once an active catalyst complex is discovered from the library, small modifications are made on the structure to try and screen the activity of neighbouring complexes.

It is interesting that non-standard conditions may also be screened, leading to the possibility that unexpected classes of catalyst may be found. **Figure 1.18** shows a carousel reactor, which is able to carry out twelve reactions in parallel, under reflux if

References for Chapter 1 begin on page 37

necessary, at variable temperature and under an inert atmosphere. Titre-plates can also be used to screen 24, 48, 96 or more parallel reactions.

Figure 1.18 Carousel reactor for high-throughput method.

The initial screening of a family of catalysts is likely to be for activity rather than to be a quantitative method. It is more efficient to screen a combinatorial catalyst library with a parallel high-throughput method rather than an off-line technique such as conventional GC or HPLC, which would be very time-consuming. Many research groups have reported rapid screening methods using different devices such as colour tests, IR imaging and ESI-MS

The simplest of these methods (a colour change) was used in a parallel assay reported by Crabtree and co-workers, which was based on a reactive dye *e.g.* **1.28** (**Figure 1.19**) that bleaches when a catalytic reaction, such as hydrosilation, took place.[59] The rapid screening is carried out in a Teflon block drilled with 70 reaction wells. This allows the rapid screening of a large set of catalysts until a "hit" is registered by the dye bleaching in one of the reaction wells. This bleaching is caused by the C=C or C=N bonds reacting and becoming saturated and therefore, destroying the conjugation with the dye.

References for Chapter 1 begin on page 37

i.e. the electronic connection between donor and acceptor is broken and the absorption coefficient of the material drops. Quantitative data can be obtained using the bleaching time, although, a drawback of this method is that a catalyst that may be active for the reactive dye may not be active using other compounds or vice-versa. Often, the reactive dyes or other labeled substrates used do not resemble the real substrates sterically or electronically.

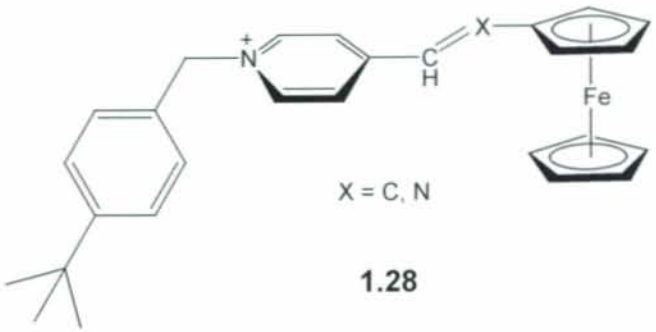

1.28

Figure 1.19 Reactive dye used by Crabtree.

In 2002, Hartwig *et al.*[60] used a colorimetric rapid screening method to obtain "lead" transition metal-catalysed hydroamination reactions. A set of reactions between morpholine and cyclohexadiene were conducted in a 96-well glass plate sealed with a glass slide. He showed that the reactions with the palest blue colour contained the lowest concentration of morpholine and, therefore, the most active catalyst.

In another high-throughput study, Ellman and co-workers used a mass spectrometric labeling strategy in the evaluation and optimization of a C-H activation reaction.[61] A mixture of aromatic heterocycles and a single alkene was subjected to catalytic C-H activation with $[Ru_3(CO)_{12}]$ and CO. The products bearing a ketone were

References for Chapter 1 begin on page 37

selectively labeled, allowing the yields of the products to be determined by ESI-MS (**Scheme 1.9**)

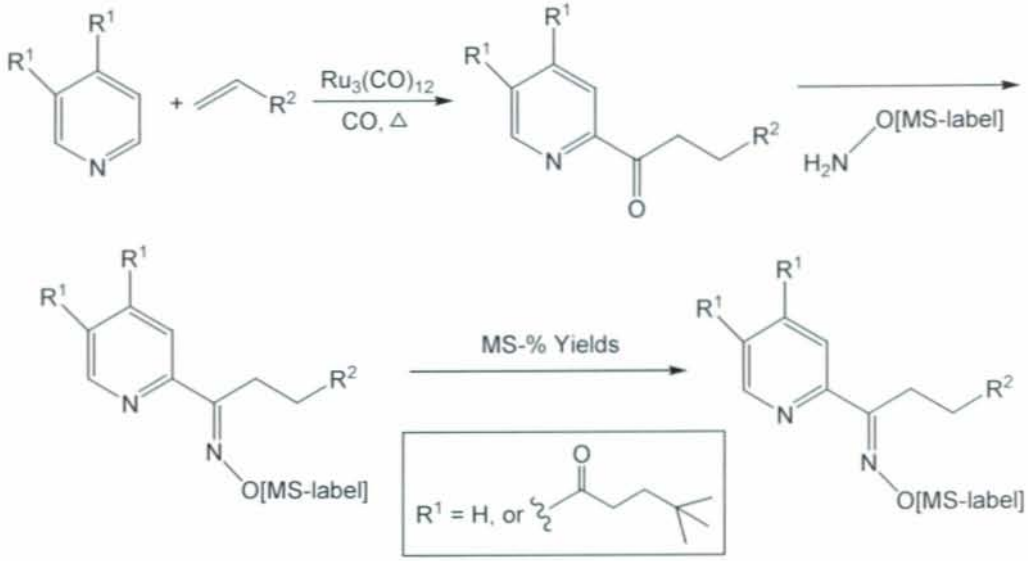

Scheme 1.9 High-throughput evaluation of C-H activation reaction by ESI-MS.

In the field of homogeneous catalysis, high-throughput screening methodologies have been employed most extensively in the discovery of exceptionally active catalysts for ethylene polymerization. Following the finding that salicylaldimines bearing bulky *ortho*-phenoxy substituents and small imine substituents gave very active chromium catalysts, Gibson and co-workers designed a library of salicylaldimine ligands bearing bulky substituents.[62] Chromium complexes of the ligands were screened in the polymerization of ethylene in order to find the most active catalysts. More recently, Mountford *et al.*[63] have reported the preparation of imidotitanium precatalysts using semi-

References for Chapter 1 begin on page 37

automated parallel synthesis procedures. Using high-throughput rapid screening techniques the group identified seven highly active ethylene polymerization precatalysts.

The work described in the following Chapters involves investigations into the use of MALDI-TOF MS for rapid screening of catalytic reactions involving extremely moisture-sensitive paramagnetic complexes. This was achieved by the synthesis of variety of lanthanide complexes and analyzing the reactions using MALDI-TOF MS. Preliminary catalytic activity of the complexes were also evaluated by testing them in the catalytic hydroamination transformation of an aminoalkyne.

References for Chapter 1 begin on page 37

1.8 References

1. (a) Cotton S. *Lanthanides and Actinides*, 1st Ed, Macmillan Education Ltd. London, **1991**, chap. 1-2; (b) Cloke, F. G. N. *Chem. Soc. Rev.*, **1993**, 17.
2. Evans W. J. *Inorg. Chem.*, **2007**, *46*, 3435.
3. Cotton, F. A.; Wilkinson, G.; Gaus, P. L. *Basic Inorganic Chemistry*. 3rd Ed. John Wiley & Sons, Inc.; New York, 1995.
4. Wilkinson, G.; Birmingham, J. M. *J. Am. Chem. Soc.*, **1954**, *76*, 6210.
5. Tsutsui, M.; Ely, N. *J. Am. Chem. Soc.*, **1974**, *96*, 4042.
6. Schumann H.; Meese-Marktscheffel J. A.; Esser, L. *Chem. Rev.*, **1995,** *95*, 865.
7. Evans, W. J. *Polyhedron*, **1987**, *14*, 453.
8. Cornils, B.; Herrmann, W. A. *Applied Homogeneous Catalysis with Organometallic Compounds; A Comprehensive Handbook*. Wiley-VCH, Weinheim, 2000.
9. (a) Thomas, J. M.; Raja, R.; Sankar, G.; Bell, R. G.; Lewis, D. W. *Pure Appl. Chem.*, **2001**, *73*, 1087; (b) Anastas, P. T.; Warner, J. C. *Green Chemistry Theory and Practice*; Oxford University Press Inc., New York, 1998.
10. Watson, P. L. *J. Am. Chem. Soc.*, **1982,** *104*, 337.
11. Gagné, M. R.; Marks, T. J. *J. Am. Chem. Soc.*, **1989**, *111*, 4108.
12. Shapiro, P. J.; Bunel, E.; Schaefer, W. P.; Bercaw, J. E. *Organometallics*, **1990,** *9*, 867.

References for Chapter 1 begin on page 37

13. Evans W. J.; Bloom, I.; Hunter, W. E.; Atwood, J. L. *J. Am. Chem. Soc.*, **1983,** *105*, 1401.

14. Molander, G. A.; Nichols, P. J. *J. Am. Chem. Soc.*, **1995,** *117*, 4415.

15. (a) St. Clair, M. A.; Santarsiero, B. D.; and Bercaw, J. E. *Organometallics*, **1989**, *8*, 17, (b) Nakayama, Y.; Yasuda, H., *J. Organomet. Chem.*, **2004,** *698*, 4489.

16. Hong, S.; Marks, T. J. *Acc. Chem. Res.*, **2004,** *37*, 673.

17. Aspinall, H. C. *Chem. Rev.* **2002,** *102*, 1807.

18. Aubrecht, K. B.; Chang, K.; Hillmyer, M. A.; Tolman, W. B. *J. Polym. Sci. Part A*, **2001**, *39*, 284.

19. Giesbrecht, G. R.; Whitener, G. D.; Arnold, J. *Dalton Trans.*, **2001**, 923.

20. Hayes, P. G.; Piers W. E.; McDonald, R. *J. Am. Chem. Soc.*, **2002**, *124*, 2132.

21. Xu, X.; Zhang, Z.; Yao, Y.; Zhang, Y.; Shen, Q. *Inorg. Chem.*, **2007**, *46*, 9379.

22. Gountchev, T. I.; Tilley, T. D. *Organometallics*, **1999**, *18*, 5661.

23. Schaverien, C. J.; Meijbooma, N.; Orpen, A. G. *J. Chem. Soc., Chem. Commun.*, **1992**, 124.

24. Duchateau, R.; Tuinstra, T.; Brussee, E. A. C.; Meetsma, A.; Duijnen, P. T.; Teuben, J. H. *Organometallics*, **1997,** *16*, 3511.

25. Kerton, F. K.; Holloway, S.; Power, A.; Soper, R. G.; Sherdan, K.; Lynam, J. M.; Whitewood, A. C.; Willans, C. E. *Can. J. Chem.*, **2008**, *85*, 435

26. Kerton, F. M.; Whitwood, A. C.; Willans, C. E. *Dalton Trans.*, **2004**, 2237.

References for Chapter 1 begin on page 37

27. Pohlki, F.; Doye, S. *Chem. Soc. Rev.*, **2003**, 104.

28. (a) Ryu, J.; Li, G. Y.; Marks, T. J. *J. Am. Chem. Soc.*, **2003**, *125*, 12584; (b) Muller, T. E.; Beller, M. *Chem. Rev.*, **1998,** *98*, 675.

29. Nobis, M.; Drieûen-Hölscher, B. *Angew. Chem. Int. Ed.*, **2001**, *40*, 3983.

30. Bytschkov, I.; Doye, S. *Eur. J. Org. Chem.*, **2003**, 935.

31. Li, Y.; Marks, T. J. *J. Am. Chem. Soc.*, **1996**, *118*, 9295.

32. Seayad, J.; Tillack, A.; Hartung, C. G.; Beller, M. *Adv. Synth. Catal.*, **2002**, *344*, 795.

33. (a) Li, Y.; Marks, T. J. *Organometallics* **1996,** *15*, 3770 (b) Kawaguchi, H.; Matsuo, T. *J. Organomet. Chem.*, **2004,** 4228.

34. Giardello, M. A.; Conticello, V. P.; Brard, L.; Gagnb, M. R.; Marks T.J. *J. Am. Chem. Soc.*, **1994,** *116*, 10241.

35. Li, Y.; Marks, T. J. *J. Am. Chem. Soc.*, **1998**, *120*, 1757.

36. Kim, Y. K.; Livinghouse, T.; Bercaw, J. E. *Tetrahedron Lett.*, **2001,** *42*, 2933.

37. Kim J. Y.; Livinghouse, T. *Org. Lett.*, **2005**, *7*, 1737.

38. Kim, Y. K.; Livinghouse, T.; Horino, Y. J. Am. Chem. Soc. **2003**, *125*, 9560.

39. Kim J. Y.; Livinghouse, T. *Org. Lett.*, **2005**, *7*, 4391.

40. Ryu, J.; Li, G. Y.; Marks, T. J. *J. Am. Chem. Soc.*, **2003**, *125*, 12584.

41. Gribkov, D. V.; Hultzsch, K.C. *Chem. Commun.*, **2004**, 730.

References for Chapter 1 begin on page 37

42. O'Shaughnessy, P. N.; Gillespie, K. M.; Knight, P. D.; Munslow I. J.; Scott, P. *Dalton Trans.*, **2004**, 2251.

43 Kawaguchi, H.; Matsuo, T. *J. Organomet. Chem.*, **2004**, *689*, 4228.

44 Piers, W. E.; Emslie, D. J. H. *Coord. Chem. Rev.* **2002**, *233-234*, 131.

45 (a) Yao, Y. M.; Ma, M. T.; Xu, X. P.; Zhang, Y.; Shen, Q.; Wong, W. T. *Organometallics*, **2005**, *24*, 4014; (b) Bonnet, F.; Cowley, A. R.; Mountford, P. *Inorg. Chem.*, **2005**, *44*, 9046.

46 Eelman, M. D.; Blacquiere, J. M.; Moriarty, M. M.; Fogg, D. E.; *Angew. Chem. Int. Ed.*, **2008**, *47*, 303; (b) Snelgrove, J. L.; Conrad, J. C.; Eelman, M. D.; Moriarty, M. M.; Yap, G. P. A.; Fogg, D. E. *Organometallics*, **2005**, *24*, 103.

47 Henderson, W.; McIndoe, J. S. *Mass Spectrometry of Inorganic and Organometallic Compounds*; John Wiley & Sons Ltd: Chichester, 2005.

48 (a) Adlhart, C.; Hinderling, C.; Baumann, H.; Chen, P. *J. Am. Chem. Soc.*, **2000,** *122,* 8204, (b) Hinderling C.; Chen P. *Angew. Chem. Int. Ed.*, **1999**, *38*, 2253.

49 Zenobi R.; Knochenmuss, R. *Mass Spectrom. Rev.*, **1998**, *17*, 337.

50 Landry, F.; Lombardo C. R.; Smith, J. W. *Anal. Biochem.*, **2000**, *279*, 1.

51 Ambre A. H.; Jagtap, R. N. *Bull. Mater. Sc.*, **2005**, *28*, 515.

52 Tanaka, K. *Angew. Chem. Int. Ed.*, **2003**, *42*, 3861.

53 Webb, M. E.; Stephens, E.; Smith A. G.; Abell, C. *Chem. Commun.*, **2003**, 2416.

54 Vitalini, D.; Mineo, P. *Macromolecules,* **1996,** *29,* 4478.

References for Chapter 1 begin on page 37

55 Corpillo, D.; Cabella, C.; Crich, S. G.; Barge, A.; Aime, S. *Anal. Chem.*, **2004**, *76*, 6012.

56 Chen, P. *Angew. Chem. Int. Ed.*, **2003**, *42*, 2832.

57 Murphy,V. *Comprehensive Organometallic Chemistry III*, Elsevier Ltd. California, **2007**, Chap. *1.13*, 341.

58 Crabtree, R. H. *Chem. Commun.*, **1999**, 1611.

59 Cooper, A. C.; McAlexander, L. H.; Lee, D.; Torres, M. T.; Crabtree R. H. *J. Am. Chem.*, **1998**, *120*, 9971.

60 Pawlas, J.; Nakao, Y.; Kawatsura, M.; Hartwig, J. F. *J. Am. Chem. Soc.*, **2002**, *124*, 3669.

61 Szewczyk, J.; Zuckerman, W. R. L.; Bergman, R. G.; Ellman, J. A. *Angew. Chem. Int. Ed.*, **2001**, *40*, 216.

62 Jones, D. J.; Gibson, V. C.; Green S. M.; Maddox, P. J. *Chem. Commun.*, **2002**, 1038.

63 Adams, N.; Arts, H. J.; Bolton, P D.; Cowell, D.; Dubberley, S. R.; Friederichs, N.; Grant, C. M.; Kranenburg, M.; Sealey, A.J.; Wang, B.; Wilson, P. J.; Cowley, A. R.; Mountford, P.; Schröder, M. *Chem. Comm.*, **2004**, 434.

References for Chapter 1 begin on page 37

Chapter 2

Synthesis and Characterization of Rare Earth Metal Complexes Using MALDI-TOF MS

2.1 Introduction and Research Objectives

The characteristic labile nature of the rare earth metal-ligand bonds and the flexibility of their coordination geometries make these metals very suitable for use as catalysts.[1] As described in Chapter 1, the rare earth metals are highly Lewis acidic and form hard M^{3+} ions with large radii. Therefore, their complexes are prone to ligand redistributions, dimerization and solvent ligation. A common method employed in preventing both dimerization and solvent coordination is to use a sterically-demanding ligand system.[1]

Multidentate ligands are able to stabilize the trivalent lanthanide centers and provide the desired environment to yield catalytic species, with specific sites being available on the metal for further reactions. In this context, amine bis(phenolate) ligand environments offer strong metal-oxygen bonds suitable for stabilizing complexes of these electropositive lanthanide metals. Various amine bis(phenol) ligands were introduced, which allowed for systematic variation of the substituent group (R′) on the tertiary nitrogen atom and those on the aromatic ring (R) (**Figure 2.1**).[2]

References for Chapter 2 begin on page 77

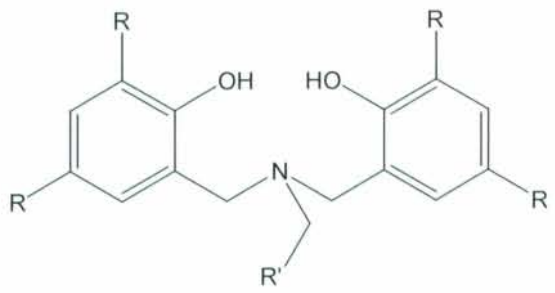

2.1 R = t-Bu
R′ = NMe_2, Py, NEt_2

Figure 2.1 Tetradentate amine bis(phenol) ligand precursor.

A recent report by Kerton *et al.*[3] described a rapid and more benign method for synthesizing a variety of amine bis(phenolate) ligands. Water was used as the solvent under microwave irradiation, which gave a faster and more quantitative yield than the conventional method.

Several reports have described the use of the lanthanide amine bis(phenolate) complexes for polymerization processes.[4-7] However, these complexes have not been used in other types of reactions that lanthanides can facilitate *e.g.* hydrogenation and hydroamination reaction. This is somewhat surprising, given the use of chiral bis(phenolate) ligands by Hultzsch and co-workers for enantioselective hydroamination reactions .[1,8]

There are numerous metal-ligand combinations that could offer interesting complexes and fascinating chemistry. But, during metal-ligand complexation, mixtures are sometimes obtained and coordination of the ligand to metal can be uncertain and in some cases, no reaction takes place at all. Moreover, most lanthanide complexes are

References for Chapter 2 begin on page 77

paramagnetic and preclude NMR analysis. If a new screening method that would support high-throughput experimentation was developed, it would play a vital role in this field of homogeneous catalysis.

Therefore, the objective of this project is directed toward investigating the efficacy of MALDI-TOF mass spectrometry as a new method for rapid probing of catalytic reactions. As well the catalytic potential of amine bis(phenolate) lanthanide complexes for hydroamination processes was explored.

2.2 Amine Bis(phenolate) Ligands

The research described in this thesis used a four ligand set of amine bis(phenolates), previously prepared in this laboratory, for the synthesis of lanthanide complexes. Two types of ligand were used as shown in **Figure 2.2**: the $[O_2N_2]$-type (**2.2** and **2.3**) and $[O_2NN']$-type (**2.4** and **2.5**). The difference between the two types of ligands is that the $[O_2N_2]$-type has their neutral nitrogen donors in the backbone of the ligand, while the $[O_2NN']$-type has one pendant nitrogen donor. The four ligands also differ in the variation of their R substituent groups. The difference between (**2.2**) and (**2.3**) lies in the steric crowding. While (**2.2**) has a methyl group as the aromatic substituent *para* to the phenol group, (**2.3**) has a *tert*-butyl group instead in this same position. On the other hand, (**2.4**) differs from (**2.5**) by having *tert*-butyl groups in both of the aromatic substituent sites *ortho* and *para* to the phenol group, while, (**2.5**) has *tert*-amyl groups in both sites.

References for Chapter 2 begin on page 77

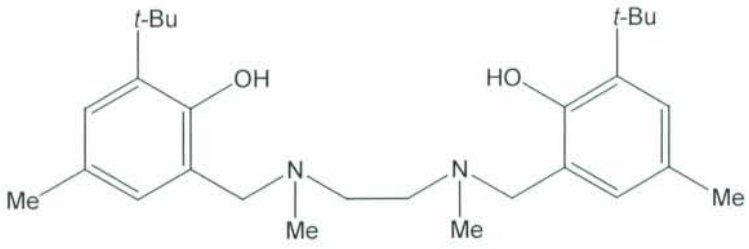

$[O_2N_2^{t\text{-}Bu,Me}]H_2$

2.2

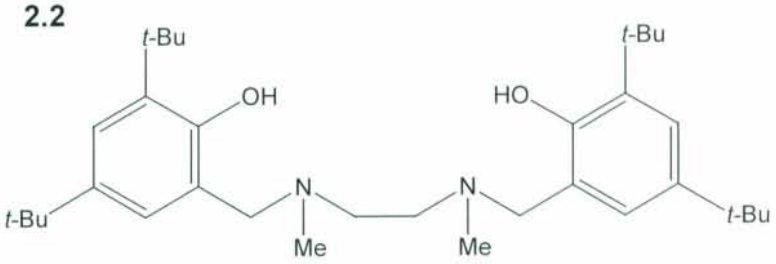

$[O_2N_2^{t\text{-}Bu}]H_2$

2.3

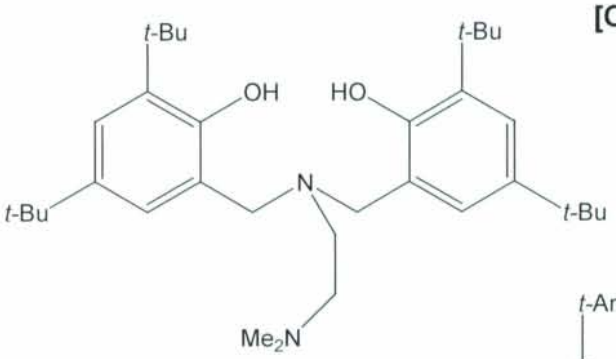

$[O_2NN'^{t\text{-}Bu}]H_2$

2.4

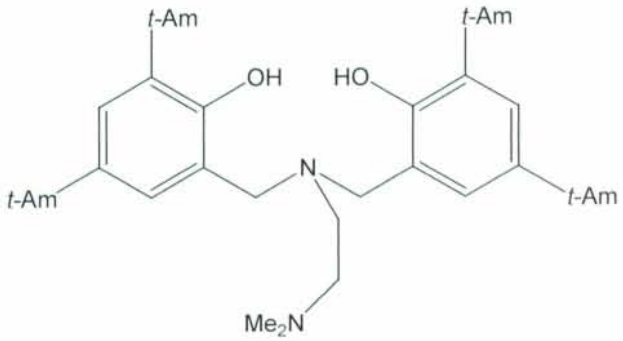

$[O_2NN'^{t\text{-}Am}]H_2$

2.5

Figure 2.2 Protio ligands used in this study

References for Chapter 2 begin on page 77

2.2.1 Drying of Amine Bis(phenol) Compounds

The amine bis(phenol) compounds were first dried using the following procedure: To a tetrahydrofuran solution of $[O_2N_2^{t\text{-}Bu,Me}]H_2$ (**2.2**), anhydrous $MgSO_4$ was added producing a white suspension. This was left to settle for 18 h, under a nitrogen atmosphere. The mixture was filtered through a canula, and the solvent was removed under vacuum to afford a dry white solid. The remaining ligands (**2.3** – **2.5**) were dried using the same procedure. The ^{1}H NMR spectra proved that all the ligands were pure and were consistent with the literature data.[3] The ^{1}H NMR spectrum of $[O_2N_2^{t\text{-}Bu,Me}]H_2$ (**2.2**) (**Figure 2.3**) showed that the ligand is symmetrical, with one singlet at δ = 10.75 ppm, which corresponds to the phenol –OH proton.

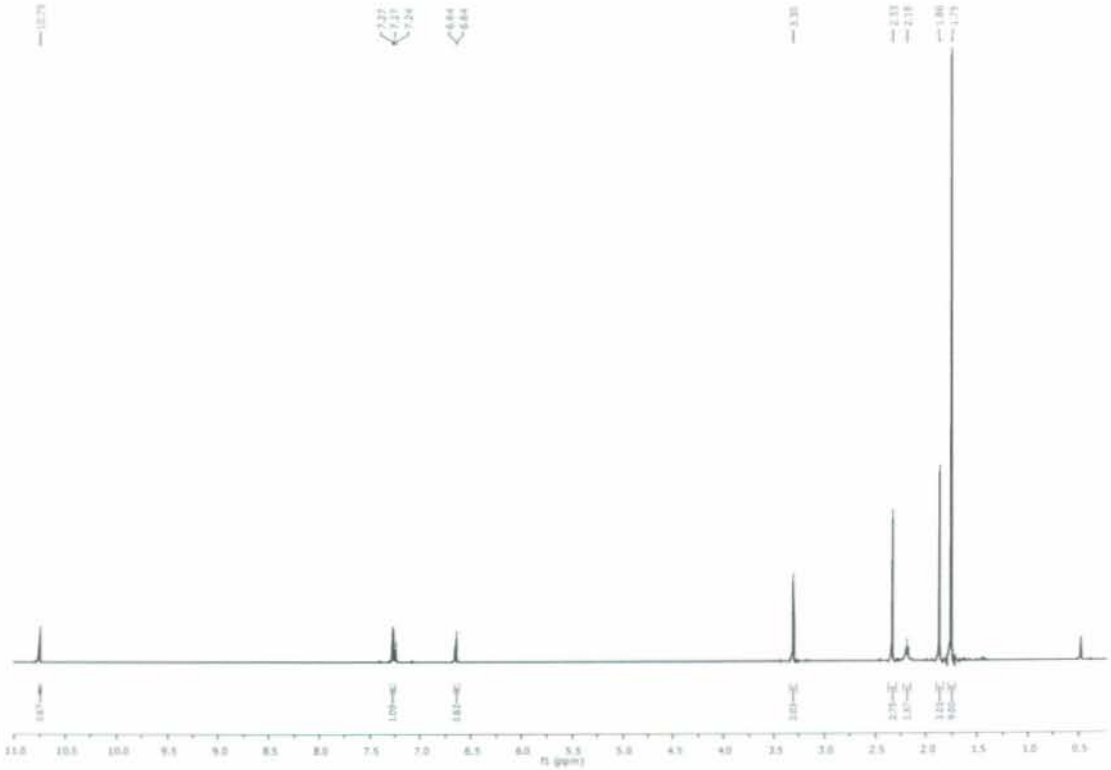

Figure 2.3 ^{1}H NMR (500 MHz) spectrum of $[O_2N_2^{t\text{-}Bu,Me}]H_2$ (**2.2**)

References for Chapter 2 begin on page 77

It also showed two sets of doublets for the aromatic protons at δ = 7.27 ppm and 6.64 ppm with coupling constants of 1.8 Hz respectively, a singlet at 3.30 ppm for the methylene group adjacent to the aromatic ring, and two singlets at δ = 2.33 ppm and 2.18 ppm for the amine methyl group and the methylene bridge respectively. The aromatic methyl group and the *tert*-butyl singlet peaks appeared at δ = 1.86 ppm and 1.75 ppm respectively. The ^{1}H NMR spectra for the remaining three ligands (**2.3** – **2.5**) are shown in **Appendix 2.1-2.3**.

2.3 Synthesis of Rare-Earth Metal Amine Bis(phenolate) Complexes

Rare-earth metal complexes can be prepared using different methods. These include salt metathesis and protonolysis of either tris(amido) or tris(alkyl) metal precursors by the ligand. Salt metathesis (salt elimination) involves the reaction of metal halide precursors with alkali metal salts of the ligand. This can lead to formation of unwanted by-products such as "ate" complexes by incorporation of the eliminated alkali halide salts into the metal coordination sphere.[1,9] The formation of undesired "ate" complexes can be prevented by using a protonolysis approach. This involves a two-step approach. For example, reacting lithium bis(trimethylsilylamide) with lanthanide chloride, followed by protonolysis with the diprotonated ligand. The rare earth metal tris(amido) complexes are convenient to prepare and are thermally robust compared to the tris(alkyl) analogues.[1] Thus, they are more frequently used in the organometallic chemistry of rare earth metals.

References for Chapter 2 begin on page 77

Lithium bis(trimethylsilyl) amide and lanthanide amide reagents used for the synthesis of the lanthanide amido bis(phenolate) complexes as described in this thesis were prepared by the reaction sequences described in the following sections using literature procedures.[10,11]

2.3.1 Synthesis of Lithium Bis(trimethylsilyl) amide[Li{N(SiMe$_3$)$_2$}]

Lithium bis(trimethylsilyl)amide [Li{N(SiMe$_3$)$_2$}] (**2.8**) was prepared by adding an ether solution of hexamethyldisilazane [HN(SiMe$_3$)$_2$] (**2.7**) to a reaction vessel. The solution was cooled to 0 °C and *n*-butyllithium (**2.6**) was added dropwise. The reaction mixture was allowed to warm up to room temperature and was stirred for 18 h under nitrogen [**Eqn. 2.1**]. Solvent removal under vacuum left a yellow solid, which was subsequently washed with cooled (0 °C) hexane. The resulting solid was dried under vacuum leaving a white powdery product in 89% yield.

$$CH_3(CH_2)_3Li + HN(SiMe_3)_2 \xrightarrow[rt,\ 18\ h]{Et_2O} Li[N(SiMe_3)_2]\cdot Et_2O \quad [2.1]$$

2.6 **2.7** **2.8**

^{1}H NMR (500 MHz) spectroscopic analysis of the white powdery solid revealed the product to be lithium bis(trimethylsilyl)amide. The spectrum (**Figure 2.4**) showed three peaks: a singlet at δ = 0.24 ppm, a triplet at δ = 1.02 ppm and a quartet at 3.33 ppm, with coupling constants of 7.0 Hz for the quartet and the triplet. The singlet corresponds to the SiMe groups of the lithium bis(trimethylsilylamide), while the triplet and the

quartet corresponded to protons of one equivalent of diethyl ether coordinated coordinated to the lithium.

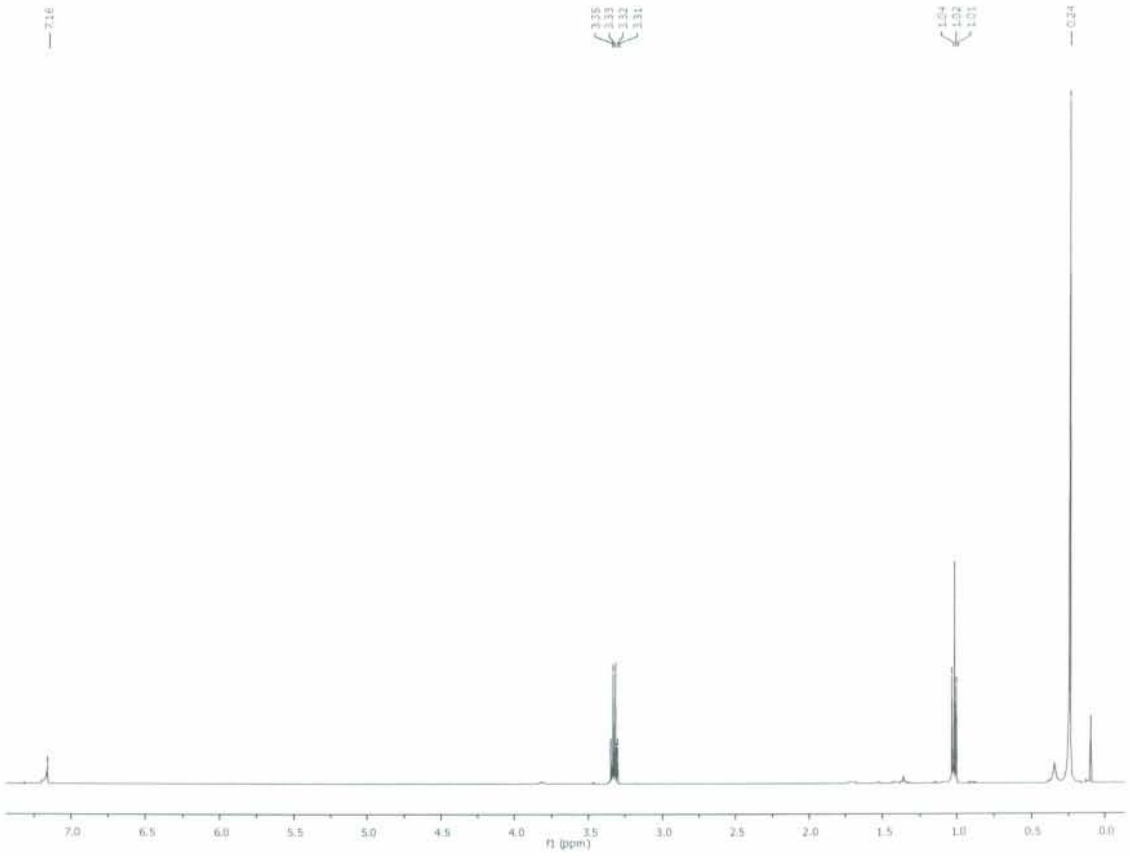

Figure 2.4 ^{1}H NMR (500 MHz) of lithium bis(trimethylsilyl)amide (**2.8**)

2.3.2 Drying of Lanthanide Trichloride Hexahydrate [Ln(III)$Cl_3 \cdot 6H_2O$]

[Ln = Gd = **2.12a,** Ho = **2.12b**, Sm = **2.12c,** La = **2.12d,** Y = **2.12e,** Yb = **2.12f]**

The lanthanide halides are highly acidic, therefore, they take up water easily when exposed to air generating lanthanide hydrate species. To obtain anhydrous lanthanide halides, commercially available lanthanide trichloride hexahydrates were dried prior to use as follows. To a tetrahydrofuran suspension of one equivalent of gadolinium

trichloride hexahydrate (**2.10**) was gradually added twenty equivalents of trimethylsilyl chloride (**2.11**) generating a colourless solution. The resulting mixture was stirred at room temperature for 18 h, during which time a pale coloured solid formed (**Eqn.2.2**). The isolated solid was dried *in vacuo*, affording a pale green powdery solid (**2.12a**) in 70% yield. Using the same procedure the anhydrous trichlorides of other lanthanides were prepared in a similar way resulting in yields ranging from 65 – 87%.

$$GdCl_3{\cdot}6H_2O + 20\ Me_3SiCl \xrightarrow[rt,\ 18\ h]{THF} GdCl_3{\cdot}(THF)_{3.5} \quad [2.2]$$

2.10 **2.11** **2.12a**

2.3.3 Synthesis of Lanthanide Tris(trimethylsilyl) Amides

[Ln{N(SiMe$_3$)$_2$}$_3$] [**Ln N″** = Ho N″ = **2.13a** , GdN″ = **2.13b,** YbN″ = **2.13c,** SmN″ = **2.13d,** LaN″ = **2.13e,** YN″ = **2.13f**]

Holmium (III) chloride (**2.12b**) was suspended in tetrahydrofuran at 0 °C. A tetrahydrofuran solution of three equivalents of lithium bis(trimethylsilyl) amide was added to the cooled suspension generating a light pink slurry. The reaction mixture was stirred at 0 °C for 4 h, allowed to warm to room temperature and subsequently stirred for 18 h (**Eqn 2.3**). The solvent was removed under vacuum to give a pink solid, which was extracted with diethyl ether. The resulting pink solution was filtered, removing solid lithium chloride. The solvent was removed from the solution *in vacuo* to generate a pink crystalline solid (**2.13a**) in 89% yield. Following the same procedure, all other lanthanide tris(trimethylsilyl) amides were obtained in good yields (43-92%).

References for Chapter 2 begin on page 77

$$HoCl_3 + 3\ Li\{N(SiMe_3)_2\} \xrightarrow[-3\ LiCl,\ rt,\ 18\ h]{THF} Ho\{N(SiMe_3)_2\}_3 \qquad [2.3]$$

2.12b **2.8** **2.13a**

The ^1H NMR spectrum of the pink crystalline solid was uninformative. The spectrum (**Figure 2.5**) showed only one significant signal, which was broad and corresponds to protons of the C_6D_6 solvent. The observed effect was a result of the paramagetic nature of the metal ion.

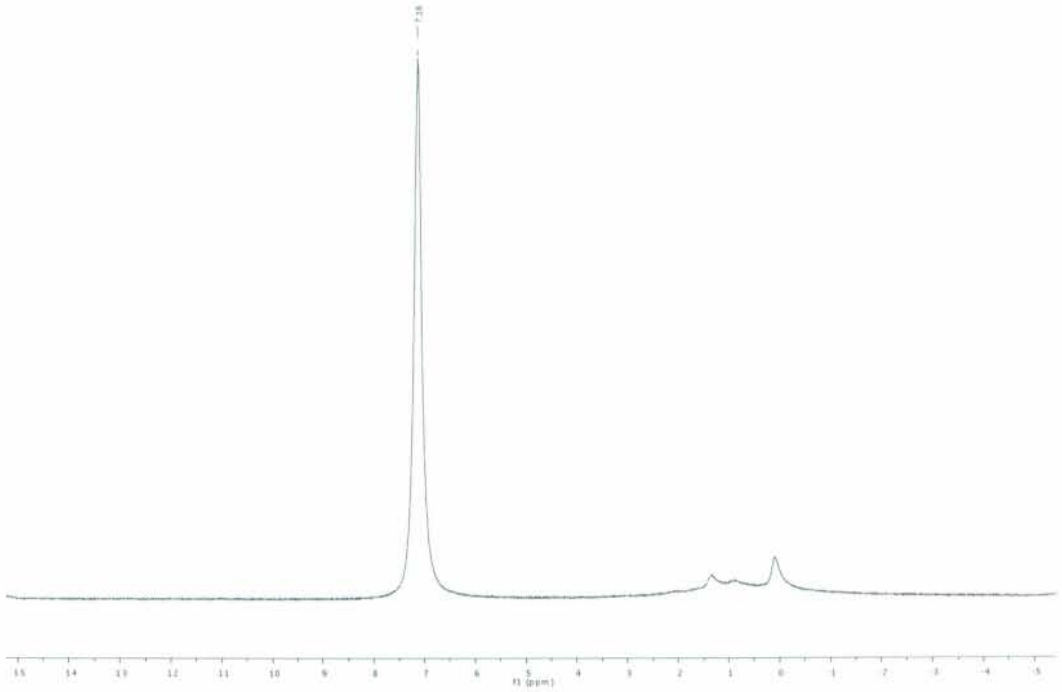

Figure 2.5 ^1H NMR (500 MHz) spectrum of holmium tris(trimethylsilyl) amide (**2.13a**)

Similar paramagnetic influences were observed for gadolinium tris(trimethylsilyl) amide (**Figure 2.6**) and samarium tris(trimethylsilyl) amide. In the case of samarium

tris(trimethylsilyl) amide (**Appendix 2.4**), the ^{1}H NMR resonances were broad and upfield shifted to –1.57 ppm.

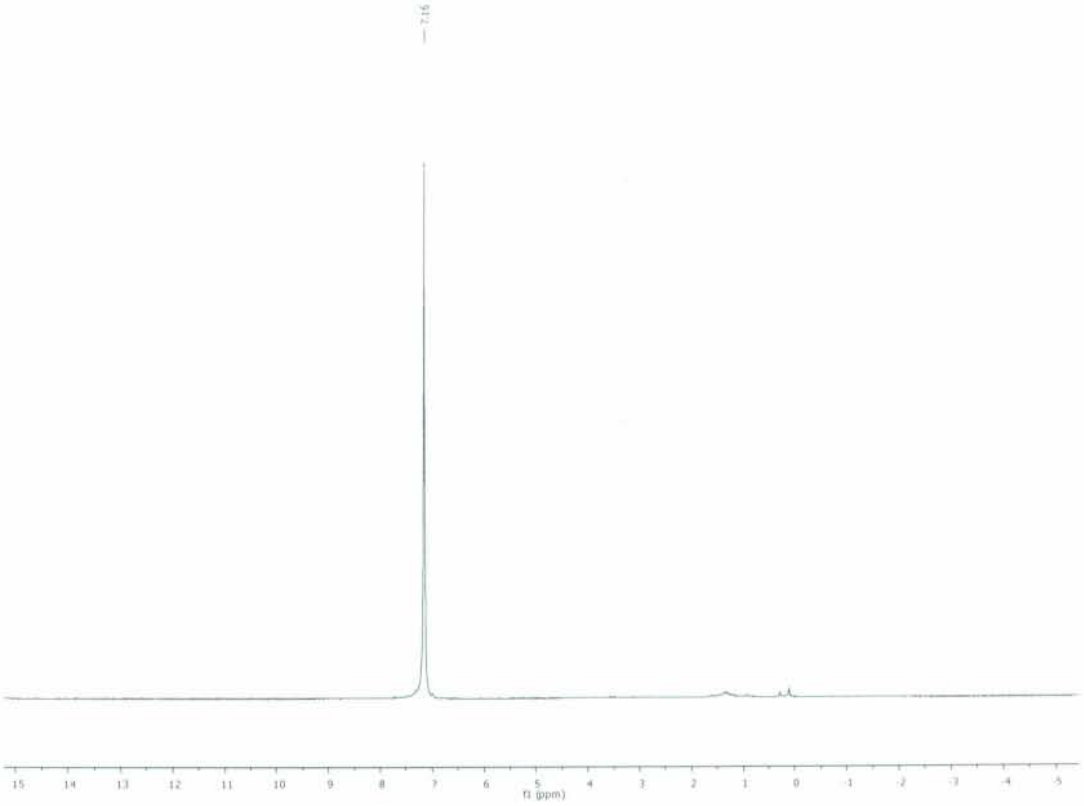

Figure 2.6 ^{1}H NMR spectrum of gadolinium tris(trimethylsilyl) amide (**2.13b**)

2.3.4 Synthesis of Lanthanide Amine Bis(phenolate) complexes

Synthetic approaches adopted for the preparation of the lanthanide amine bis(phenolate) complexes in this research were based on the previous work in the Kerton laboratory.[4] The complexation of each of the six lanthanide amide reagents $[Ln\{N(SiMe_3)_2\}_3]$ (**2.13a-2.13f**) with the four different amine bis(phenolate) ligands (**2.2-2.5**) were carried out by transamination reactions. **Table 2.1** shows the codes for the lanthanide complexes, which were prepared as described below.

References for Chapter 2 begin on page 77

Table 2.1 Names and code numbers of lanthanide complexes used

Ligand	Lanthanide Amide	Complex	Code #
$[O_2N_2^{t\text{-}Bu,Me}]$	$Ho\{N(SiMe_3)_2\}_3$	$[O_2N_2^{t\text{-}Bu,Me}]HoN(SiMe_3)_2$	**2.14a**$_{2.2}$
$[O_2N_2^{t\text{-}Bu}]$	" "	$[O_2N_2^{t\text{-}Bu}]HoN(SiMe_3)_2$	**2.14a**$_{2.3}$
$[O_2NN'^{t\text{-}Bu}]$	" "	$[O_2NN'^{t\text{-}Bu}]HoN(SiMe_3)_2$	**2.14a**$_{2.4}$
$[O_2NN'^{t\text{-}Am}]$	" "	$[O_2NN'^{t\text{-}Am}]HoN(SiMe_3)_2$	**2.14a**$_{2.5}$
$[O_2N_2^{t\text{-}Bu,Me}]$	$Gd\{N(SiMe_3)_2\}_3$	$[O_2N_2^{t\text{-}Bu,Me}]GdN(SiMe_3)_2$	**2.14b**$_{2.2}$
$[O_2N_2^{t\text{-}Bu}]$	" "	$[O_2N_2^{t\text{-}Bu}]GdN(SiMe_3)_2$	**2.14b**$_{2.3}$
$[O_2NN'^{t\text{-}Bu}]$	" "	$[O_2NN'^{t\text{-}Bu}]GdN(SiMe_3)_2$	**2.14b**$_{2.4}$
$[O_2NN'^{t\text{-}Am}]$	" "	$[O_2NN'^{t\text{-}Am}]GdN(SiMe_3)_2$	**2.14b**$_{2.5}$
$[O_2N_2^{t\text{-}Bu,Me}]$	$Yb\{N(SiMe_3)_2\}_3$	$[O_2N_2^{t\text{-}Bu,Me}]YbN(SiMe_3)_2$	**2.14c**$_{2.2}$
$[O_2N_2^{t\text{-}Bu}]$	" "	$[O_2N_2^{t\text{-}Bu}]YbN(SiMe_3)_2$	**2.14c**$_{2.3}$
$[O_2NN'^{t\text{-}Bu}]$	" "	$[O_2NN'^{t\text{-}Bu}]YbN(SiMe_3)_2$	**2.14c**$_{2.4}$
$[O_2NN'^{t\text{-}Am}]$	" "	$[O_2NN'^{t\text{-}Am}]YbN(SiMe_3)_2$	**2.14d**$_{2.5}$
$[O_2N_2^{t\text{-}Bu,Me}]$	$Sm\{N(SiMe_3)_2\}_3$	$[O_2N_2^{t\text{-}Bu,Me}]SmN(SiMe_3)_2$	**2.14d**$_{2.2}$
$[O_2N_2^{t\text{-}Bu}]$	" "	$[O_2N_2^{t\text{-}Bu}]SmN(SiMe_3)_2$	**2.14d**$_{2.3}$
$[O_2NN'^{t\text{-}Bu}]$	" "	$[O_2NN'^{t\text{-}Bu}]SmN(SiMe_3)_2$	**2.14d**$_{2.4}$
$[O_2NN'^{t\text{-}Am}]$	" "	$[O_2NN'^{t\text{-}Am}]SmN(SiMe_3)_2$	**2.14d**$_{2.5}$
$[O_2N_2^{t\text{-}Bu,Me}]$	$La\{N(SiMe_3)_2\}_3$	$[O_2N_2^{t\text{-}Bu,Me}]LaN(SiMe_3)_2$	**2.14e**$_{2.2}$
$[O_2N_2^{t\text{-}Bu}]$	" "	$[O_2N_2^{t\text{-}Bu}]LaN(SiMe_3)_2$	**2.14e**$_{2.3}$
$[O_2NN'^{t\text{-}Bu}]$	" "	$[O_2NN'^{t\text{-}Bu}]LaN(SiMe_3)_2$	**2.14e**$_{2.4}$
$[O_2NN'^{t\text{-}Am}]$	" "	$[O_2NN'^{t\text{-}Am}]LaN(SiMe_3)_2$	**2.14e**$_{2.5}$
$[O_2N_2^{t\text{-}Bu,Me}]$	$Y\{N(SiMe_3)_2\}_3$	$[O_2N_2^{t\text{-}Bu,Me}]YN(SiMe_3)_2$	**2.14f**$_{2.2}$
$[O_2N_2^{t\text{-}Bu}]$	" "	$[O_2N_2^{t\text{-}Bu}]YN(SiMe_3)_2$	**2.14f**$_{2.3}$
$[O_2NN'^{t\text{-}Bu}]$	" "	$[O_2NN'^{t\text{-}Bu}]YN(SiMe_3)_2$	**2.14f**$_{2.4}$
$[O_2NN'^{t\text{-}Am}]$	" "	$[O_2NN'^{t\text{-}Am}]YN(SiMe_3)_2$	**2.14f**$_{2.5}$

References for Chapter 2 begin on page 77

A toluene solution of one molar equivalent of holmium tris(trimethylsilyl) amide [Ho{N(SiMe$_3$)$_2$}$_3$] (**2.13a**) was added to a toluene suspension of one molar equivalent [$O_2N_2^{tBu}$]H$_2$ (**2.3**) at –78 0 °C, giving a pale orange solution. The solution was allowed to warm to room temperature and was stirred for 18 h (**Eqn. 2.4**). Removal of the solvent under vacuum afforded a pale pink solid (**2.14a$_{2.3}$**). The pink solid was washed with pentane at 0 °C and the product was isolated in excellent yield (93%). Other lanthanide complexes were synthesized using the same procedure. Crystalline materials were obtained by cooling a saturated toluene/hexamethyldisiloxane solution to –35 °C in an inert atmosphere glove box. However, the crystallized species were not suitable for X-ray diffraction analysis due to the extreme moisture-sensitive nature of the complexes. The crystals desolvated as they were brought out of the glove box, which resulted in cracking of the crystals. ^{1}H NMR spectra were extremely broad due to the paramagnetic and fluxional nature of the complexes. As a result, no meaningful interpretation was obtained.

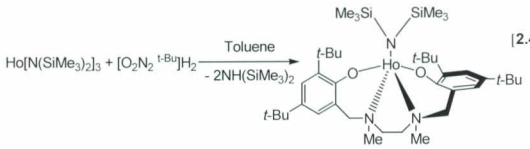

2.13a **2.3** **2.14a$_{2.3}$**

2.4 Characterization of Lanthanide Complexes Using MALDI-TOF Mass Spectrometry

MALDI-TOF MS was used for screening the complexation of the lanthanide amide reagents with amine bis(phenolate) ligands by mixing a toluene solution of the

lanthanide amide reagent *e.g.* $Gd\{N(SiMe_3)_2\}_3$ with a toluene solution of the ligand precursor *e.g.* $[O_2N_2{}^{t\text{-}Bu,Me}]H_2$. The mixture was stirred for 18 h at room temperature in an inert atmosphere glove box. An equal volume of a toluene solution of anthracene was added to the reaction mixture and was stirred for a further two minutes. The resulting solution was spotted on a MALDI sample plate and allowed to dry. Alongside the sample of the reaction mixture, a toluene solution of ligand alone *e.g.* $[O_2N_2{}^{t\text{-}Bu,Me}]H_2$, mixed with anthracene was spotted on another space on the sample plate and allowed to dry. The sample plate was placed inside two Ziploc bags and was removed from the glove box and rapidly transferred to the spectrometer for analysis. MALDI-TOF mass spectra of the isolated complexes and the free ligands were obtained under uniform instrument conditions. **Figure 2.7** shows a typical MALDI sample plate with 10 × 10-numbered positions where samples can be spotted.

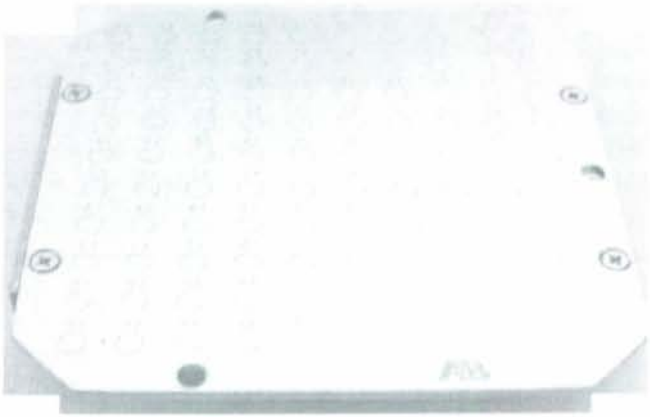

Figure 2.7 Example of a MALDI sample plate

2.4.1 MALDI-TOF MS Analysis Optimization

Prior to focusing on using toluene as a solvent for the study, various solvents such as hexane, acetonitrile and THF, were screened. Of these, toluene gave a better solubility

for both the analytes and matrix. It has been noted that the quality of MALDI analysis depends strongly on the matrix and the deposition of the samples.[12,13] MALDI matrices should contain laser energy-absorbing structures with high molar absorptivity.[14] Crystalline pyrene and anthracene meet this requirement, as they possess aromatic rings with extended electron π-conjugation. However, they do not contain functional groups that would react with moisture-sensitive complexes such as the organolanthanide species of interest. These two matrices have previously been used by Fogg and co-workers in the analysis of organotransition metal complexes.[15] Thus, these two matrices were screened for their potentials as matrices for the MALDI-TOF MS analysis of the organolanthanide complexes. The use of anthracene was generally found to give optimal spectra, although the differences between the two matrices were only marginal. As well, different matrix-to-analyte ratios (10:1, 5:1; 1:1) were screened. The higher matrix-to-analyte ratios afforded spectra that were dominated by matrix ions. The matrix-to-analyte ratio of 1:1 (anthracene:analyte) provided spectra with a good signal-to-noise ratio. This is in contrast with the previous studies where very large matrix excess has been used for organometallic species.[12,15] However, in our studies, the ligands may also act to absorb and transfer the laser energy. Therefore, in addition to screening the reaction with matrix, direct laser desorption ionization (LDI) without matrix was conducted but this did not afford interpretable spectra. This finding is in contrast to other results obtained in the Kerton group using Ti amide reagents.[16]

In our standard method, the sample plate was exposed (2-10 seconds) briefly to air when introduced to the spectrometer, but no product of a hydrolysis reaction was observed. Presumably the matrix covered the sample and prevented decomposition. In the

References for Chapter 2 begin on page 77

study performed by Fogg *et al.*, the MALDI-TOF MS was directly interfaced with an inert atmosphere glove box. Therefore to assess the viability of our approach (using a Ziploc or glove bag), samples were intentionally exposed to air, and were compared with our standard method. The resulting spectra contained no higher mass peaks; and the only assignable signals were for the protonated ligands. Therefore, rapid transfer of the plate into the instrument is essential.

2.4.2 Analysis of Isolated Lanthanide Complexes

In mass spectrometry, isotope abundance patterns are extremely useful in identifying the molecular formula and thereby, the species present. Sm, Gd, and Yb each have 7 naturally occurring isotopes, while Ho has only 1 naturally occurring isotope.[17] Thus, in this research, peaks with *m/z* higher than that of the protonated ligand were interpreted using their isotope distribution pattern.

Figure 2.8 shows the MALDI–TOF mass spectra for two isolated lanthanide amine bis(phenolate) amide complexes. These compounds had also been characterized using elemental analysis. The mass spectrum of the isolated $[O_2N_2^{t\text{-Bu,Me}}]GdN(SiMe_3)_2$ (**2.14b$_{2.2}$**) presented in **Figure 2.8(a)** shows an intense fragment peak at *m/z* 596, which corresponds to the loss of the bis(trimethylsilyl) amide group, $[N(SiMe_3)_2]$. Also, the peak at *m/z* 631 could be attributed to the loss of a methyl and two *tert*-butyl groups.

The MALDI mass spectrum of isolated $[O_2N_2^{t\text{-Bu,Me}}]HoN(SiMe_3)_2$(**2.14a$_{2.3}$**) (**Figure 2.8(b)**) shows a similar major peak at *m/z* 687, which was formed also by losing the bis(trimethylsilyl) amide group, $[N(SiMe_3)_2]$. The spectra **Figure 2.8** (**a**) and (**b**) insets contain the isotope patterns for the fragments; $[(O_2N_2^{t\text{-Bu,Me}})Gd]^+$ and $[(O_2N_2^{t\text{-}}$

^{Bu})Ho]$^+$ at *m/z* 596 and 687 respectively. The calculated (top) and the observed (bottom) isotope patterns are in good agreement, confirming the assignments.

The observation of the $[(O_2N_2^{t\text{-}Bu,Me})Gd]^+$ and $[(O_2N_2^{t\text{-}Bu})Ho]^+$ ion fragments, corresponding to the loss of $[N(SiMe_3)_2]$ in both spectra indicates probably that there were gas phase reactions occurring within the spectrometer. In a MALDI-TOF MS speciation study of poly(amidoamine)-platinum(II) complexes, Romeo *et al.*[18] also observed gas phase reactions and fragmentation despite this being a 'soft' mass spectrometric technique. In addition, the cleavage of the Ln-N$(SiMe_3)_2$ bond presumably indicates that under the mass spectrometry conditions, the coordinated bonds of oxygen donor to the lanthanide metal center are more stable than that of the Ln-N$(SiMe_3)_2$. This is in agreement with solution state reactivity.[4,5,7]

Fogg *et al.*[15] in their work reported that Cu(II) complexes resisted one-electron oxidation to yield the cation through electron transfer MALDI, as a result of the metal center being in its highest common oxidation state. This can be used to explain why in our study intact molecular ion peaks $[M]^+$ were not observed as the metals centers are also in their highest common oxidation state of 3+.

Beside the peaks observed at the expected region of peaks (*m/z* 600-800), clusters of less intense peaks between m/z 1000 and 1300 were observed in the spectra of almost all of the complexes investigated. To verify if these high masses were a general mass spectrometric trend for lanthanide species supported by the amine bis(phenolate) ligands, additional experiments were carried out with crude reaction mixtures.

References for Chapter 2 begin on page 77

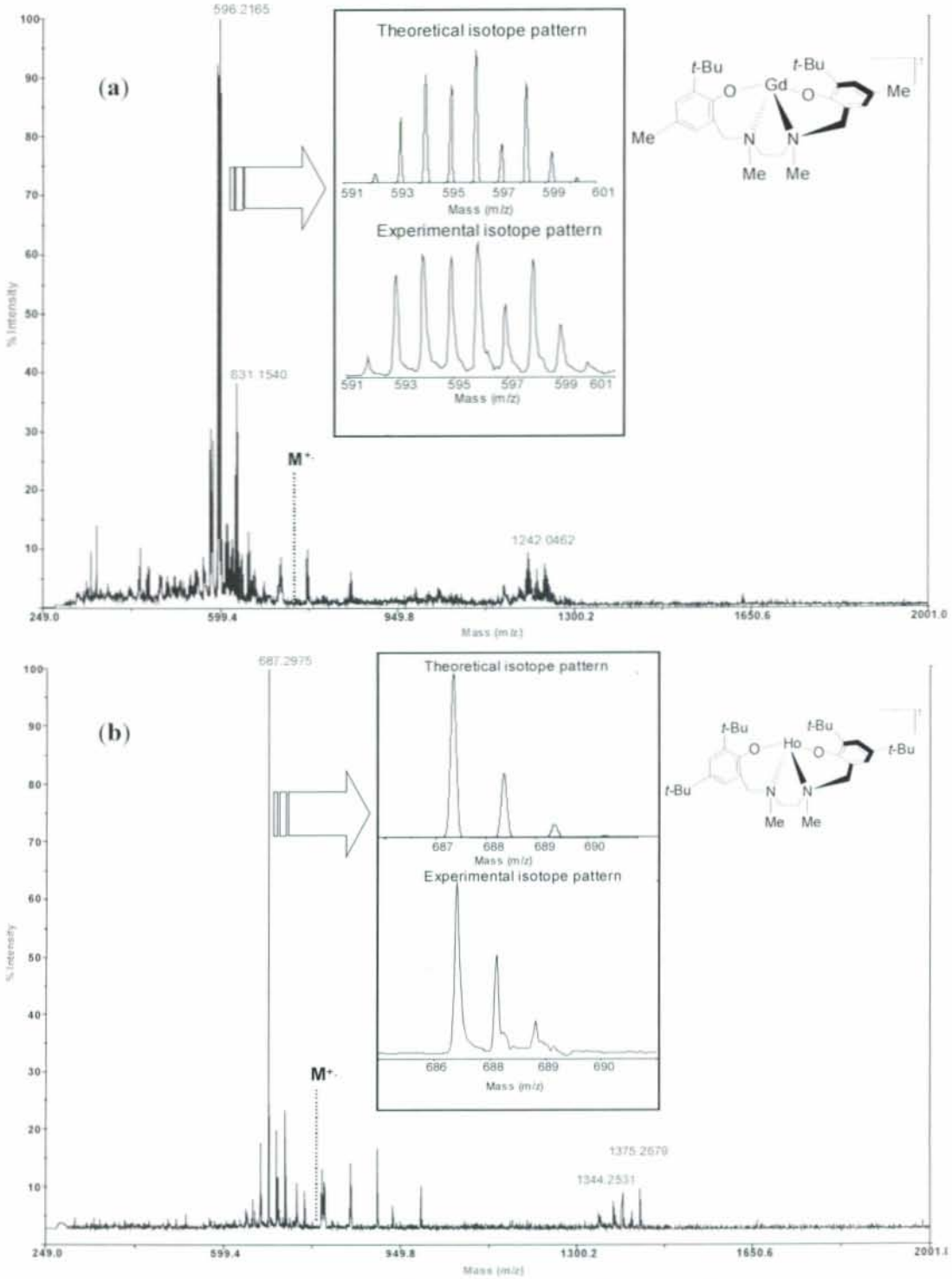

Figure 2.8 (**a**) Mass spectrum of $[O_2N_2^{t\text{-Bu,Me}}]GdN(SiMe_3)_2$; (**b**) mass spectrum of $[O_2N_2^{t\text{-Bu}}]HoN(SiMe_3)_2$. Dotted line indicates expected position of the molecular ions.

References for Chapter 2 begin on page 77

2.4.3 Analysis of The Crude Reaction Mixtures

The abbreviation **N″** is used in this study to represent bis(trimethylsilyl)amide [$N(SiMe_3)_2$] for the assignment of peaks in the MS spectra. The spectrum of the free ligand ([$O_2N_2^{t\text{-Bu,Me}}$]H_2 (**2.2**)) and the spectrum resulting from the MALDI analysis of the complexation reaction between Gd{$N(SiMe_3)_2$}$_3$ (**2.13b**) with [$O_2N_2^{t\text{-Bu,Me}}$]H_2 (**2.2**) are shown in **Figure 2.9** (**a**) and (**b**) respectively. It should be noted that the lanthanide amide reagents *e.g.* Gd{$N(SiMe_3)_2$}$_3$ (**2.13b**) alone did not give interpretable spectra due to their volatility under the mass spectrometric conditions. The spectra of free ligand in all the examples studied showed a single intense peak at *m/z* corresponding to the molecular masses of the various ligands. For example, in the case of spectrum **Figure 2.9** (**a**) the intense single peak at *m/z* 440 corresponds exactly to the molecular masses of [$O_2N_2^{t\text{-Bu,Me}}$]H_2 (**2.2**). In comparison, the mass spectra obtained from the reaction mixtures contained several peaks. For example, **Figure 2.9** (**b**) contains three major peaks at *m/z* 597, 630, 684, which were assigned respectively to [($O_2N_2^{t\text{-Bu,Me}}$)GdN″ - $SiMe_3$ – *t*-Bu – 2Me]$^+$, [($O_2N_2^{t\text{-Bu,Me}}$)GdN″– 2 *t*-Bu – Me]$^+$ and [($O_2N_2^{t\text{-Bu,Me}}$)GdN″ – $SiMe_3$]$^+$. As can be seen clearly from the spectrum, molecular ion peaks were not observed. However, as in other spectra, peaks could be assigned to loss of either methyl, $SiMe_3$ or $N(SiMe_3)$ groups. For all the reaction mixtures studied, the spectra showed that the ligands coordinated to the metal centers and the presence of [$(O_2N_2)Ln$]$^+$ or [$(O_2NN')Ln$]$^+$ fragments.

References for Chapter 2 begin on page 77

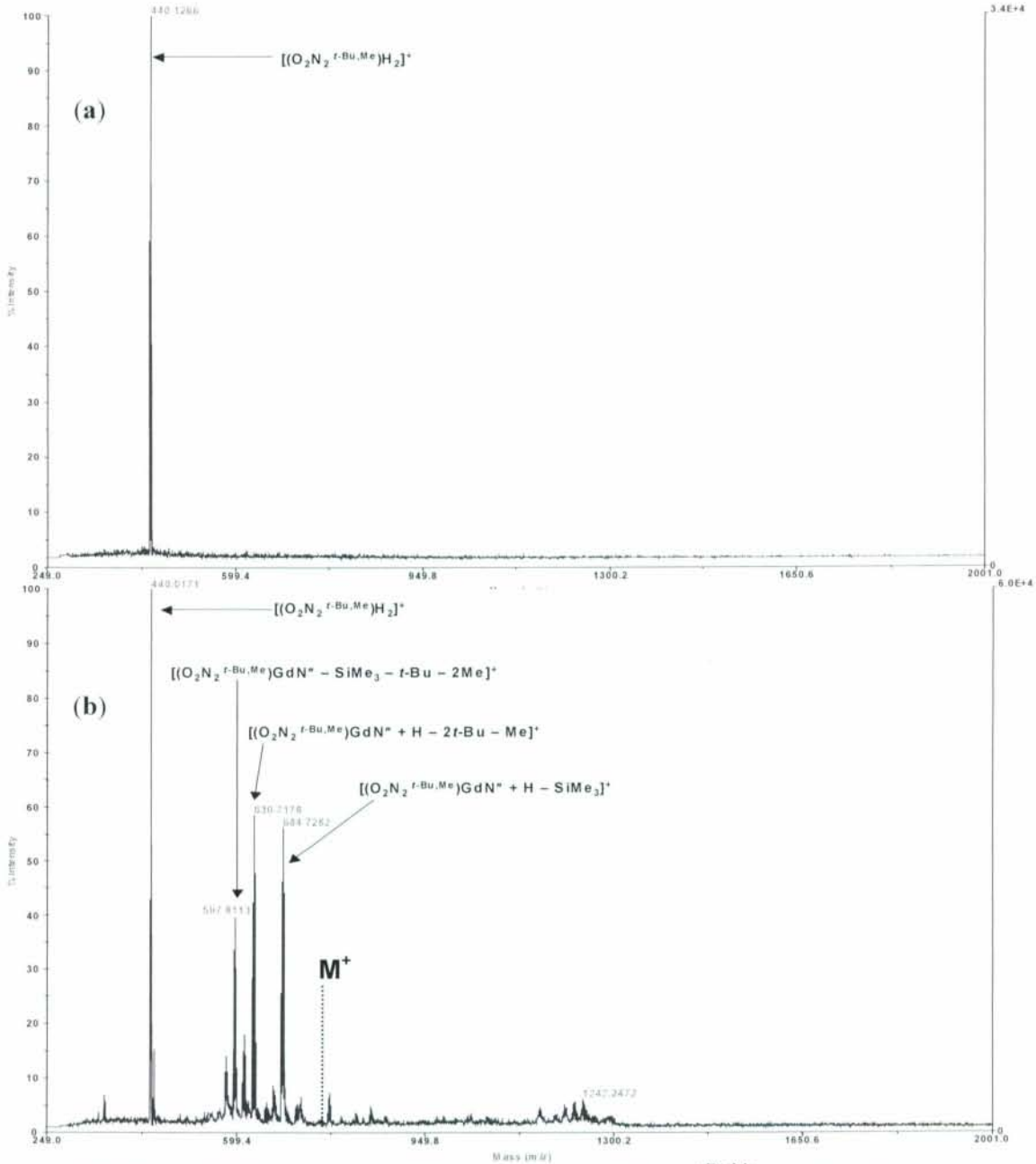

Figure 2.9 Comparison of mass spectra of (**a**) free $[O_2N_2{}^{t\text{-Bu,Me}}]H_2$ (**2.2**) and (**b**) reaction mixture containing $Gd(N'')_3$ and $[O_2N_2{}^{t\text{-Bu,Me}}]H_2$.

References for Chapter 2 begin on page 77

Also, as observed in the spectra of the isolated complexes, all the spectra of the crude reaction mixtures studied indicate the presence of higher mass peaks (m/z >900). The reaction of $Yb\{N(SiMe_3)_2\}_3$ with $[O_2NN'^{t\text{-}Am}]H_2$, **Figure 2.10** clearly shows the higher mass peaks at m/z 1032 and1089.

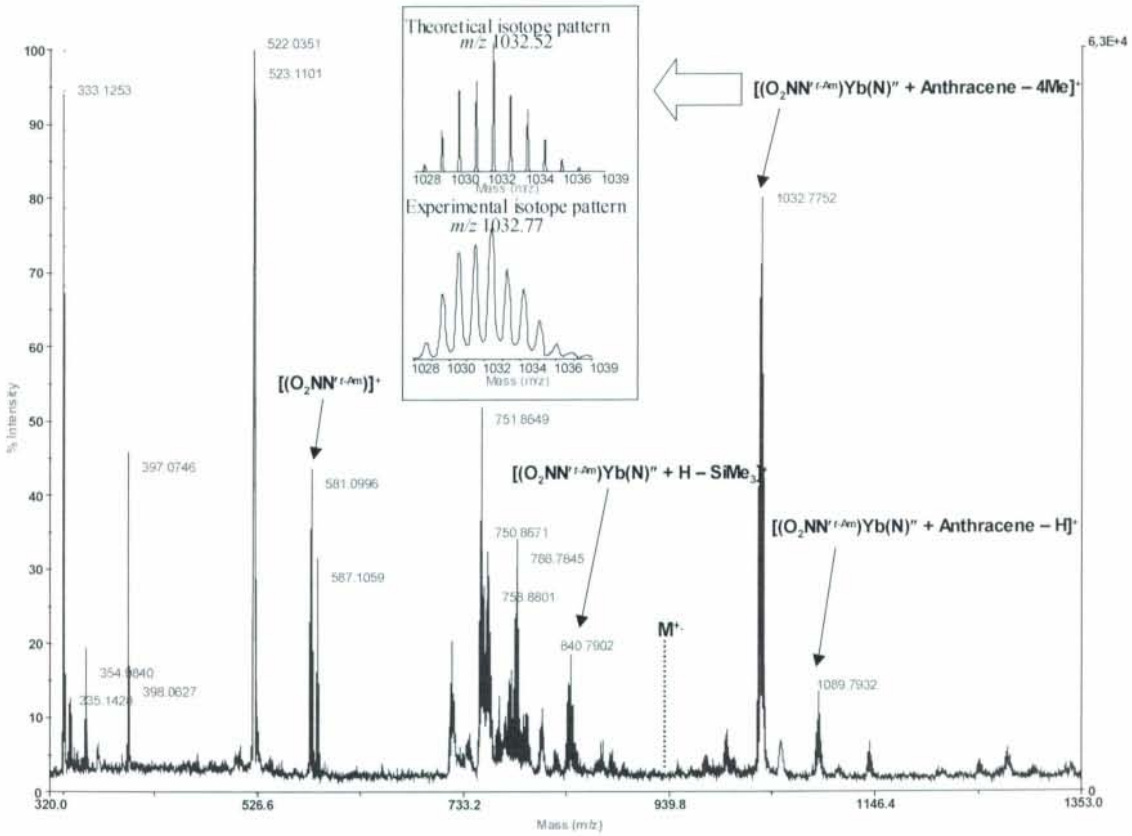

Figure 2.10 Mass spectrum of reaction mixture containing $Yb(N'')_3$ and $[O_2NN'^{t\text{-}Am}]H_2$, inset includes isotope patterns for the fragment $[(O_2NN'^{tAm})Yb\ N'' + C_{14}H_{10} - 4Me]^+$; theoretical (*top*) and experimental (*bottom*).

These high mass peaks were attributed to monomeric and dimeric arene complexes. Evaluations of the isotopic distributions labeled in the inset (**Figure 2.10**) showed that the theoretical (top) and the observed values were in good agreement. **Table 2.2** shows the

References for Chapter 2 begin on page 77

assignment of some arene adducts detected by the MALDI-TOF MS during our study. MALDI-TOF mass spectra of other complexes are shown in **Appendix 2.7.1-2.7.20**

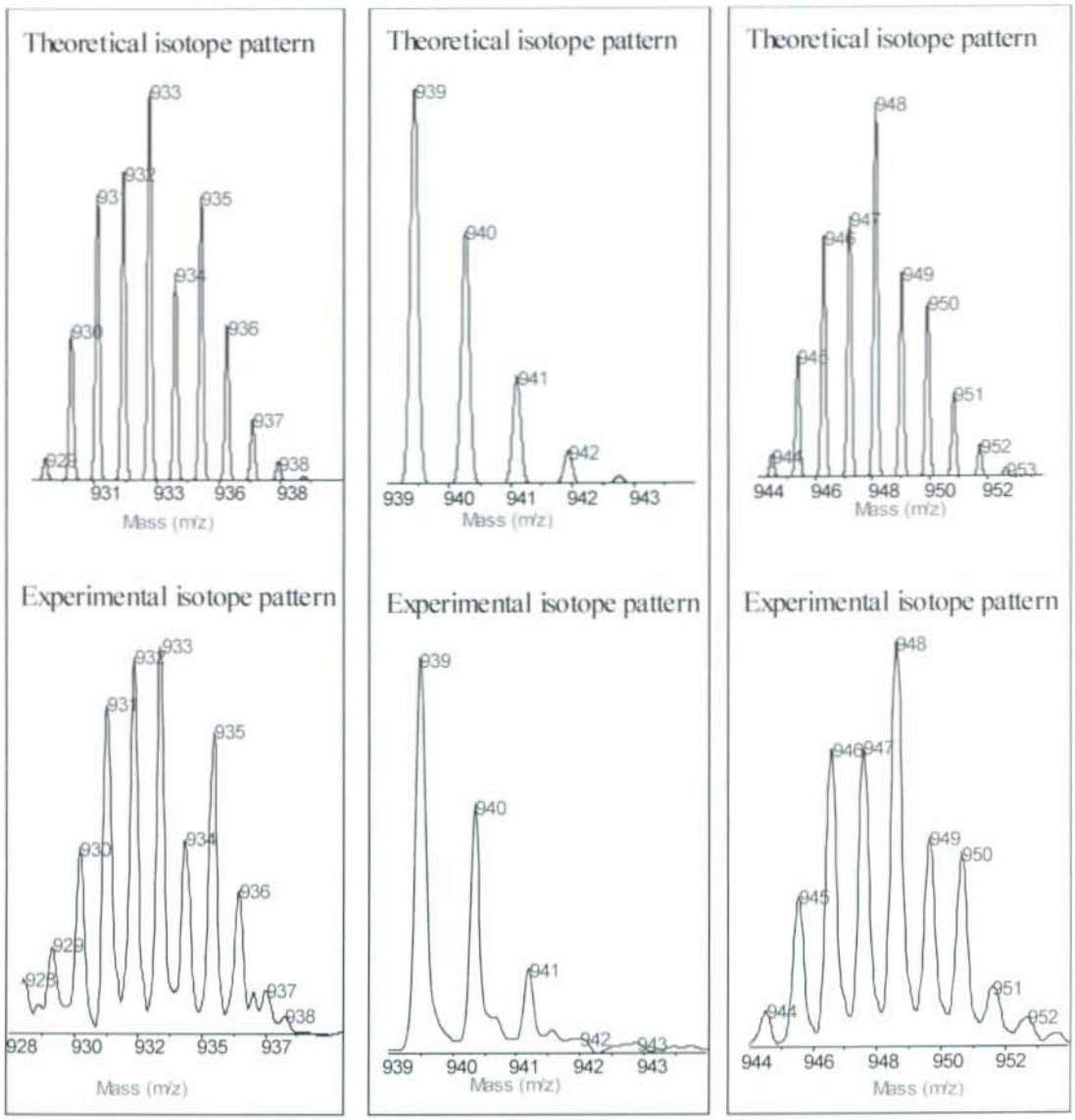

Figure 2.11 Theoretical and experimental isotope patterns of toluene adduct peaks (a) $[(O_2N_2^{t\text{-}Bu,Me})GdN'' + \text{toluene}]^+$ (b) $[(O_2NN'^{t\text{-}Bu})HoN'' + \text{toluene}]^+$ and (c)$[(O_2NN'^{t\text{-}Bu})YbN'' + \text{toluene}]^+$.

References for Chapter 2 begin on page 77

Table 2.2 Lanthanide-arene adducts detected by MALDI-TOF MS

Ln	Ligand	*m/z*	Assignment
Gd	$[O_2N_2^{t\text{-Bu,Me}}]^{2-}$	1298	$[\{(O_2N_2^{t\text{-Bu,Me}})Gd\}_2$ + anthracene – *t*-Bu - Me$]^+$
Gd	$[O_2N_2^{t\text{-Bu,Me}}]^{2-}$	1242	$[\{(O_2N_2^{t\text{-Bu,Me}})Gd\}_2$ + anthracene – 2 *t*-Bu - Me$]^+$
Gd	$[O_2NN'^{t\text{-Bu}}]^{2-}$	932	$[(O_2NN'^{t\text{-Bu}})GdN''$ + toluene$]^+$
Gd	$[O_2NN'^{t\text{-Am}}]^{2-}$	1220	$[\{(O_2NN'^{t\text{-Am}})Gd\}_2$+ anthracene - 6 *t*-Am - 2H$]^+$
Ho	$[O_2NN'^{t\text{-Am}}]^{2-}$	1233	$[\{(O_2NN'^{t\text{-Am}})Ho\}_2$ + anthracene - 6 *t*-Am$]^+$
Ho	$[O_2NN'^{t\text{-Bu}}]^{2-}$	940	$[(O_2NN'^{t\text{-Bu}})HoN''$ + toluene$]^+$
Yb	$[O_2NN'^{t\text{-Bu}}]^{2-}$	948	$[(O_2NN'^{t\text{-Bu}})YbN''$ + toluene$]^+$
Yb	$[O_2NN'^{t\text{-Am}}]^{2-}$	1089	$[(O_2NN'^{t\text{-Am}})YbN''$ + anthracene - H$]^+$

MALDI-TOF MS ionization mechanisms for characterization of polar organic and bioorganic molecules, have been predominantly proton-transfer between the analyte and acidic organic matrix.[19] On the other hand, Limbach and co-workers reported a charge-transfer ionization mechanism with the use of non-polar matrices for the characterization of a series of transition metal complexes.[20] Charge-transfer occurs in the gas-phase when photoabstraction of an electron from the matrix generates a radical cation, which

References for Chapter 2 begin on page 77

subsequently becomes involved in a charge-transfer reaction with the desorbed analyte as shown in **Scheme 2.1**.[15,20]

However, in our study, the exact matches of the theoretical and the experimental isotope patterns of the higher mass peaks (**Figure 2.10** and **Figure 2.11**) facilitated assignment of peaks (**Table 2.1**) and suggest that the ionization occurred through adduct formation. Probably toluene that co-crystallized with the sample during preparation has become associated with the coordinatively unsaturated lanthanide metal center during the mass spectrometric analysis. This observation was consistent with the studies of Fogg and co-workers, in which matrix-adduct formation was observed in the spectra of coordinatively unsaturated two-coordinate Pd and Au complexes.[15] Also, in 1998, O'Hair *et al.*[21] demonstrated that coordinatively unsaturated metal complexes in electrospray ionization experiments react with neutral reagents (aminoacids and peptides) in the gas phase to also form adducts.

As pointed out in the preceding Chapter, large lanthanide metal centers have a tendency to form complexes with high-coordination numbers (6 to 12). Therefore it is not surprising that adducts are seen in all our spectra. In the solid-state related lanthanide complexes typically coordinate a Lewis basic solvent *e.g.* THF or DME to form 6- or 7-coordinate monomeric species.[5,7]

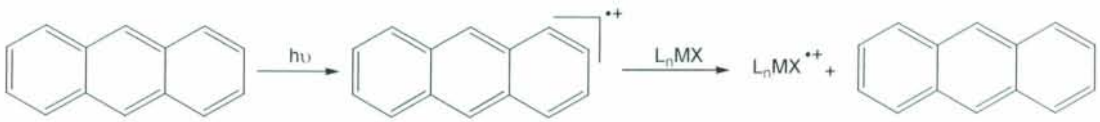

Scheme 2.1 Ionization by charge-transfer in MALDI-TOF mass spectrometry with arene matrices.

References for Chapter 2 begin on page 77

The dimeric metal species containing anthracene formed in the spectrometer probably possess structures similar the complexes isolated by Fryzuk *et al.*,[22] in which the isolable species were supported with amido-phosphine ligands, $[\{(^{t}P_2N_2^{t})Ln\}_2(\mu\text{-}C_{14}H_{10})]$ and $[\{(^{t}P_2N_2^{t})Ln\}_2(\mu\text{-}C_{12}H_{10})]$. These unusual structurally authenticated Ln-arene complexes consist of Ln^{3+} metal centers coordinated to a dianionic tetradentate mixed-donor ligand with the third anionic ligand being a bridging delocalized anthracene or biphenyl dianion. Our hypothesis, as shown in **Scheme 2.2** is that in our study, $[Ln(O_2N_2)]^+$ species formed *in situ*, react within the spectrometer with gaseous anthracene to yield similar $[\{(O_2N_2)Ln\}_2(\mu\text{-}C_{14}H_{10})]^+$ species *i.e.* the $[Ln(O_2N_2)]^+$ scavenges neutral gas-phase anthracene molecules and this results in the appearance of a range of high *m/z* peaks in our experiments.

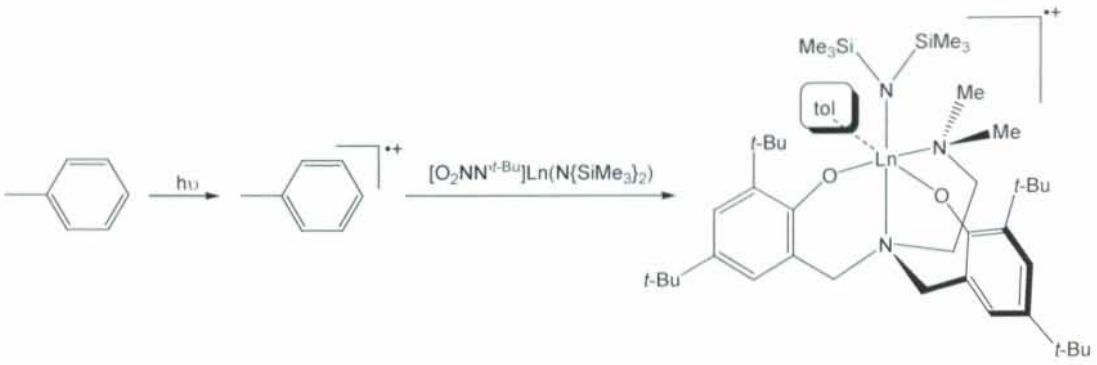

Scheme 2.2 Proposed ionization by adduct formation in MALDI-TOF MS of Lanthanide complexes with arene matrices or solvents, tol = toluene.

References for Chapter 2 begin on page 77

2.5 Summary

In this study, it has been demonstrated that MALDI-TOF MS can be used for rapid screening of the reactions of moisture-sensitive lanthanide species. The preliminary reactions can be carried out on a sub-50 mM scale, thereby reducing consumption of reagents. In addition, the MALDI-TOF MS technique has been shown by others to support high-throughput methods and therefore, as this preliminary investigation shows, libraries of lanthanide compound can be screened, making it possible to reduce the overall time of analysis. Additionally, there was very good agreement between the experimental and theoretical isotope patterns. This demonstrated that the technique permits the rapid confirmation of the coordination of amine bis(phenolate) ligands to the lanthanide metal centers, which cannot be obtained with NMR spectroscopy due to the paramagnetic nature of most of the lanthanide metal ions. *e.g.* Gd^{3+}, Ho^{3+}. The fragmentation ions observed could be correlated to known ablation processes inside the MALDI instrument. It was also observed that arene adducts are formed *in situ* during the mass spectrometric experiment, presumably due to electron scrambling between the anthracene and analyte, or between analyte and toluene. It is therefore believed that polyaromatic hydrocarbons affect the results obtained in MALDI-TOF analysis with metals that are extremely coordinatively unsaturated as shown in this study and by Fogg *et al.*

References for Chapter 2 begin on page 77

2.6 Experimental Section

2.6.1 Materials

Chemical reagents were purchased from Aldrich, Alfa Aesar, Lancaster and Strem. Solvents (toluene, diethyl ether, THF, hexane) were dried over sodium or sodium-benzophenone and distilled under nitrogen. Anthracene was purified by recrystallization from hexane solution, which was dried over anhydrous $MgSO_4$. Ligands and lanthanide reagents were prepared using standard literature procedures. [10,11]

2.6.2 Methods

All reactions were performed under an inert atmosphere using standard Schlenk line procedures, or in a glove box, with O_2 and H_2O levels below 5 ppm.

2.6.3 Instruments

^{1}H NMR spectra were recorded on a Bruker Avance 500 MHz spectrometer at 298 K and were referenced internally using the residual proton resonances of the solvent. Data are reported as follows: Chemical shift, multiplicity (s = singlet, d = doublet, dd = doublet of doublets, t = triplets, br = broad, m = multiplet), coupling constant (*J*, Hz), integration and assignment. ^{1}H NMR spectra were processed using MestReNova software.

Elemental analyses were performed by Guelph Chemical Laboratories Ltd., Guelph, ON, Canada.

The MALDI-TOF mass spectra were acquired using a Voyager-DE RP Biospectrometry workstation (Applied Biosystems, Toronto, Canada) that uses a pulsed nitrogen laser (337 nm). The spectra were obtained in reflectron positive mode at 20 kV

References for Chapter 2 begin on page 77

accelerating voltage with delay ion extraction set to 145 ns and accumulating 50 shots for each spectrum. The instrument has a monoisotopic resolution of 10,000.

2.6.4 MALDI Sample Preparation

A solution of the anthracene matrix was prepared by dissolving 10 mg of anthracene in 1.00 mL of toluene. A 10 mg/mL solution of $Gd\{N(SiMe_3)_2\}_3$ was obtained by dissolving $Gd\{N(SiMe_3)_2\}_3$ (5.0 mg, 7.8 μmol) in toluene (500 μL). A 10 mg/mL solution of $[O_2N_2^{t\text{-Bu,Me}}]H_2$ was obtained by dissolving $[O_2N_2^{t\text{-Bu,Me}}]H_2$ (2.20 mg, 5.0 μmol) in toluene (220 μL). 200 μL of the gadolinium amide solution and 200 μL of the $[O_2N_2^{t\text{-Bu,Me}}]H_2$ solution were mixed (1:1 v/v) in a vial and stirred for 18 h. 50 μL of the gadolinium amide and $[O_2N_2^{t\text{-Bu,Me}}]H_2$ mixture was added to 50 μL of the anthracene solution (1:1 v/v) and the mixture was stirred for a further 2 minutes. Approximately 1 μL of the resulting solution was applied on the plate (10 × 10 letter/number grid) and allowed to dry. At the same time, alongside the samples of reaction mixture, 1 μL of the original 10 mg/mL solution of $[O_2N_2^{t\text{-Bu,Me}}]H_2$ also mixed with the matrix and was spotted on another space on the plate and allowed to dry. All MALDI samples were prepared in similar manner.

2.6.5 Drying of Amine Bis(phenolate) Ligands

2.6.5.1 $[O_2N_2^{t\text{-Bu,Me}}]H_2$ (2.2)

An Erlenmeyer flask was charged with $[O_2N_2^{t\text{-Bu,Me}}]H_2$ (3.00 g, 6.8 mmol). THF (20.0 mL) was added to the Erlenmeyer flask. $MgSO_4$ was added to the THF solution of $[O_2N_2^{t\text{-Bu,Me}}]H_2$, giving a white suspension. The mixture was covered with parafilm and

References for Chapter 2 begin on page 77

allowed to settle for 18 h. Using filter paper, the resulting solution was filtered into a Schlenk tube and removal of the solvent under vacuum afforded dry $[O_2N_2^{t\text{-}Bu,Me}]H_2$ as a white crystalline solid .

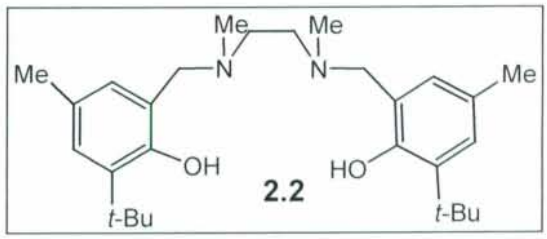

2.2

^{1}H NMR (500 MHz, $CDCl_3$): δ 10.75 (s, 2H, O*H*); 7.27 (d, 2H, $^4J_{HH}$ = 1.8 Hz, Ar*H*); 6.64 (d, 2H, $^4J_{HH}$ = 1.8 Hz, Ar*H*); 3.30 (s, 4H, Ar-CH_2-N); 2.33 (s, 6H, NCH_3); 2.18 (s, 4H, N-C_2H_4-N); 1.86 (s, 6H, CCH_3); 1.75 (S, 18H, C$(CH_3)_3$). Other ligands were dried using the same procedure.

2.6.5.2 $[O_2N_2^{t\text{-}Bu}]H_2$ (2.3)

^{1}H NMR (500 MHz, $CDCl_3$): δ 10.87 (s, 2H, O*H*); 7.59 (d, 2H, $^4J_{HH}$ = 2.4 Hz, Ar*H*); 6.96 (d, 2H, $^4J_{HH}$ = 2.4 Hz, Ar*H*); 3.34(s, 4H, Ar-CH_2-N); 2.20 (s, 4H, N-C_2H_4-N); 1.86 (s, 6H, NCH_3); 1.79 (S, 18H, C$(CH_3)_3$); 1.44 (s, 18H, C$(CH_3)_3$).

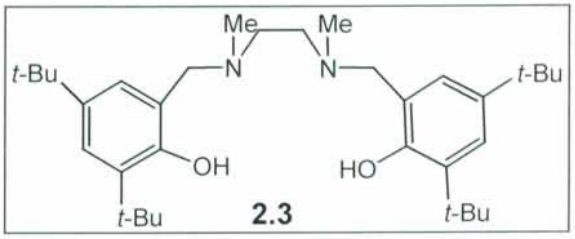

2.3

2.6.5.3 $[O_2NN'^{t\text{-}Bu}]H_2$ (2.4)

^{1}H NMR (500 MHz, $CDCL_3$): δ 9.78 (s, 2H, O*H*); 7.16 (d, 2H, $^4J_{HH}$ = 2.4 Hz, Ar*H*); 6.84 (d, 2H, $^4J_{HH}$ = 2.4 Hz, Ar*H*); 3.57 (s, 4H, Ar-CH_2-N); 2.64 (br, 4H, N-C_2H_4-N); 2.29 (s, 6H, N$(CH_3)_2$); 1.36 (s, 18H, 2C$(CH_3)_3$); 1.24 (s, 18H, 2C$(CH_3)_3$).

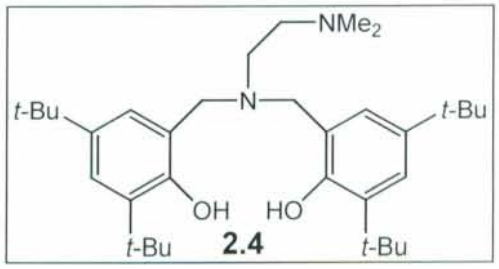

2.4

2.6.5.4 $[O_2NN^{t\text{-}Am}]H_2$ (2.5)

^{1}H NMR (500 MHz, $CDCl_3$): δ (s, 2H, O*H*); 7.44 (d, 2H, $^4J_{HH}$ = 2.4 Hz, Ar*H*); 7.03 (d, 2H, $^4J_{HH}$ = 2.4 Hz, Ar*H*); 3.51 (s, 4H, Ar-CH_2-N); 2.29 (q, 4H, $^3J_{HH}$ = 7.4 Hz, CH_2CH_3); 2.02 (s, 6H, N(CH_3)$_2$); 1.72 (q, 4H, $^3J_{HH}$ = 7.4 Hz, 2CCH_2CH$_3$); 1.68 (s, 12H, 2C(CH_3)$_2$); 1.39 (s, 12H, 2C(CH_3)$_2$); 0.95 (t, 6H, $^3J_{HH}$ = 7.4 Hz, CH_2CH_3); 0.82 (t, 6H, $^3J_{HH}$ = 7.4 Hz, CH_2CH_3)

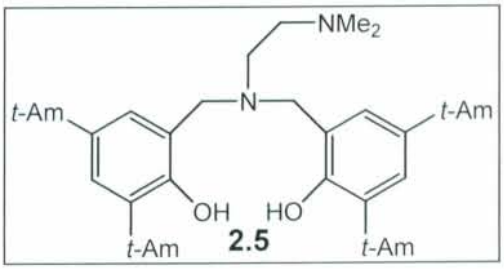

2.5

2.7 Synthesis

2.7.1 Syntheses of Lithium Bis(trimethylsilyl)Amide[Li{N(SiMe$_3$)$_2$}] (2.8)

A 500 mL reaction vessel was cycled on a Schlenk line and charged hexamethyldisilazane (6.46 g, 40.0 mmol, 8.3 mL) (**2.7**). Diethyl ether (60.0 mL) was transferred into the reaction vessel and the resulting solution was cooled to 0 °C. *n*-butyllithium (2.56 g, 40.0 mmol, 25 mL) (**2.6**) was added dropwise to the cooled solution. The resulting yellow reaction mixture was allowed to warm to room temperature and stirred for 18 h under nitrogen. The solvent was removed under vacuum to afford a yellow solid. Impurities were removed by washing the yellow solid with hexane (2 × 30 mL) cooled to 0 °C. The solvent was removed by filtration and the ensuing solid was dried under vacuum leaving a white powdery product (5.94 g, 89% yield).

^{1}H NMR (500 MHz, C_6D_6): δ 3.33 (q, 4H, $^3J_{HH}$ = 7.0 Hz, Et_2O); 1.02 (t, 6H, $^3J_{HH}$ = 7.0 Hz, Et_2O); 0.24 (s, 18H, SiMe$_3$)

References for Chapter 2 begin on page 77

2.7.2 Drying of Lanthanide Trichloride Hexahydrate [Ln(III)Cl_3·$6H_2O$]

A Schlenk tube was charged with gadolinium (III) chloride hexahydrate (15.00 g, 40.3 mmol), a stir bar and THF (60.0 mL). Another Schlenk tube was charged with trimethylsilyl chloride (87.56 g, 806 mmol, 103.0 mL). Both Schlenk tubes were cycled on the Schlenk line. Using a cannula, the trimethylsilyl chloride was added slowly to the gadolinium chloride suspension and the mixture stirred at room temperature for 18 h. The mixture was filtered and the resulting white solid dried *in vacuo* giving a white powdery solid (14.5 g, 71% yield). Employing the above procedure the trichloride hexahydrate of other lanthanides were dried as shown in **Table 2.2** below: **Ln** = Gd = **2.12a** Ho = **2.12b,** Sm = **2.12c,** La, = **2.12d,** Y = **2.12e**, Yb = **2.12f**

Table 2.3 Data for drying of lanthanide (III) chloride hexahydrates.

Ln	Starting materials					Products		
	$LnCl_3·6H_2O$		Me_3SiCl			$LnCl_3(THF)_x$		
	Mass (g)	mole (mmol)	Mass (g)	mole (mmol)	Vol. (mL)	Colour	Mass (g)	% yield
2.12a	15.0	40.3	87.56	806.0	103.0	White	14.75	71
2.12b	10.0	26.4	57.36	528.0	67.5	Pink	13.83	87
2.12c	10.0	27.4	59.56	548.0	70.1	Pale Yellow	9.00	65
2.12d	10.0	28.0	61.49	566.0	72.3	White	9.36	63
2.12e	10.0	49.4	107.40	988.9	126.4	Yellow	12.45	83
2.12f	10.0	25.8	56.07	67.0	67.0	Yellow	10.00	78

References for Chapter 2 begin on page 77

2.7.3 Synthesis of Tris(trimethylsilyl) Amide[Ln{N(SiMe$_3$)$_2$}$_3$]

2.7.3.1 [Ho{N(SiMe$_3$)$_2$}$_3$] (2.13a)

Holmium trichloride, [$HoCl_3(THF)_{3.5}$] (**2.12b**) (5.01 g, 9.6 mmol) was weighed into a Schlenk tube. Another Schlenk tube was charged with lithium bis(trimethylsilyl) amide, [Li{$N(SiMe_3)_2$}] (**2.8**) (6.39 g, 28.7 mmol, 3 equiv). The Schlenk tubes were cycled on a Schlenk line, and THF (60 mL) pre-cooled to 0 °C was added to the Schlenk tube containing lithium bis(trimethylsilyl) amide. The solution was transferred slowly using cannula to the Schlenk tube containing holmium trichloride cooled to 0 °C. The reaction mixture was stirred for 4 h and gradually warmed to room temperature. The mixture was stirred for an additional 18 h. The solvent was removed under vacuum, the residue was extracted with diethyl ether (60 mL) and the mixture was filtered using a cannula into another Schlenk tube, leaving lithium chloride (white solid) behind. Diethyl ether was removed under vacuum affording a dry pale pink crystalline solid (6.75 g, 89% yield).

The ^{1}H NMR (500 MHz, C_6D_6), spectrum was extremely broad due to the paramagnetic nature of the compound. As a result, meaningful interpretation was not possible. Following the same procedure all other lanthanide tris(trimethylsilyl) amides were obtained in good yields

References for Chapter 2 begin on page 77

2.7.3.2 [Gd{N(SiMe$_3$)$_2$}$_3$] (2.13b)

[GdCl$_3$(THF)$_{3.5}$] (**2.12a**) (5.00 g, 9.7 mmol) and [Li{N(SiMe$_3$)$_2$}](**2.8**) (6.49 g, 29.1 mmol, 3 equiv) in THF (60 mL) afforded a white crystalline solid (3.96 g, 52% yield). ^{1}H NMR (500 MHz, C_6D_6), spectrum was extremely broad due to the paramagnetic nature of the compound. As a result meaningful interpretation was not possible.

2.7.3.3 [Yb{N(SiMe$_3$)$_2$}$_3$] (2.13c)

[YbCl$_3$(THF)$_3$] (**2.12f**) (3.54 g, 7.1 mmol) and [Li{N(SiMe$_3$)$_2$}](**2.8**) (4.78 g, 21.4 mmol, 3 equiv) in THF (60 mL) afforded a pale yellow crystalline solid (4.17 g, 67% yield). ^{1}H NMR (500 MHz, C_6D_6), spectrum was extremely broad due to the paramagnetic nature of the compound. As a result meaningful interpretation was not possible

2.7.3.4 [Sm{N(SiMe$_3$)$_2$}$_3$] (2.13d)

[SmCl$_3$(THF)$_{3.5}$] (**2.12c**) (5.00 g, 9.8 mmol) and [Li{N(SiMe$_3$)$_2$}](**2.8**) (6.57 g, 29.5 mmol, 3 equiv) in THF (60 mL) afforded a pale yellow crystalline solid. (8.84 g, 92% yield). ^{1}H NMR (500 MHz, C_6D_6), spectrum is paramagnetically broadened

2.7.3.5 [La{N(SiMe$_3$)$_2$}$_3$] (2.13e)

[LaCl$_3$(THF)$_4$] (**2.12d**) (2.67 g, 5.0 mmol) and [Li{N(SiMe$_3$)$_2$}](**43**) (3.76 g, 16.0 mmol, 3 equiv) in THF (60 mL) gave a pale yellow crystalline solid (1.80 g, 43% yield).

^{1}H NMR (500 MHz, C_6D_6): δ 3.66 (br, 4H,THF), 1.29 (br, 4H, THF), 0.36 (s, 54H, SiMe$_3$).

References for Chapter 2 begin on page 77

2.7.3.6 [Y{N(SiMe$_3$)$_2$}$_3$] (2.13f)

[YCl$_3$(THF)$_3$] (**2.12e**) (2.00 g, 8.0 mmol) and [Li{N(SiMe$_3$)$_2$}](**2.8**) (1.15 g, 2.8 mmol, 3 equiv) in THF (60 mL) afforded a pale yellow crystalline solid (1.76 g, 80% yield).

^{1}H NMR (500 MHz, C_6D_6): δ 3.63 (t, 4H, J = 6.4Hz, THF), 1.35 – 1.21 (m, 4H, THF), 0.37 (s, 54H, SiMe$_3$)

2.7.4 Synthesis of Lanthanide Amine Bis(phenolate) Complexes

2.7.4.1 [O$_2$N$_2$$^{t\text{-Bu}}$]Ho{N(SiMe$_3$)$_2$} (2.14a$_{2.3}$)

Ho{N(SiMe$_3$)$_2$}$_3$ (2.77 g, 3.5 mmol) was weighed into a Schlenk tube equipped with a stir bar and toluene (30 mL) was added. To this suspension was added a toluene solution (25 mL) of [O$_2$N$_2$$^{t\text{-Bu}}$]H$_2$ (1.84 g, 3.5 mmol) at –78 °C. The resulting mixture was stirred for 18 h at room temperature. The solvent was removed under vacuum and the resulting solid was washed was with pentane (2 × 15 mL) at 0 °C. A pale pink solid, [O$_2$N$_2$$^{t\text{-Bu}}$]Ho{N(SiMe$_3$)$_2$}, was obtained (2.77 g, 93%). Anal. Calcd for [C$_{40}$H$_{72}$HoN$_3$O$_2$Si$_2$]: C, 56.65; H, 8.56; N, 4.95. Found: C, 56.41; H, 8.47; N, 4.75. MALDI-TOF MS (anthracene matrix): *m/z* (peak identified): 697 ([(O$_2$N$_2$$^{t\text{-Bu}}$)Ho]$^+$). The same procedure was used to prepare 3 other complexes on a ~ 3mmol scale. However, it should be noted that many more complexes were prepared on an analytical scale for MS analysis.

2.7.4.2 [O$_2$N$_2$$^{t\text{-Bu,Me}}$]Gd{N(SiMe$_3$)$_2$} (2.14b$_{2.2}$)

Gd{N(SiMe$_3$)$_2$}$_3$ (2.74 g, 3.5 mmol) and [O$_2$N$_2$$^{t\text{-Bu,Me}}$]H$_2$ (1.54 g, 3.5 mmol) afforded [O$_2$N$_2$$^{t\text{-Bu,Me}}$]Gd{N(SiMe$_3$)$_2$} (2.40 g, 91%). Anal. Calcd for C$_{34}$H$_{60}$GdN$_3$O$_2$Si$_2$:

C, 54.00; H, 8.00; N, 5.56. Found: C, 53.92; H, 7.93; N, 5.68: MALDI-TOF MS (anthracene matrix): *m/z* (peak identified): 596 ([$(O_2N_2{}^{t\text{-}Bu,Me})$Gd]$^+$)

2.7.4.3 [$O_2NN'^{t\text{-}Bu}$]Yb{$N(SiMe_3)_2$} (2.14c$_{2.4}$)

Yb{$N(SiMe_3)_2$}$_3$ (2.68 g, 3.1 mmol) and [$O_2NN'^{t\text{-}Bu}$]H_2 (1.62 g, 3.1 mmol) afforded [$O_2NN'^{t\text{-}Bu}$]Yb{$N(SiMe_3)_2$} (1.45 g, 54%). Anal. Calcd for $C_{40}H_{72}N_3O_2Si_2Yb$: C, 56.11; H, 8.48; N, 4.91. Found: C, 56.02; H, 8.37; N, 4.47; MALDI-TOF MS (anthracene matrix): *m/z* (peak identified): 696 ([$O_2NN'^{t\text{-}Bu}$]Yb]$^+$), 731 ([$O_2NN'^{t\text{-}Bu}$]YbN″ + H – 2 *t*-Bu – Me]$^+$), 949 ([$O_2NN'^{t\text{-}Bu}$]YbN″ + toluene]$^+$), 1006 ([$O_2NN'^{t\text{-}Bu}$]YbN″ + Anthracene – 2Me]$^+$), 1166 ({[$O_2NN'^{t\text{-}Bu}$]YbN″}$_2$ – 4 *t*-Bu – 2 N$(SiMe_3)_2$]$^+$.

2.7.4.4 [$O_2NN'^{t\text{-}Am}$]Ho{$N(SiMe_3)_2$} (2.14a$_{2.5}$)

Ho{$N(SiMe_3)_2$}$_3$ (2.60 g, 3.3 mmol) and [$O_2NN'^{t\text{-}Am}$] (1.91 g, 3.3 mmol) afforded [$O_2NN'^{t\text{-}Am}$]Ho{$N(SiMe_3)_2$} (0.52 g, 17%). Anal. Calcd for $C_{44}H_{80}HoN_3O_2Si_2$: C, 58.44; H, 8.92; N, 4.65. Found: C, 58.76; H, 8.66; N, 4.31; MALDI-TOF MS (anthracene matrix): *m/z* (peak identified): 743 ([$(O_2NN'^{t\text{-}Am})$Ho]$^+$), 778 ([$(O_2NN'^{t\text{-}Am})$HoN″ + H – *t*-Am – 4 Me]$^+$), 1024([$(O_2NN'^{t\text{-}Am})$HoN″ + anthracene – 4 Me]$^+$), 1081([$(O_2NN'^{t\text{-}Am})$HoN″ + anthracene – H]$^+$), 1233 ([{$(O_2NN'^{t\text{-}Am})$HoN″}$_2$ – 3 *t*-Am – 2 N$(SiMe_3)_2$ – 3 Me + H]$^+$).

2.8 References:

1. Piers, W. E.; Emslie, D. J. H. *Coord. Chem. Rev.* **2002**, *233-234*, 131.
2. (a) Tshuva, E. Y.; Goldberg, I.; Kol, M. *Organometallics*, **2001**, *20*, 3017; (b) Groysman, S.; Sergeeva, E.; Goldberg, I.; Kol, M. *Inorg. Chem.*, **2005**, *44*, 8188.
3. Kerton, F. M.; Holloway, S.; Power, A.; Soper, R. G.; Sherdan, K.; Lynam, J. M.; Whitewood, A. C.; Willans, C. *Can. J. Chem.*, **2008**, *85*, 435.
4. Kerton, F. M.; Whitwood, A. C.; Willans, C. E. *Dalton Trans.*, **2004**, 2237.
5. Amgoune, A.; Thomas, C. M.; Roisnel, T.; Carpentier, J. *Chem. Eur., J.* **2006**, *12*, 169.
6. Yao, Y.; Ma, M.; Xu, X.; Zhang, Y.; Shen, Q.; Wong, W. *Organometallics* **2005**, *24*, 4014.
7. Dyer,H. E.; Huijser, S; Schwarz, A. D.; Wang, C.; Duchateau, R.; Mountford, P. *Dalton Trans.*, **2008**, 32.
8. Gribkov, D. V.; Hampel, F.; and Hultzsch, K. C. *Eur. J. Inorg. Chem.*, **2004**, 4091
9. (a) Emslie, D. J. H.; Piers, W. E.; MacDonald, R. *J. Chem. Soc., Dalton Trans.*, **2002**, 293; (b) Riegert, D.; Collin, J.; Meddour, A.; Schulz, E.; Trifonov, A. *J. Org. Chem.*, **2006**, *71*, 2514; (c) Ma, M.; Xu, X.; Yao, Y.; Zhang, Y.; Shen, Q. *J. Mol. Struct.*, **2005**, *740*, 69.
10. Piers, W. E.; Shapiro, P. J.; Bunel E. E.; Bercaw J. E. *Synlett.*, **1990**, 74.

References for Chapter 2 begin on page 77

11. Bradley, D. C.; Ghotra, J. S.; Hart, F. A. *J. Chem. Soc. Dalton. Trans.*, **1973**, 1021.

12. Hunsucker, S. W.; Watson, R. C.; Tissue, B. M. *Rapid Commun. Mass Spectrom.*, **2001**, *15*, 1334.

13. Lou, X.; van Buijtenen, J.; Bastiaansen, J. J. A. M.; de Waal, B. F. M.; Langeveld, B. M. W.; van Dongen, J. L. J. *J. Mass Spectrom.*, **2005**, *40*, 654.

14. Busch, K. L. *J. Mass Spectrom.*, **1995**, *30*, 233.

15. Eelman, M. D.; Blacquiere, J. M.; Moriarty, M. M.; Fogg, D. E.; *Angew. Chem. Int. Ed.*, **2008**, *47*, 303.

16. Butt, S. M. Honours Thesis, Memorial University of Newfoundland, 2008.

17. Henderson, W.; McIndoe, J. S. *Mass Spectrometry of Inorganic and Organometallic Compounds*; John Wiley & Sons Ltd: Chichester, 2005.

18. Mazzaglia, A.; Scolaro, L. M.; b, Garozzo, D.; Malvagna, P.; Romeo, R. *J. Organomet. Chem.*, **2005**, *690*, 1978.

19. (a) Knochenmuss, R. *Analyst*, **2006**, 131, 966; Knochenmuss, R.; Zenobi, R. *Chem Rev.*, **2003**, *103*, 441; (b) Karas, M.; Kruger, R. *Chem. Rev.*, **2003,** *103*, 427.

20. Macha, S. F.; McCarley, T. D.; Limbach, P. A. *Anal. Chim. Acta.*, **1999**, *397*, 235.

21. Reid, G. E.; O'Hair, R.A. J.; Styles, M. L. W.; McFadyen, D.; Simpson, R. J. *Rapid Commun. Mass Spectrom.*, **1998**, *12*, 1701.

22. Fryzuk, M. D.; Jafarpour, L.; Kerton, F. M.; Love, J. B.; Patrick, B. O.; and Rettig, S. J. *Organometallics* **2001,** *20*, 1387.

References for Chapter 2 begin on page 77

Chapter 3

Organolanthanide-Mediated Hydroamination/cyclization of Aminoalkyne Screened by MALDI-TOF MS

3.1 Introduction

As indicated in Chapter 2, amine bis(phenolate)-based organolanthanide complexes have been utilized widely as highly efficient homogeneous precatalysts for a variety of chemical processes such as polymerization.[1] Hitherto, these complexes had never been used as catalysts for intramolecular hydroamination-cyclization. Therefore, they were selected for our study. With the lanthanide amine bis(phenolate) complexes prepared in Chapter 2 on hand, the attention in this present Chapter will be focused on the preparation of an aminoalkyne substrate, followed by hydroamination reactions to explore the potential of various amine bis(phenolate)complexes as hydroamination catalysts. As well, rapid screening of the reactions using MALDI-TOF mass spectrometry will be presented.

3.2 Preparation of the Aminoalkyne Substrate

The synthesis of 5-phenyl-4-pentyn-1-amine as a substrate for intramolecular hydroamination has been reported,[2] but the chemical yield 22% for the last step of its preparation is rather low. However, the research described in this thesis modified the literature procedure to increase the yield. The procedure for the synthesis of the aminoalkyne substrate involves a three-step approach.

References for Chapter 3 begin on page 111

3.2.1 5-Chloro-1-phenyl-1-pentyne (3.3)

The first step in the synthesis of 5-phenyl-4-pentyn-1-amine (**3.7**) is the preparation of 5-chloro-1-phenyl-1-pentyne, which involves gradual addition of one molar equivalent of lithium phenylacetylide to a THF solution of one molar equivalent of 3-bromo-1-chloropropane, while stirring at 0 °C for 2 h. The reaction mixture was allowed to warm to room temperature and stirred for an additional 6 h (**Eqn. 3.1**). The reaction mixture was poured into deionized water, and formed two layers. The organic and aqueous phases were separated and the water layer was extracted with diethyl ether. The combined ether extract was washed with brine, and dried over anhydrous $MgSO_4$. The resulting mixture was allowed to settle for half an hour and then filtered. Diethyl ether and THF were removed by rotary evaporation and the resulting light brown liquid was distilled under vacuum at 105 °C to give a colourless liquid product (**3.3**) in 61% yield. The ^{1}H NMR analysis was in agreement with the literature.[2]

[3.1]

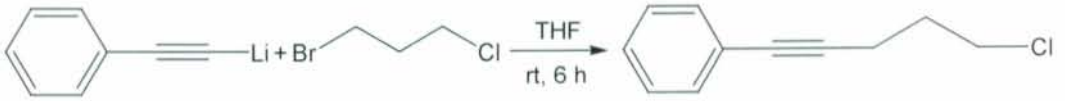

3.1 **3.2** **3.3**

3.2.2 *N*-(5-Phenyl-4-pentynyl)phthalimide (3.5)

The second step includes the addition of *N*-(5-chloro-1-phenyl-1-pentyne) (**3.3**) to a DMF solution of potassium phthalimide (**3.4**). The reaction mixture was heated at reflux 100 °C for 18 h (**Eqn. 3.2**). The resulting yellow/brown reaction mixture was allowed to

References for Chapter 3 begin on page 111

cool to room temperature and then was poured into an equal mixture of trichloromethane and deionized water, which formed two layers. The layers were separated and the water layer was extracted with trichloromethane. The organic and aqueous extracts were combined and washed with aqueous KOH and subsequently, with deionized water to remove unreacted phthalimide. The extract was dried over anhydrous $MgSO_4$ and the resulting mixture was then filtered. The trichloromethane was removed under vacuum, giving a white solid residue, which was triturated with diethyl ether. After collection by filtration, the solid residue was dried at reduced pressure, affording a white crystalline solid (**3.5**) in 74% yield. ^{1}H NMR analysis was consistent with the literature data.[2]

[3.2]

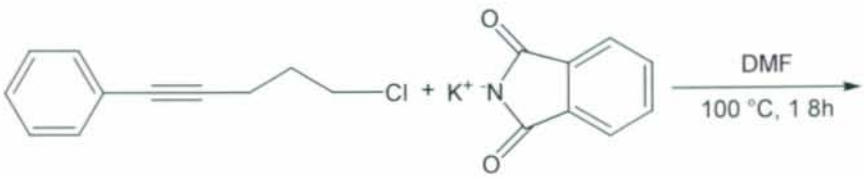

3.3 **3.4**

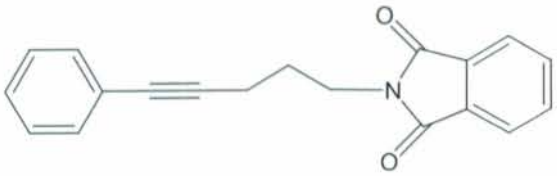

3.5

3.2.3 5-Phenyl-4-pentyn-1-amine (3.7)

To a methanol solution of *N*-(5-phenyl-4-pentylnyl)phthalimide (**3.5**) was added two molar equivalents of hydrazine monohydrate (**3.6**). The resulting mixture was heated at reflux 80 °C for 18 h (**Eqn. 3.3**) and then allowed to cool to room temperature. At this

step, upon workup, a yellow precipitate was obtained, but the literature procedure reported that a liquid product was formed. However, a literature search revealed that hydrazinolysis of *N*-substituted phthalimide produces a precipitate of phthalhydrazide along with the primary amine, which makes it difficult to separate the primary amine.[3] In the work described in this thesis, the aminoalkyne was obtained by treating the yellow precipitate with concentrated HCl, which converted the primary amine to the quaternary ammonium chloride, followed by addition of deionized water (**Eqn 3.3**). The amine salt was subsequently deprotonated with aqueous NaOH and the aqueous phase and organic phases were extracted with dichloromethane. The resulting solution was dried over anhydrous $MgSO_4$, filtered and the solvent was removed by rotary evaporation. The resulting brown liquid was distilled at 100 °C to afford a colourless oily liquid (**3.7**) in 42% yield. ^{1}H NMR analysis was in agreement with literature data.[2]

[3.3]

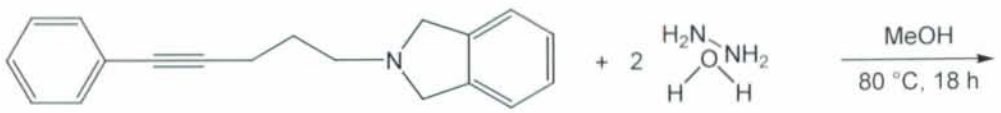

3.5 **3.6**

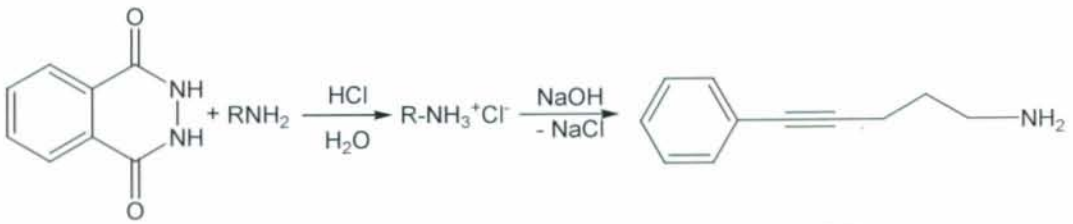

3.7

References for Chapter 3 begin on page 111

3.3 Results & Discussion

3.3.1 Catalytic Hydroamination-Cyclization of Aminoalkyne

The lanthanide amine bis(phenolate) complexes described in Chapter 2 were investigated as catalysts for the hydroamination of aminoalkyne substrate (**3.7**) to the corresponding azacycle (**3.8**) as shown in a typical hydroamination-cyclization in **Eqn. 3.4**. The preparative-scale hydroamiantion reaction was conducted by loading a reaction flask with the lanthanide amine bis(phenolate) complex *e.g.* $[O_2N_2^{t\text{-}Bu,Me}]HoN(SiMe_3)_2$, followed by addition of benzene at 0 °C. A benzene solution of 5-phenyl-4-pentyne-1-amine was transferred to the reaction flask. The resulting reaction mixture was freeze-pump-thawed and was stirred at room temperature for 48 h. The product was separated from the catalyst *in vacuo* and the solvent was removed by atmospheric pressure distillation to afford a light yellow oily liquid.

[3.4]

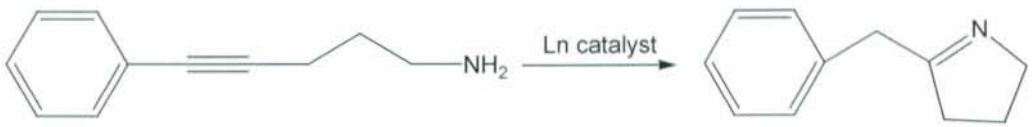

3.7 **3.8**

3.3.2 NMR Characterization of Hydroamination Reaction Product

The ^1H NMR spectrum (**Figure 3.1**) of the resulting light yellow oily liquid reveals that the product resonances are paramagnetically broadened. Therefore, no definitive information could be obtained.

References for Chapter 3 begin on page 111

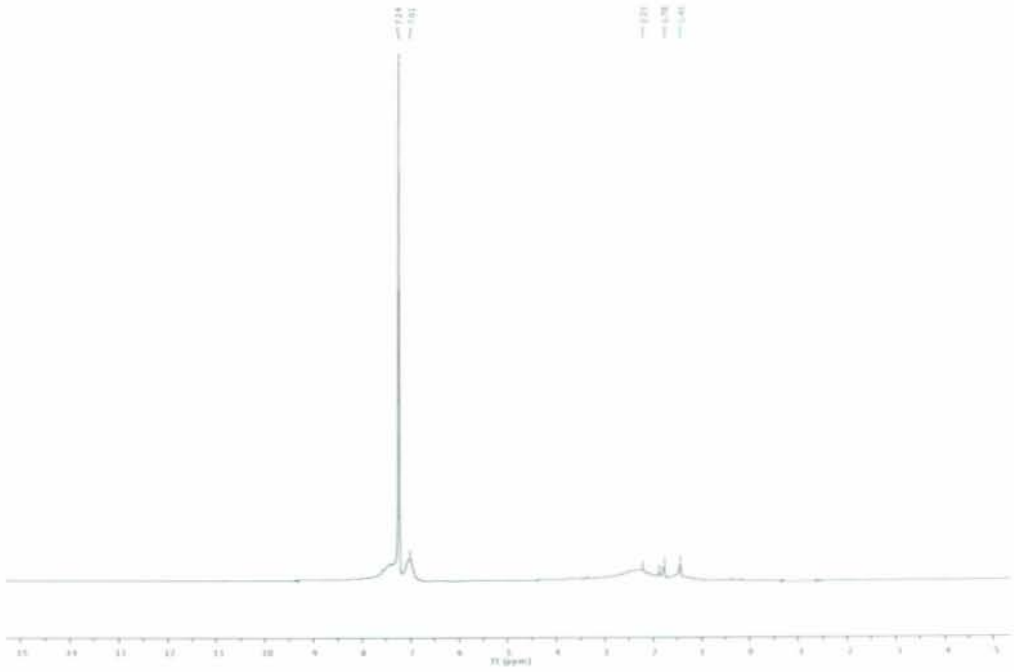

Figure 3.1 ^{1}H NMR spectrum of the hydroamination reaction product

Isolation of the product from the paramagnetic material was carried out by column chromatography on neutral alumina, using diethyl ether as eluent and removing the solvent was by rotary evaporation. After the product was chromatographed twice, it was found that no hydroamination product was obtained; rather, the starting material was recovered quantitatively. **Figure 3.2** shows a comparison of ^{1}H NMR spectra for the aminoalkyne substrate (**a**) relative to (**b**) first chromatographed and (**c**) second chromatographed hydroamination product. Although, the resonances were still broadened and shifted, formation of no product was evidenced by the resonances of the recovered material comparatively matching with that of the starting aminoalkyne. This is similar to

the observation made by Marks *et al.*[4] for paramagnetic Nd^{3+} ($4f^3$) and Sm^{3+} ($4f^5$) catalysts in an investigation of the kinetics of enantioselective hydroamination-cyclization of amino olefins. Many papers discuss the monitoring of hydroamination-cyclization reactions using diagnostic ^1H NMR resonances.[2,5] However, in our study, the presence of paramagnetic lanthanide ions in the product precluded the direct NMR analysis.

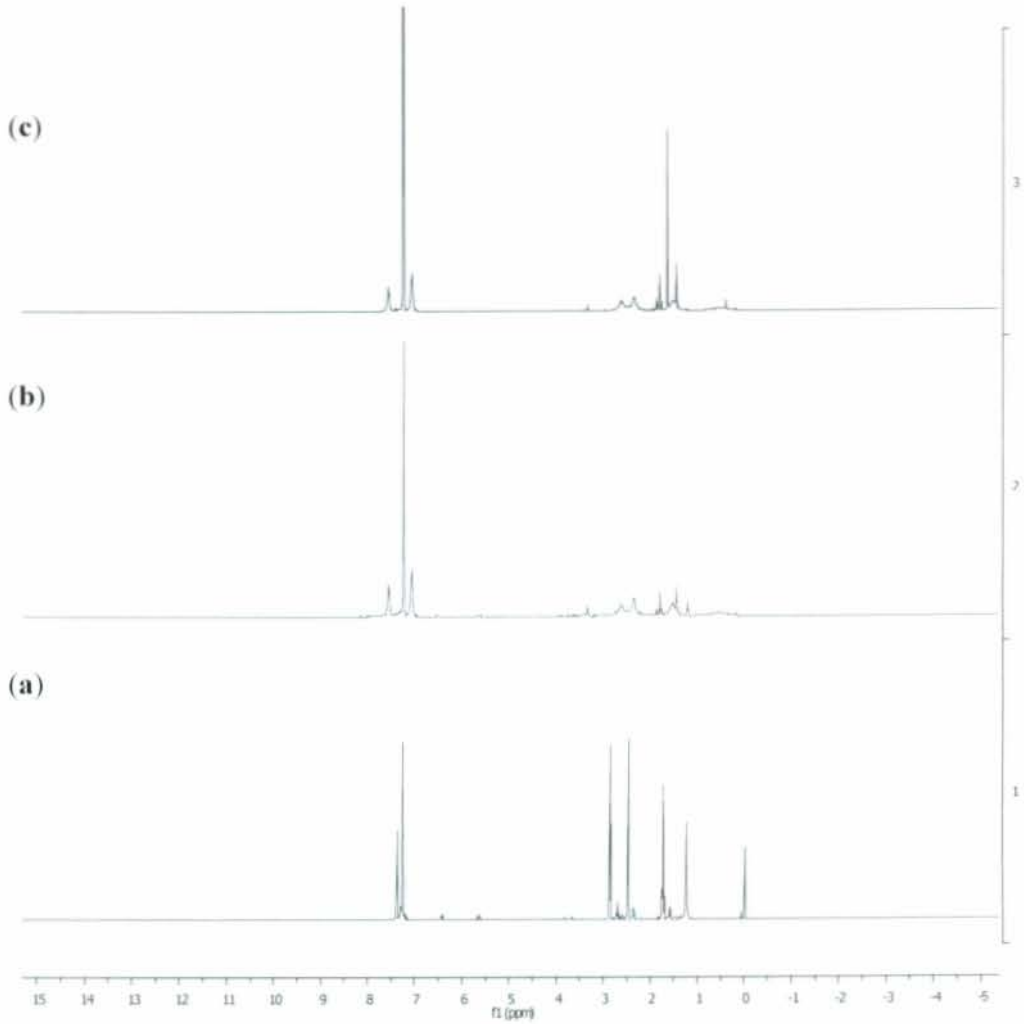

Figure 3.2 ^1H NMR spectra (**a**) the starting material (aminoalkyne (**3.7**)) (**b**) hydroamination product after the first chromatograph and (**c**) after second chromatograph.

References for Chapter 3 begin on page 111

3.3.3 MALDI-TOF MS Characterization of Hydroamination Reactions

Since the primary objective of this research lies in the investigation of MALDI-TOF MS as a rapid screening technique for paramagnetic lanthanide species and hydroamination reactions, crude hydroamination reaction mixtures were prepared and assayed. The analytical scale hydroamination-cyclization reaction samples for MALDI-TOF MS were prepared by mixing a toluene solution of lanthanide amide reagent *e.g.* $Ho\{N(SiMe_3)_2\}_3$ with the amine bis(phenol) ligand *e.g.* $[O_2N_2^{t\text{-}Bu,Me}]H_2$ to generate *in situ* the corresponding complex (**Figure 3.3**). The mixture was stirred for 4 h at room temperature, after which the aminoalkyne substrate was added. The resulting reaction mixture was stirred for an additional 2 h. Equal volumes of the reaction mixture (analyte) and a toluene solution of anthracene (matrix) were mixed and stirred for two minutes to ensure homogeneity. An aliquot of the mixture was spotted on the sample plate and allowed to dry. Alongside the spotted reaction mixture, on another position the corresponding lanthanide amide-ligand mixture was spotted as a reference. They were allowed to dry before transferring the plate to the spectrometer.

MALDI-TOF mass spectra for the hydroamination reactions of the aminoalkyne substrate (**3.7**) were assigned by comparison with the spectra for the *in situ* generated lanthanide complexes $\mathbf{2.14a_{2.2}}$ – $\mathbf{2.14c_{2.5}}$ shown in **Figure 3.3**.

References for Chapter 3 begin on page 111

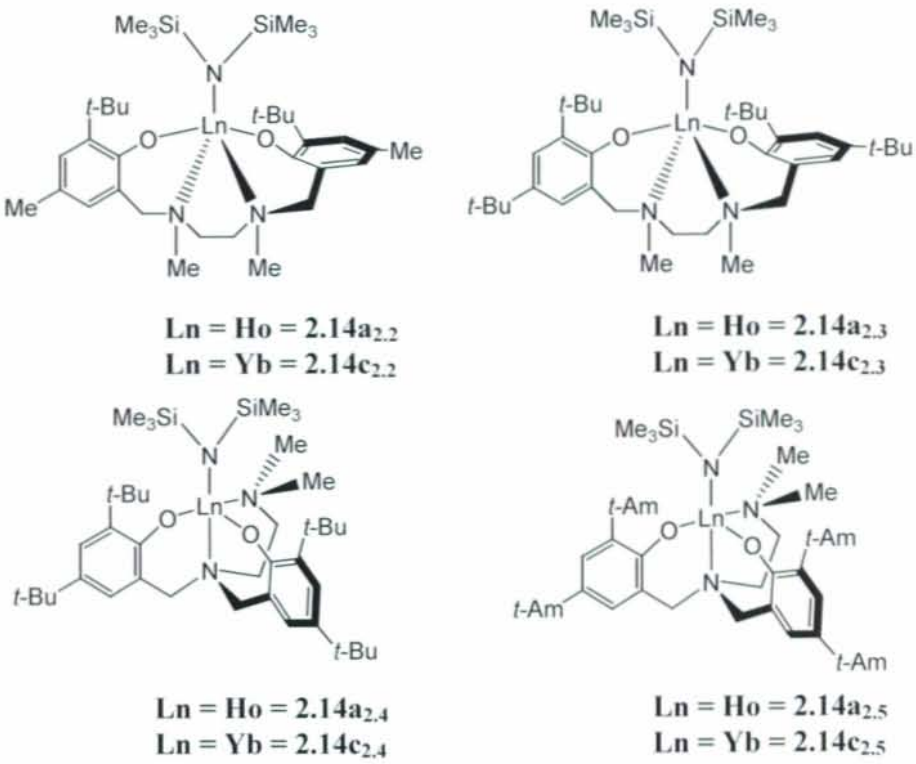

Figure 3.3 *In situ* generated lanthanide amine bis(phenolate) complexes used for hydroamination reaction.

To evaluate the performance of MALDI-TOF MS as a screening technique, the results of each of the reaction mixtures are discussed on a case-by-case basis. The MALDI-TOF mass spectrum of the reaction of holmium amide reagent and $[O_2N_2^{t\text{-Bu,Me}}]H_2$ ligand (**2.14a$_{2.2}$**) is shown in **Figure 3.4** (**a**). A number of peaks are observed, which can be attributed to loss of alkyl, amide or SiMe groups as discussed in chapter 2.

References for Chapter 3 begin on page 111

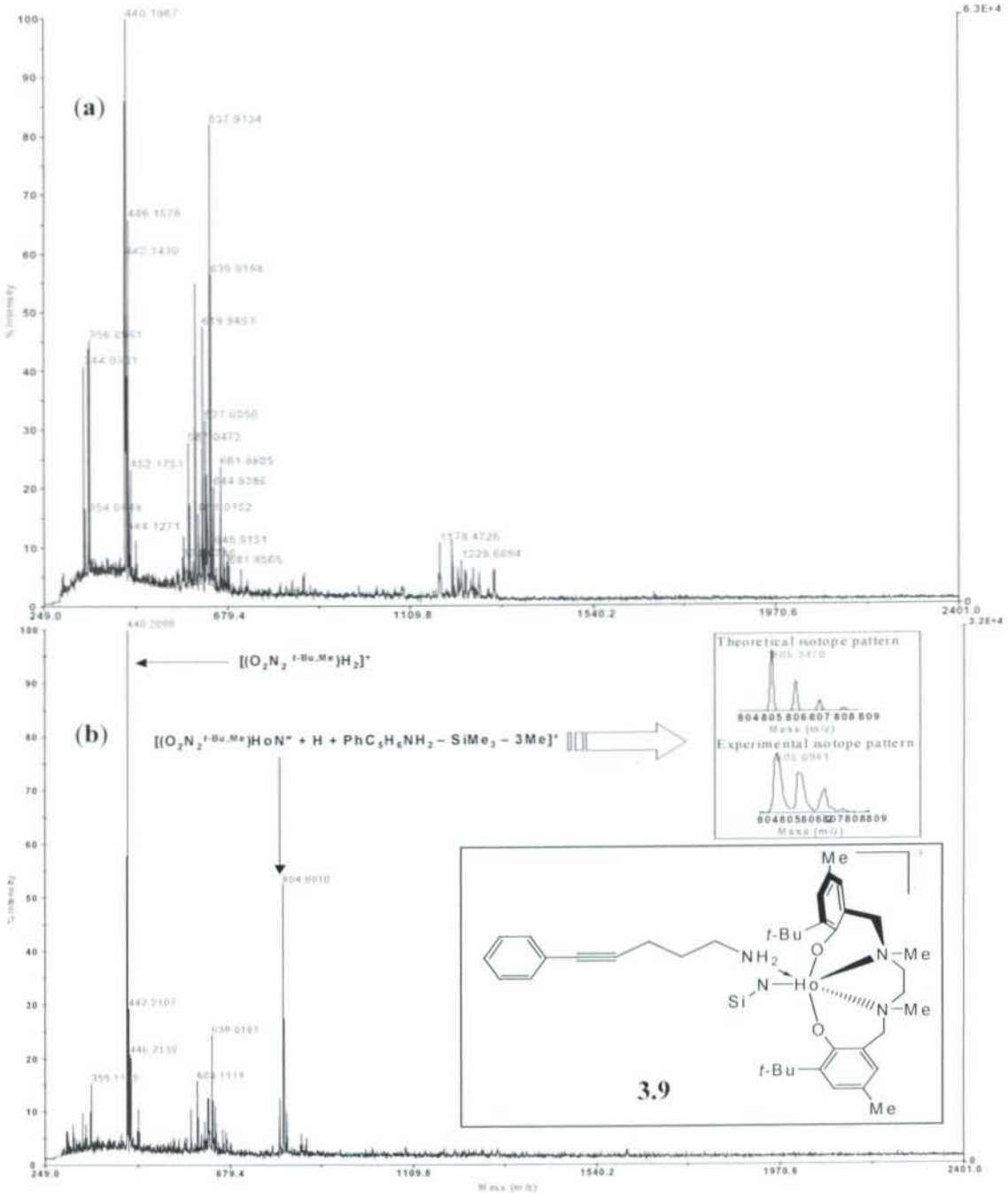

Figure 3.4 MALDI mass spectra of (**a**) reaction of holmium amide reagent with $[O_2N_2^{t\text{-}Bu,Me}]$ (**b**) hydroamination reaction mixture from $[O_2N_2^{t\text{-}Bu,Me}]HoN(SiMe_3)_2$ and aminoalkyne, inset; (*top*) isotope distribution patterns (*bottom*) proposed structure of an observed peak.

References for Chapter 3 begin on page 111

The MALDI-TOF MS spectrum **Figure 3.4** (**b**) from the hydroamination reaction mixture of the aminoalkyne substrate (**3.7**) exhibited a prominent fragment ion at *m/z* 804 corresponding to loss of a $SiMe_3$ and three methyl groups and coordination of the aminoalkyne. The absence of this peak in **Figure 3.4** (**a**) indicates that a reaction took place between the substrate and the lanthanide complex. A possible structural assignment of the peak is an aminoalkyne coordination complex (**3.9**) of the lanthanide, as shown in **Figure 3.4** (**b**). This observed peak was interpreted using the isotope distribution pattern, in which the theoretical and experimetal isotope patterns are in good agreement as shown in **Figure 3.4** (**b**) inset (top). The peak at *m/z* 638 corresponds to the loss of a methyl and two *tert*-butyl groups from $[O_2N_2^{t\text{-}Bu,Me}]HoN(SiMe_3)_2$ and aminoalkyne reaction mixture.

The MALDI-TOF mass spectrum (**Appendix 3.4** (**b**)) of the hydroamination reaction of aminoalkyne substrate (**3.7**) with holmium complex $[O_2N_2^{t\text{-}Bu}]HoN(SiMe_3)_2$ (**2.14a**$_{2.3}$) showed similar fragmentation patterns as observed in **Figure 3.4** (**b**). The peak at *m/z* 889 corresponds to the aminoalkyne substrate being coordinated to the holmium complex. The structural assignment is proposed based on the theoretical and experimental isotope patterns, which are in good agreement. Another peak observed at *m/z* 722 also gave evidence towards the loss of a methyl and two *tert*-butyl groups from$[O_2N_2^{t\text{-}Bu}]HoN(SiMe_3)_2$ and aminoalkyne reaction mixture similar to the peak observed in the mass spectrum of **Figure 3.4** (**b**).

The comparison of the MALDI-TOF mass spectra of the *in situ* holmium complex $[O_2NN^{t\text{-}Am}]HoN(SiMe_3)_2$ (**2.14a**$_{2.5}$) alone **Figure 3.5**(**a**) and that of the corresponding hydroamination reaction mixture **Figure 3.5** (**b**) exhibited some similarities in the region

of *m/z* 600-900. However, beyond *m/z* 900, it was observed that in **Figure 3.5** (**b**), the higher mass peaks became more intense and pronounced. The fragmented ions observed at *m/z* 1024 and 1081 correspond to $[(O_2NN'^{t\text{-Am}})Ho(N'') + \text{Anthracene} - 4Me]^+$ and $[(O_2NN'^{t\text{-Am}})Ho(N'') + \text{anthracene} - H]^+$ respectively.

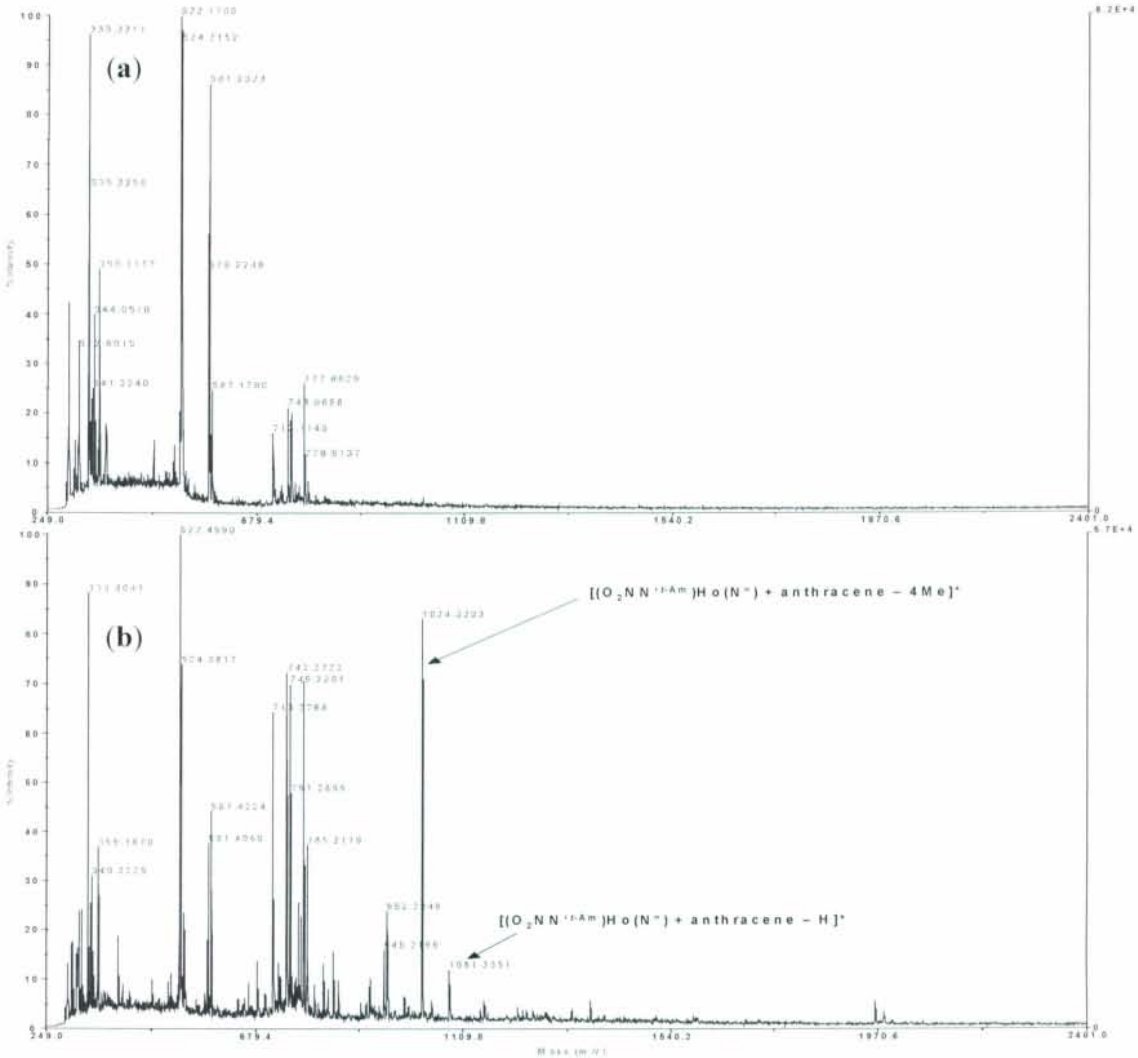

Figure 3.5 MALDI mass spectra of (**a**) reaction of holmium amide reagent with $[O_2NN'^{t\text{-Am}}]$; (**b**) hydroamination reaction mixture from $[O_2NN'^{t\text{Am}}]HoN(SiMe_3)_2$ and aminoalkyne.

Evaluation of the MALDI mass spectra resulting from the analysis of holmium complex $[O_2NN'^{t\text{-}Bu}]HoN(SiMe_3)_2$ alone **Figure 3.6** (**a**) and that of the corresponding hydroamination reaction **Figure 3.6** (**b**) showed similar enhancement of the higher mass peaks as observed for **Figure 3.5** (**b**). Structural assignments reveal that the peaks correspond to arene complexes. It is not apparent why the arene complex peaks are enhanced in the hydroamination reaction mixture.

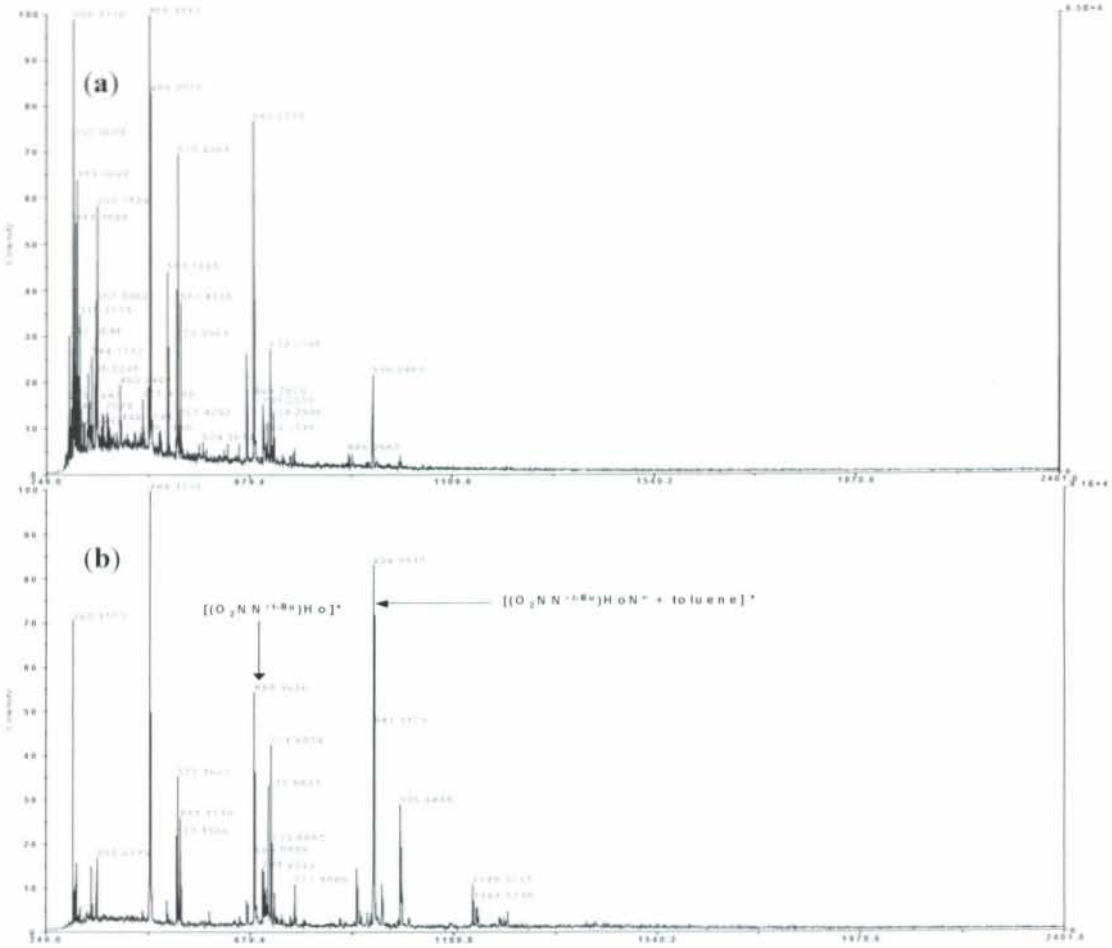

Figure 3.6 MALDI-TOF mass spectra of (**a**) in situ generated $[O_2NN'^{t\text{-}Bu}]HoN(SiMe_3)_2$ (**b**) hydroamination reaction of aminoalkyne substrate with $[O_2NN'^{t\text{-}Bu}]HoN(SiMe_3)_2$.

References for Chapter 3 begin on page 111

Some researchers have observed enhanced matrix-analyte adduct formation, which they attributed to the degree of photon energy that influences the photochemical reactions between matrix and analyte.[6-8] In this case, the mass spectrometric analyses were conducted under uniform spectrometric conditions. Thus, the observed similarities and differences in the spectra of the hydroamination reactions could be attributed to a more significant role of other factors; for instance, geometry of the complexes, ligand effect and substrate effect. In order to find out whether matrix-analyte reactions in the gas phase are responsible for the observed differences, additional experiments with ytterbium complexes were performed.

Analogously to **Figure 3.4** (**b**), the mass spectrum of the hydroamination reaction shown in **Figure 3.7** (**b**) mediated by $[O_2N_2^{t\text{-}Bu,Me}]YbN(SiMe_3)_2$ (**2.14c**$_{2.2}$) exhibited a major peak at *m/z* 814 corresponding to the aminoalkyne substrate being coordinated to the ytterbium metal center and the loss of a $SiMe_3$ and three methyl groups. A possible structure for the observed peak is shown in **Figure 3.7** (**b**) inset (bottom (**3.10**)). The assignment of these peaks was confirmed by the isotopic distribution patterns. The experimental isotope pattern is in good agreement with the theoretical isotope pattern as shown in **Figure 3.7** (**b**) inset (top). In addition to this, fragment was observed at *m/z* 647 for the loss of a methyl and two *tert*-butyl groups from hydroamination reaction mixture of $[O_2N_2^{t\text{-}Bu,Me}]YbN(SiMe_3)_2$ and aminoalkyne.

References for Chapter 3 begin on page 111

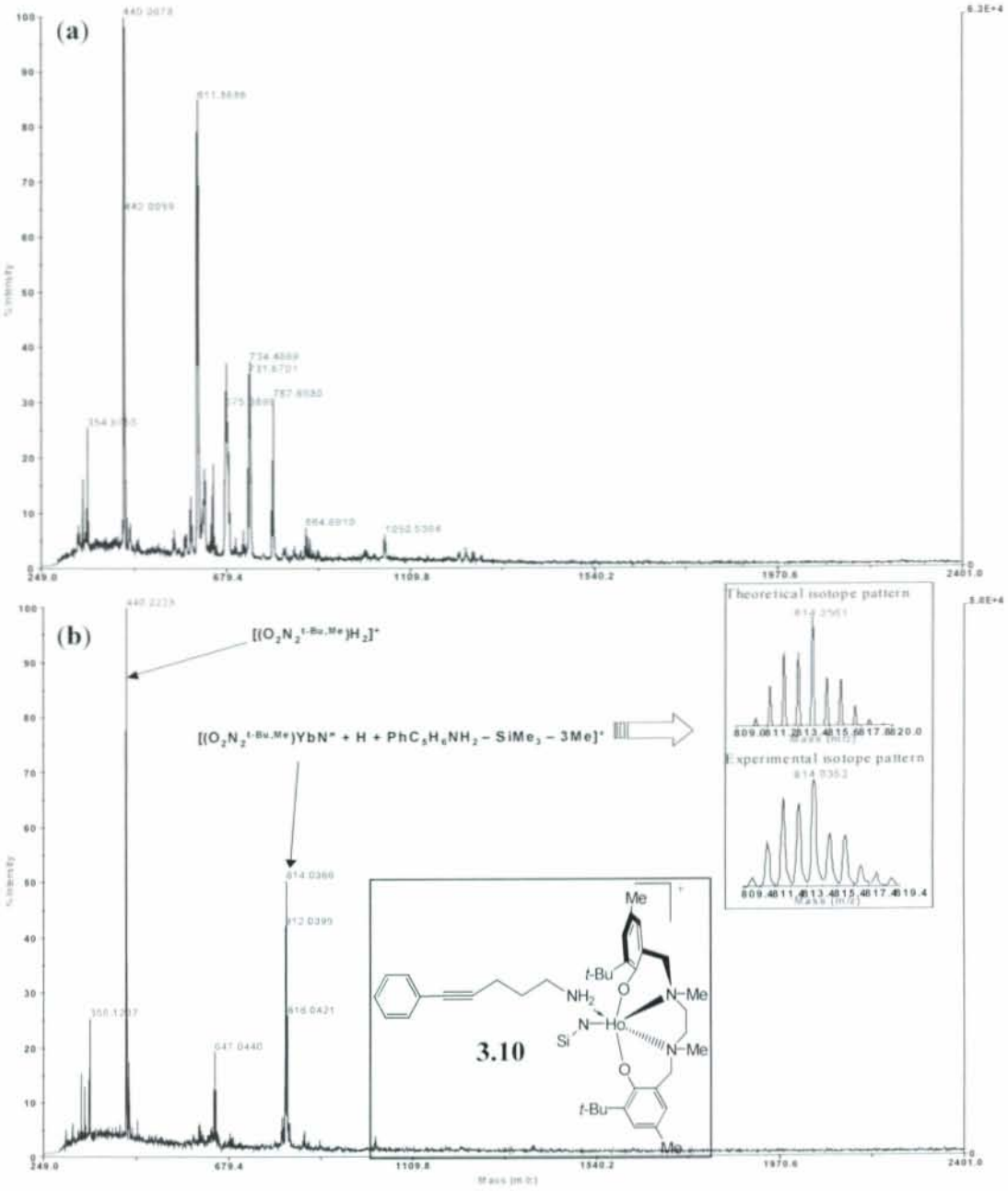

Figure 3.7 MALDI mass spectra of (**a**) reaction of ytterbium amide reagent with $[O_2N_2^{t\text{-}Bu,Me}]H_2$; (**b**) (**b**) hydroamination reaction mixture of aminoalkyne substrate with $[O_2NN^{t\text{-}Bu,Me}]YbN(SiMe_3)_2$; inset; (*top*) isotope distribution patterns and (*bottom*) proposed structure of an observed peak.

References for Chapter 3 begin on page 111

Interestingly, the mass spectrum resulting from the hydroamination reaction mixture with $[O_2N_2^{t\text{-}Bu}]YbN(SiMe_3)_2$ **Figure 3.8 (b)** exhibited a fragmentation pattern similar to those observed for the Holmium analogue in **Figure 3.4(b)** and **Figure 3.7 (b)**. Significant peaks were observed at *m/z* 731 corresponding to the loss of a $SiMe_3$ and three methyl groups along with a fragmentation at *m/z* 889 assigned to the loss of a methyl and two *tert*-butyl groups from the reaction mixture of $[O_2N_2^{t\text{-}Bu}]YbN(SiMe_3)_2$ and aminoalkyne.

Figure 3.9 (b) shows the MALDI-MS spectrum of the hydroamination reaction mixture with $[O_2NN'^{t\text{-}Am}]YbN(SiMe_3)_2$ (**2.14c$_{2.5}$**). Surprisingly, no peak for the aminoalkyne substrate being coordinated to the metal center was observed, rather enhanced signals for arene complexes at *m/z* 1032 and 1089 were observed. A similar pattern was also observed for $[O_2NN'^{t\text{-}Bu}]YbN(SiMe_3)_2$ (**2.14c$_{2.4}$**) as shown in **Figure 3.10 (b)**. These patterns of fragmentation are consistent with the previous observations made for their analogous holmium complexes. **Table 3.1** shows the assignment of all prominent peaks observed in all the hydroamination reaction mixtures studied by MALDI-TOF MS in this work.

References for Chapter 3 begin on page 111

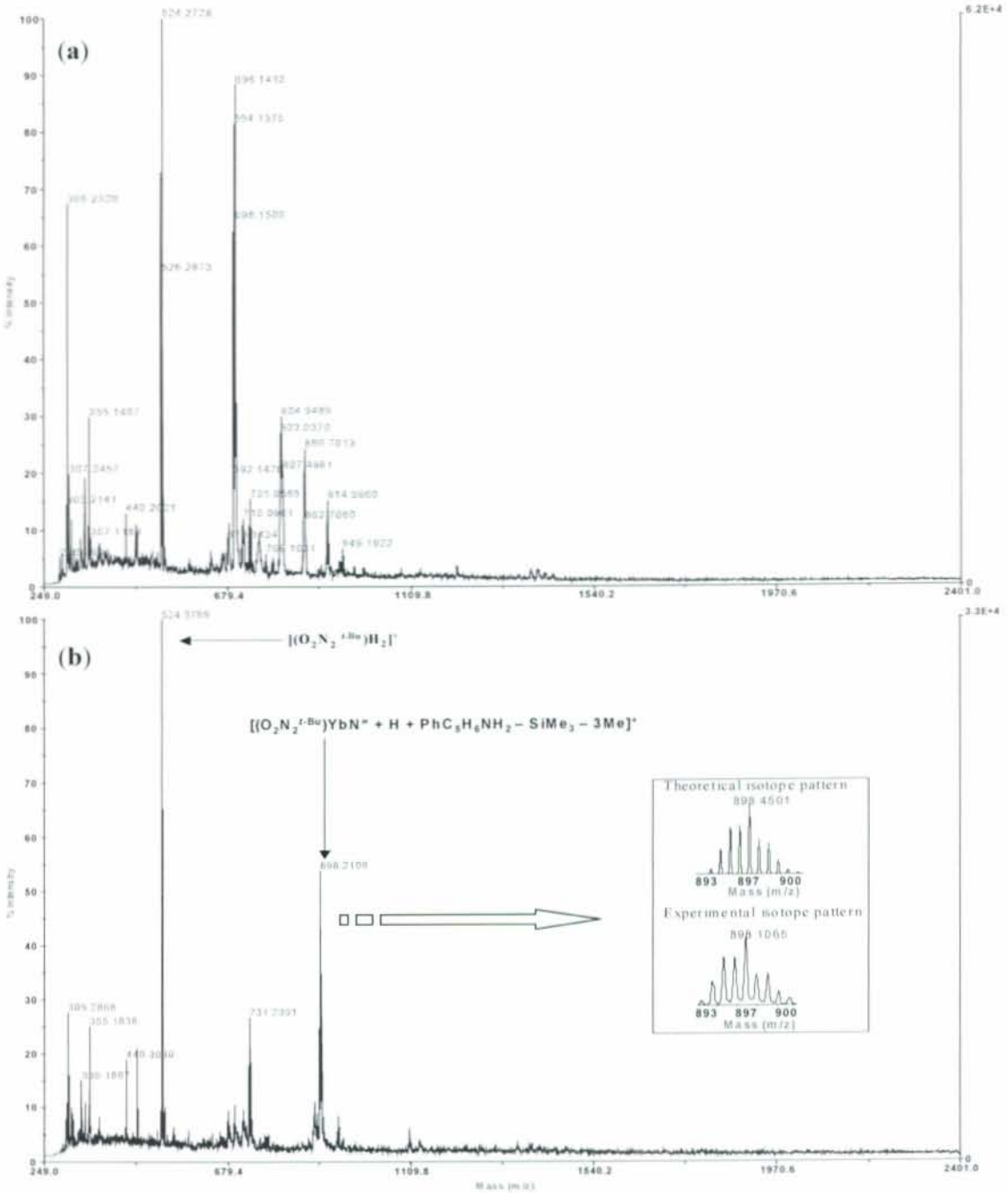

Figure 3.7 MALDI-TOF mass spectra of (**a**) in situ generated $[O_2N_2^{t\text{-}Bu}]YbN(SiMe_3)_2$ (**b**) hydroamination reaction of aminoalkyne substrate(**3.7**) with $[O_2N_2^{t\text{-}Bu}]YbN(SiMe_3)_2$.

References for Chapter 3 begin on page 111

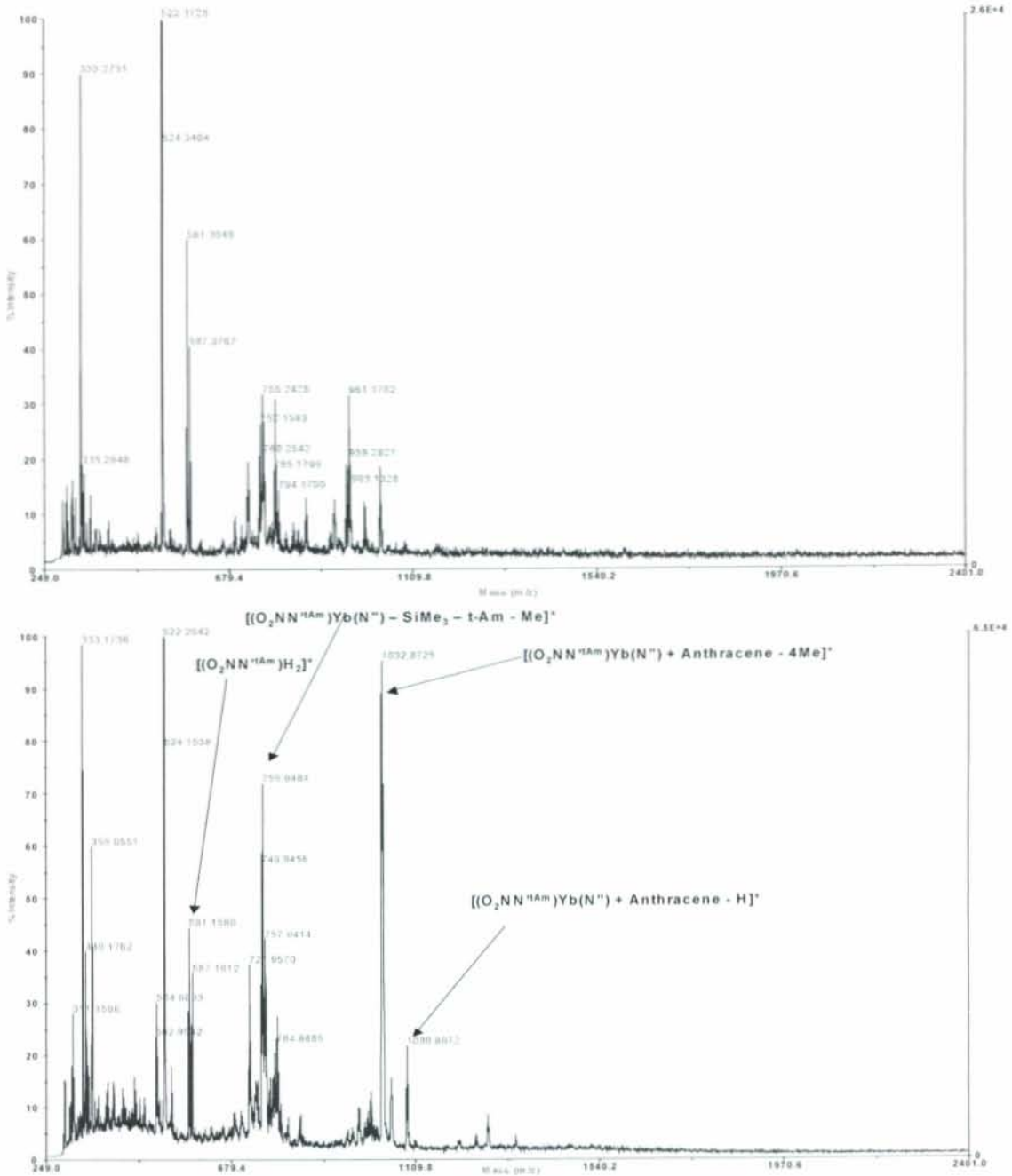

Figure 3.9 MALDI mass spectra of (**a**) reaction of $YbN(SiMe_3)_2$ with $[O_2NN^{t\text{-}Am}]H_2$; (**b**) hydroamination reaction mixture of $[O_2NN^{t\text{-}Am}]YbN(SiMe_3)_2$ and aminoalkyne substrate.

References for Chapter 3 begin on page 111

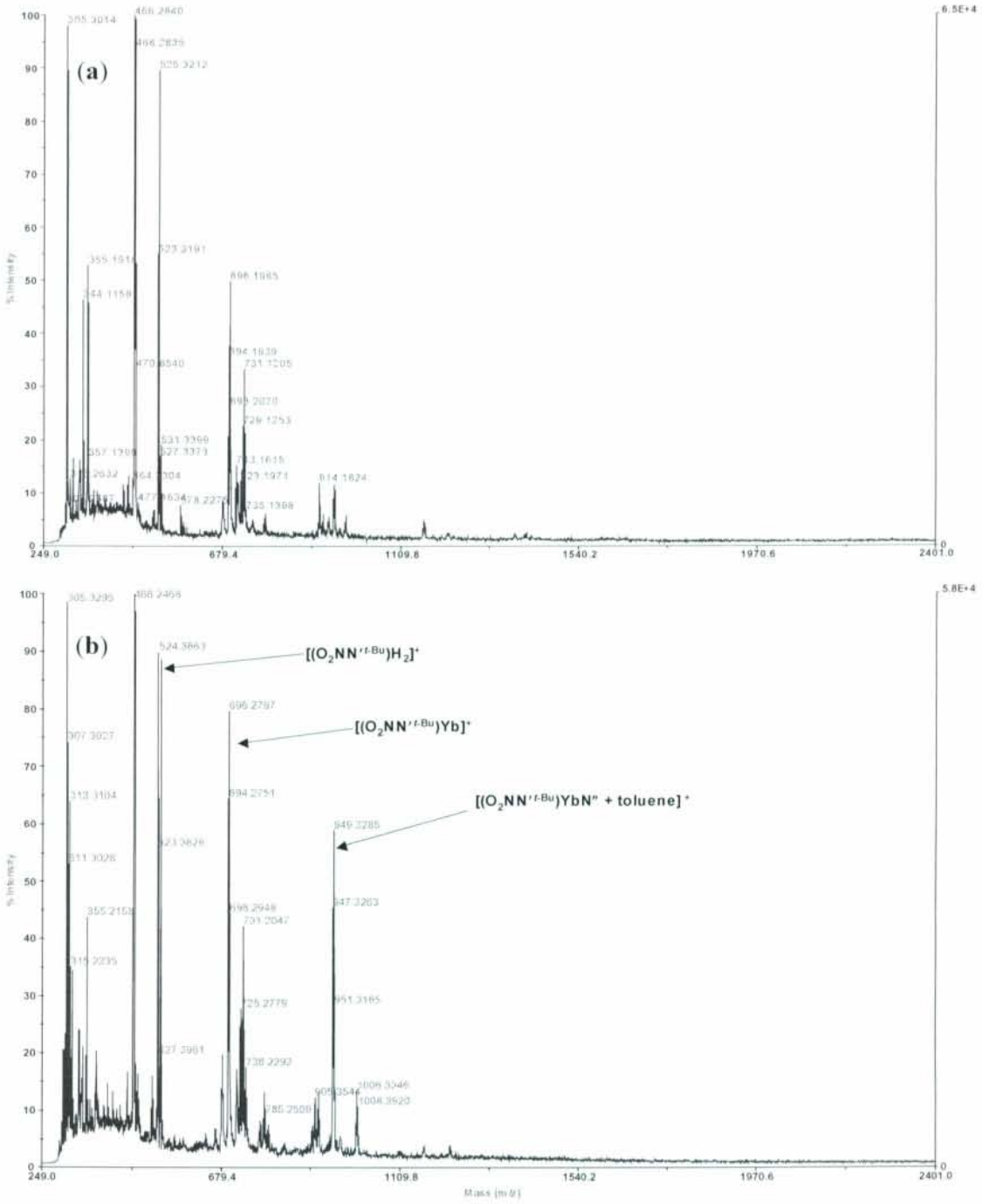

Figure 3.10 MALDI-TOF mass spectra of (**a**) in situ generated $[O_2NN'^{t\text{-}Bu}]YbN(SiMe_3)_2$; (**b**) hydroamination reaction of aminoalkyne substrate(**3.7**) with $[O_2NN'^{t\text{-}Bu}]YbN(SiMe_3)_2$.

References for Chapter 3 begin on page 111

Table 3.1 Assignment of prominent peaks observed in the MALDI-TOF MS analysis for the hydroamination reactions mediated by *in situ* generated holmium and ytterbium amine bis(phenolate) complexes.

Hydroamination Reaction mixture	$[M]^+$	$[M - N(SiMe_3)]^+$	$[M + H - 2\ t\text{-Bu} - Me]^+$	$[M - SiMe_3 - t\text{-Am} - Me]^+$	$[M + H + Sub - SiMe_3 - 3\ Me]^+$
$[O_2N_2^{t\text{-Bu,Me}}]HoN'' + Sub$	(763)	—	638	—	804
$[O_2N_2^{t\text{-Bu}}]HoN'' + Sub$	(847)	—	722	—	889
$[O_2NN'^{t\text{-Bu}}]HoN'' + Sub$	(847)	686	721	—	—
$[O_2NN'^{t\text{-Am}}]HoN'' + Sub$	(904)	—	—	—	—
$[O_2N_2^{t\text{-Bu,Me}}]YbN'' + Sub$	(772)	—	647	—	814
$[O_2N_2^{t\text{-Bu}}]YbN'' + Sub$	(856)	—	731	—	898
$[O_2NN'^{t\text{-Bu}}]YbN'' + Sub$	(856)	696	731	—	—
$[O_2NN'^{t\text{-Am}}]YbN'' + Sub$	(912)	—	—	755	—

	$[M + Toluene]^+$	$[M + Anthracene - 2Me]^+$	$[M + Anthracene - 4Me]^+$	$[M + Anthracene - H]^+$
$[O_2N_2^{t\text{-Bu,Me}}]HoN'' + Sub$	—	—	—	—
$[O_2N_2^{t\text{-Bu}}]HoN'' + Sub$	—	—	—	—
$[O_2NN'^{t\text{-Bu}}]HoN'' + Sub$	939	997	—	—
$[O_2NN'^{t\text{-Am}}]HoN'' + Sub$	—	—	1024	1081
$[O_2N_2^{t\text{-Bu,Me}}]YbN'' + Sub$	—	—	—	—
$[O_2N_2^{t\text{-Bu}}]YbN'' + Sub$	—	—	—	—
$[O_2NN'^{t\text{-Bu}}]YbN'' + Sub$	948	1006	—	—
$[O_2NN'^{t\text{-Am}}]YbN'' + Sub$	—	—	1032	1089

$[M]^+$ = molecular ion of the complex.; Sub = aminoalkyne substrate; N'' = $N(SiMe_3)_2$; Values in parenthesis ( ) are expected molecular masses not observed.

3.4 Summary and Interpretation of Data from MALDI-TOF MS of Hydroamination Reaction Mixtures

The results summarized in **Table 3.1** indicate that the spectra for the hydroamination reactions mediated by the complexes $[O_2N_2^{t\text{-}Bu,Me}]HoN(SiMe_3)_2$ (**2.14a$_{2.2}$**) and $[O_2N_2^{t\text{-}Bu,Me}]YbN(SiMe_3)_2$ (**2.14c$_{2.2}$**) exhibit similar fragmentation patterns. Both complexes show similar fragmentation via the loss of a methyl and two *tert*-butyl groups and similar coordination of the aminoalkyne substrate to the metal centers. These patterns were also observed for complexes: $[O_2N_2^{t\text{-}Bu}]HoN(SiMe_3)_2$ (**2.14a$_{2.3}$**) and $[O_2N_2^{t\text{-}Bu}]YbN(SiMe_3)_2$ (**2.14c$_{2.3}$**). In contrast, the spectra for the hydroamination reactions with complexes $[O_2NN'^{t\text{-}Bu}]HoN(SiMe_3)_2$ (**2.14a$_{2.4}$**), $[O_2NN'^{t\text{-}Am}]HoN(SiMe_3)_2$ (**2.14a$_{2.5}$**), $[O_2NN'^{t\text{-}Bu}]YbN(SiMe_3)_2$ (**2.14c$_{2.4}$**), and $[O_2NN'^{t\text{-}Am}]YbN(SiMe_3)_2$ (**2.14c$_{2.5}$**) showed no fragmentation peak corresponding to the aminoalkyne being coordinated to the metal center, rather the peaks corresponding to arene complex formation were enhanced.

These results show a clear trend and differences in reactivity between $[O_2N_2]$- and $[O_2NN']$-based complexes. In all the cases studied, no coordination of the aminoalkyne substrate was observed for any of the $[O_2NN']$-based complexes. This apparent difference in reactivity may be attributed to structural differences between the two classes of ligands coordinated to the metals. Several studies have shown that the pendant nitrogen donor has a major effect on reactivity especially for polymerization catalysts.[1a,9] However, from the results in **Table 3.1**, the $[O_2N_2]$-based complexes, which contain both amines in the backbone of the ligand, demonstrated coordination of the aminoalkyne to the metal center. A possible explanation for this behaviour is that the $[O_2N_2]$ ligand environment

References for Chapter 3 begin on page 111

wrapped around the metal center provides a relatively open site for the incoming aminoalkyne to coordinate with. On the other hand, the pendant donor may have created greater steric congestion around the metal center that results in non-coordination of the aminoalkyne.

3.4.1 Catalytic Cycle

Many papers have been published which discuss the mechanistic studies of organolanthanide-catalyzed intramolecular hydroamination/cyclization of aminoalkenes,[10] aminodienes,[11] and aminoallenes.[12] Marks and co-workers[13] have proposed a general intramolecular hydroamination-cyclization catalytic mechanism for aminoalkynes. A schematic representation of the mechanism is shown (**Scheme 1.4**) in Chapter 1 and involves the coordination of the amino group of the substrate to the metal center through proton transfer from the substrate to the leaving amide or hydrocarbyl ligand of the precatalyst. This process cleaves the lanthanide-amide or lanthanide-hydrocarbyl bond, thereby generating the active catalyst. This step is followed by insertion of the alkyne triple bond into the lanthanide-nitrogen bond forming lanthanide-alkyl species, which is subsequently protonolyzed rapidly by the amino group of another aminoalkyne substrate to release the product and regenerate the catalyst.[13]

In his mechanistic investigation, Marks found that the activation of the precatalyst occurs through rapid protonolysis. However, in our study it was observed that the aminoalkyne substrate coordinated to the metal center did not lead to catalytic activity. One possible explanation for the observed lanthanide-substrate adduct is that electron density from the lone pair on the nitrogen is donated to the Lewis acidic lanthanide center

References for Chapter 3 begin on page 111

which stabilized the adduct species (Dead, end, **Scheme 3.1**). Thus, we propose that an equilibrium was established which hampered the formation of the active species that would have been incorporated into an efficient catalytic cycle. Therefore, this led to "dead end" as illustrated in **Scheme 3.1**. The fact that the catalytic pathway was impeded due to stability of the lanthanide-substrate adduct, probably led to the failure in formation of the hydroamination product. This is not surprising considering that hydroamination/cyclization of aminoalkynes catalyzed by most active organolanthanide catalysts are conducted at elevated temperature.[14,15] Presumably, elevation of the experimental temperature could facilitate facile H transfer from the substrate to the leaving amide ligand, and generate an active hydroamination catalyst. In our initial investigations, all reactions have been performed at room temperature.

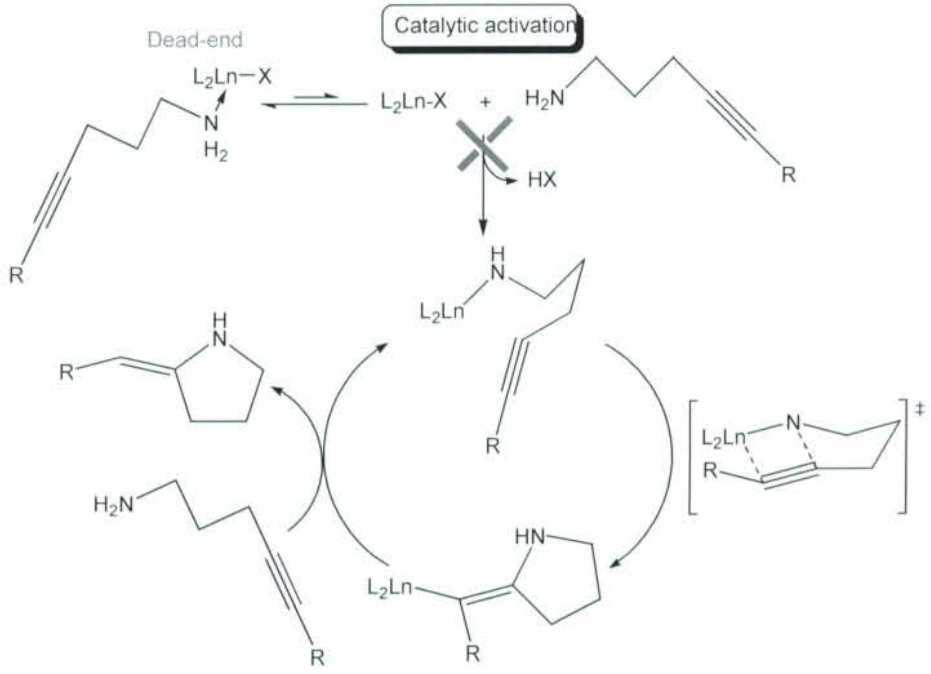

Scheme 3.1 Proposed hydroamination catalytic pathway

References for Chapter 3 begin on page 111

3.5 Summary

In the MALDI-TOF mass spectrometric analysis of reactions between organolanthanides and an aminoalkyne, mass spectra were generated in which the aminoalkyne substrate was observed to coordinate to the lanthanide metal center. The results of our study revealed differences in the trend of reactivity between $[O_2N_2]$ and $[O_2NN']$ ligand-based complexes. The observed peaks of the substrate coordinating to the metal center suggests that the $[O_2N_2]$-based complexes could be potential candidates for the generation of active catalysts for intramolecular hydroamination-cyclization of aminoalkynes with variation of the experimental conditions, such as for example, temperature. The observed spectra presumably indicate that the differences in the catalytic activity of the two classes of ligand-based complexes may be as a result of structural parameters *e.g.* sterics.

Our results demonstrate that MALDI-TOF MS can be successfully applied to the analysis of three component mixtures in organolanthanide chemistry. However, further experiments are required to gain a better understanding of the data obtained to-date. Despite this, it has been shown that MALDI-TOF MS can be a useful rapid screening technique towards extremely moisture-sensitive paramagnetic organolanthanide and other metal-catalyzed reactions.

References for Chapter 3 begin on page 111

3.6 Experimental Section

3.6.1 Materials

Chemical reagents were purchased from Aldrich, Alfa Aesar, Lancaster and Strem. Before using solvents (toluene, diethyl ether, THF, hexane, dichloromethane) they were dried over sodium or sodium-benzophenone or calcium hydride and distilled under nitrogen. Chloroform-*d* and benzene-d_6 used for NMR analysis were purchased from Cambridge Isotope Laboratories, purified by distillation and stored in sealable Schlenk tubes in the glove box.

3.6.2 Instruments

^{1}H NMR spectra were recorded on a Bruker Avance 500 MHz spectrometer at 298 K and were referenced internally using the residual proton resonances of the solvent. Chemical shifts (δ) are quoted in ppm, the downfield direction being positive. Coupling constants (*J*) are given in Hz. The following abbreviations are used for convenience in reporting the multiplicity of NMR resonances: s = singlet, d = doublet, dd = doublet of doublets, t = triplets, q = quartet, p = pentet, br = broad, m = multiplet. Integration and assignments of ^{1}H NMR spectra were processed using MestReNova software.

The MALDI-TOF mass spectra were acquired using a Voyager-DE RP Biospectrometry workstation (Applied Biosystems, Toronto, Canada) that uses a pulsed nitrogen laser (337 nm). The spectra were obtained in reflectron positive mode at 20 kV accelerating voltage with delay ion extraction set to 145 ns and accumulating 50 shots for each spectrum.

References for Chapter 3 begin on page 111

3.6.3 Experimental Methods

All manipulations of metal complexes and air sensitive reagents were performed under an inert atmosphere using standard Schlenk line procedures or in M Braun nitrogen-filled glove box with O_2 and H_2O levels below 5 ppm. Solvents were removed using Schlenk lines or a rotary evaporator. Anhydrous $MgSO_4$ was used as a drying agent for some organic reagents. Structural assignments of peaks for the mass spectrometric study were based on comparison of the experimental isotope patterns with corresponding theoretical isotope patterns.

3.7 Synthesis of Amnioalkyne

3.7.1 5-Chloro-1-phenyl-1-pentyne (3.3)

To a solution of 1-bromo-3-chloropropane (15.74 g 0.1 mol) in THF (80 mL) was added lithium phenylacetylide (100 mL, 0.1 mol) dropwise while stirring at 0 °C for 2 h. The reaction mixture was allowed to warm to room temperature and was stirred for an additional 6 h. The reaction mixture was poured into deionized water (20 mL), which formed two layers. The organic and aqueous phases were separated and the water layer extracted with diethyl ether (3×10 mL). The combined ether extract was washed with brine (20 mL), dried over anhydrous $MgSO_4$, and filtered. The resulting mixture was allowed to settle for 0.5 h and then filtered. Diethyl ether and THF were removed by rotary evaporation giving a light brown liquid, which was subsequently distilled under vacuum at 105 °C to afford a colourless liquid product (10.86 g, 61% yield). ^{1}H NMR (500 MHz, $CDCl_3$): δ 7.37 (dd, 2H, J = 2.8 Hz, Ar*H*), 7.28 – 7.25 (m, 3H, Ar*H*), 3.70 (t,

2H, J = 6.4 Hz, CH_2Cl), 2.59 (t, 2H, J = 6.8 Hz, C≡C– CH_2), 2.05 (p, 2H, J = 6.6 Hz, CH_2–CH_2–CH_2).

3.7.2 *N*-(5-Phenyl-4-pentynyl)phthalimide (3.5)

N-(5-chloro-1-phenyl-1-pentyne) (4.75 g, 0.026 mol) was added to potassium phthalimide (4.93 g, 0.026 mol) in DMF (45 mL) and the reaction mixture was heated to 100 °C for 18 h. The resulting yellow/brown reaction mixture was allowed to cool to room temperature and then poured into a mixture of trichloromethane (65 mL) and deionized water (65 mL) was added, which formed two layers. The layers were separated and the aqueous phase was extracted with trichloromethane (3 × 20 mL). The combined extract was washed with aqueous KOH (60 mL, 0.2 M) and subsequently, with deionized water (60 mL) to remove any unreacted phthalimide. The solution was dried over anhydrous $MgSO_4$ and the resulting mixture was filtered. Trichloromethane was removed under vacuum giving a white solid residue, which was triturated with diethyl ether (2 × 20 mL) and filtered. The resulting solid residue was dried at reduced pressure affording a white crystalline solid (5.66 g, 74% yield). ^{1}H NMR (500 MHz, $CDCl_3$): δ 7.80 (dd, 2H, J = 3.1 Hz, ArH), 7.65 (dd, 2H, J = 3.0 Hz, ArH), 7.26 (dd, 2H, J = 3.1, ArH), 7.20 (dd, 3H, J = 1.8 Hz, ArH), 3.85 (t, 2H, J = 7.0 Hz, CH_2N), 2.48 (t, 2H, J = 7.0 Hz, C≡C– CH_2), 2.01 (p, 2H, J = 7.0 Hz, CH_2–CH_2–CH_2).

3.7.3 5-Phenyl-4-pentyn-1-amine (3.7)

Two molar equivalents of hydrazine monohydrate (10.86 g, 0.08 mol) were added to a methanol solution (70 mL) of one molar equivalent of *N*-(5-phenyl-4-

pentynyl)phthalimide (12.26 g, 0.04 mol). The resulting mixture was heated at reflux 80 °C for 18 h, allowed to cool to room temperature, after which concentrated hydrochloric acid (12 mL) was added and the mixture was heated at reflux for an additional 4 h. The reaction mixture was then cooled to room temperature and filtered to afford a white precipitate. The white solid was washed with methanol (3 × 10 mL) and the solvent was removed *in vacuo*. Deionized water (60 mL) was added to the resulting white solid, followed by addition of aqueous NaOH (150 mL, 1.0 M). The layers were separated and the aqueous phase was extracted with dichloromethane (3 × 20 mL). The combined extract was dried over anhydrous $MgSO_4$, filtered and the resulting solution was rotary evaporated to give a brown liquid. The liquid was distilled at 110 °C to afford a colourless oily liquid (2.92 g, 42% yield). ^{1}H NMR (500 MHz, $CDCl_3$): δ 7.36 (dd, 2H, J = 2.3 Hz, Ar*H*), 7.25 (dd, 3H, J = 2.1 Hz, Ar*H*), 2.85 (t, 2H, J = 6.9 Hz, CH_2N), 2.46 (t, 2H, J = 7.0 Hz, C≡C–CH_2), 1.72 (p, 2H, J = 6.9 Hz, CH_2–CH_2–CH_2), 1.22 (s, 2H, NH_2).

3.8 Attempted Preparative-Scale Catalytic Hydroamination/Cyclization Reactions

In the glove box, lanthanide amine bis(phenolate) complex *e.g.* $[O_2NN'^{t\text{-Bu}}]$HoN(SiMe$_3$)$_2$ (51.2 mg, 60.4 μmol) was loaded into a sealable reaction vessel equipped with a magnetic stirrer bar followed by benzene (10 mL). To another sealable reaction vessel was added 5-Phenyl-4-pentyn-1-amine (503 mg, 3.2 mmol) and benzene (4 mL). Both reaction vessels were brought out of the glove box, cycled on a Schlenk line and while under nitrogen flow, the 5-Phenyl-4-pentyn-1-amine/benzene mixture was transferred to the benzene/precatalyst mixture at 0 °C by syringe. The mixture was freeze-

pump-thaw degassed, warmed to room temperature and allowed to stir for 48 h. The solution was vacuum transferred into another sealable reaction vessel and the resulting yellow solution was transferred to a microdistillation vessel where atmospheric pressure distillation was conducted to afford a clear yellow oily liquid. The ^{1}H NMR analysis of the oily liquid was not informative as the signals were paramagnetically broadened. The oily liquid product was chromatographed on neutral alumina (600 mg), using diethyl ether (10 mL) as the eluent. The eluent was rotary evaporated to recover a yellow oily liquid quantitatively. ^{1}H NMR analysis showed the starting material resonances, however, the resonances were still paramagnetically broad.

3.9 Analytical-Scale Reactions of Ln Species with Aminoalkyne Substrate

In the glove box, a 10 mg/mL solution of lanthanide amide reagent *e.g.* $Yb\{N(SiMe_3)_2\}_3$ was obtained by dissolving $Yb\{N(SiMe_3)_2\}_3$ (5.7 mg, 6.5 μmol) in toluene (570 μL). A 10 mg/mL solution of amine bis(phenol) ligand *e.g.* $[O_2N_2^{t\text{-}Bu,Me}]H_2$ was obtained by dissolving $[O_2N_2^{t\text{-}Bu,Me}]H_2$ (2.20 mg, 5.0 μmol) in toluene (220 μL). 200 μL of the ytterbium amide solution and 200 μL of the $[O_2N_2^{t\text{-}Bu,Me}]H_2$ solution were mixed (1:1 v/v) in a vial and stirred for 4 h at room temperature. A 10 mg/mL solution of the 5-Phenyl-4-pentyne-1-amine was obtained by dissolving 5-Phenyl-4-pentyne-1-amine (41.4 mg, 26.0 mmol) in toluene (4.14 mL). 100 μL of the $Yb\{N(SiMe_3)_2\}_3$-$[O_2N_2^{t\text{-}Bu,Me}]H_2$ mixture and 100 μL of the 5-phenyl-4-pentyne-1-amine solution were mixed (1:1 v/v) in a vial and the hydroamination reaction mixture was stirred for an additional 2 h.

References for Chapter 3 begin on page 111

Using the same procedure, the 7 other analytical-scale hydroamination reactions were performed.

3.10 MALDI-TOF MS Analysis of Hydroamination Reaction Mixtures

MALDI-TOF MS analysis of the 8 hydroamination reaction mixtures were performed as follows: A 10 mg/mL solution of the anthracene matrix was prepared by dissolving 10 mg of anthracene in 1000 μL of toluene. 50 μL of the hydroamination reaction mixture e.g $Yb\{N(SiMe_3)_2\}_3$ and $[O_2N_2^{t\text{-}Bu,Me}]H_2$ was added to 50 μL of the anthracene solution (1:1 v/v) and the mixture was stirred for 2 minutes. Approximately 1 μL of the resulting solution was spotted on the plate (10 × 10 number grid) and allowed to dry. At the same time, alongside the of reaction mixture samples, 1 μL of the original 10 mg/mL solution of hydroamination reaction mixture *e.g.* $Yb\{N(SiMe_3)_2\}_3$ and $[O_2N_2^{t\text{-}Bu,Me}]H_2$ also mixed with matrix was spotted on another space on the plate and allowed to dry. When dry, the sample plate was placed inside two Ziploc bags, removed from the glove box and rapidly transferred to the spectrometer for analysis.

$Yb\{N(SiMe_3)_2\}_3$-$[O_2N_2^{t\text{-}Bu,Me}]H_2$ + $PhC_5H_6NH_2$

MALDI-TOF MS (anthracene matrix): *m/z* (peak identified): 647 ($[(O_2N_2^{t\text{-}Bu,Me})YbN'' + H - 2\ t\text{-}Bu - Me]^+$), 814 ($[(O_2N_2^{t\text{-}Bu,Me})YbN'' + H + PhC_5H_6NH_2 - SiMe_3 - 3\ Me]^+$)

$Yb\{N(SiMe_3)_2\}_3$-$[O_2N_2^{t\text{-}Bu}]H_2$ + $PhC_5H_6NH_2$

MALDI-TOF MS (anthracene matrix): *m/z* (peak identified): 731 ($[(O_2N_2^{t\text{-}Bu})YbN'' + H - 2\ t\text{-}Bu - Me]^+$), 898 ($[(O_2N_2^{t\text{-}Bu})YbN'' + H + PhC_5H_6NH_2 - SiMe_3 - 3\ Me]^+$)

$Yb\{N(SiMe_3)_2\}_3$-$[O_2NN'^{t\text{-}Bu}]H_2$ + $PhC_5H_6NH_2$

MALDI-TOF MS (anthracene matrix): *m/z* (peak identified): 696 ($[(O_2NN'^{t\text{-}Bu})Yb]^+$), 731 ($[(O_2NN'^{t\text{-}Bu})YbN'' + H - 2\ t\text{-}Bu - Me]^+$), 948 ($[(O_2NN'^{t\text{-}Bu})YbN'' + toluene]^+$), 1006 ($[(O_2NN'^{t\text{-}Bu})YbN'' + anthracene - 2\ Me]^+$).

$Yb\{N(SiMe_3)_2\}_3$-$[O_2NN'^{t\text{-}Am}]H_2$ + $PhC_5H_6NH_2$

MALDI-TOF MS (anthracene matrix): *m/z* (peak identified): 775 ($[O_2NN'^{t\text{-}Am})YbN'' - SiMe_3 - t\text{-}Am - Me]^+$), 1032 ($[O_2NN'^{t\text{-}Am})YbN'' + anthracene - 4\ Me]^+$), 1089 ($[O_2NN'^{t\text{-}Am})YbN'' + anthracene - H]^+$).

$Ho\{N(SiMe_3)_2\}_3$-$[O_2N_2^{t\text{-}Bu,Me}]H_2$ + $PhC_5H_6NH_2$

MALDI-TOF MS (anthracene matrix): *m/z* (peak identified): 638 ($[(O_2N_2^{t\text{-}Bu,Me})HoN'' + H - 2\ t\text{-}Bu - Me]^+$), 804 ($[(O_2N_2^{t\text{-}Bu,Me})HoN'' + H + PhC_5H_6NH_2 - SiMe_3 - 3\ Me]^+$).

Ho{N(SiMe$_3$)$_2$}$_3$-[O$_2$N$_2^{t\text{-Bu}}$]H$_2$ + PhC$_5$H$_6$NH$_2$

MALDI-TOF MS (anthracene matrix): *m/z* (peak identified): 722 ([(O$_2$N$_2^{t\text{-Bu}}$)HoN″ + H– 2 *t*-Bu – Me]$^+$), 889 ([(O$_2$N$_2^{t\text{-Bu}}$)HoN″ + H + PhC$_5$H$_6$NH$_2$ – SiMe$_3$ – 3 Me]$^+$).

Ho{N(SiMe$_3$)$_2$}$_3$-[O$_2$NN$^{t\text{-Bu}}$]H$_2$ + PhC$_5$H$_6$NH$_2$

MALDI-TOF MS (anthracene matrix): m/z (peak identified): 686 ([(O$_2$NN$^{t\text{-Bu}}$)Ho]$^+$), 721 ([(O$_2$NN$^{t\text{-Bu}}$)HoN″ + H– 2 *t*-Bu – Me]$^+$), 939 ([(O$_2$NN$^{t\text{-Bu}}$)HoN″ + toluene]$^+$), 997 ([(O$_2$NN$^{t\text{-Bu}}$)HoN″ + anthracene – 2 Me]$^+$).

Ho{N(SiMe$_3$)$_2$}$_3$-[O$_2$NN$^{t\text{-Am}}$]H$_2$ + PhC$_5$H$_6$NH$_2$

MALDI-TOF MS (anthracene matrix): m/z (peak identified): 747 ([(O$_2$NN$^{t\text{-Am}}$)HoN″ – SiMe$_3$ – *t*-Am2 – 2Me]$^+$), 1024 ([(O$_2$NN$^{t\text{-Am}}$)HoN″ + anthracene – 4 Me]$^+$), 1081 ([(O$_2$NN$^{t\text{-Am}}$)HoN″ + anthracene – H]$^+$).

3.11 References:

1. (a) Kerton, F. M.; Whitwood, A. C.; Willans, C. E. *Dalton Trans.*, **2004**, 2237; (b) Yao, Y.; Ma, M.; Xu, X.; Zhang, Y.; Shen, Q.; Wong, W. *Organometallics* **2005,** *24,* 4014.

2. Li, Y.; Marks T. J. *J. Am. Chem. Soc.*, **1996,** *118,* 9295.

3. Khan, M. N. *J. Org. Chem.*, **1996,** *61,* 8063; (b) Khan, M. N. *J. Org. Chem.*, **1995**, *60*, 4536.

4. Giardello, M. A.; Conticello, V. P.; Brard, L.; Gagné, M. R.; Marks, T. J. *J. Am. Chem. Soc.*, **1994**, *116,* 10241.

5. Kim, H.; Livinghouse, T.; Seomoon, D.; Lee, P. H. *Bull. Korean Chem. Soc.*, **2007**, *28*, 1127.

6. Beavis, R. C.; Chait, B. T. *Rapid Commun. Mass Spectrom.*, **1989**, *3*, 233.

7. Horneffer, V.; Dreisewerd, K.; Luedemann, H. C.; Hillenkamp, F.; Laege, M.; Strupat, K. *Int. J. Mass Spectrom.*, **1999**, *85/186/187*, 859.

8. Knochenmuss, R.; Zenobi, R. *Chem Rev.*, **2003**, *103,* 441.

9. Tshuva, E. Y.; Goldberg, I.; Kol, M. *Organometallics,* **2001,** *20,* 3017.

10. Motta, A.; Lanza, G.; Fragala, I. L.; Marks, T. J. *Organometallics,* **2004,** *23,* 4097.

11. Tobisch, S. *J. Chem. Soc.*, **2005**, *127*, 11979.

12. Tobisch, S. *Chem. Eur. J.*, **2006**, *12*, 2520.

13. Motta, A.; Fragala, I. L.; Marks, T. J. *Organometallics,* **2006,** *25,* 5533.

References for Chapter 3 begin on page 111

14. Panda, T. K.; Zulys, A.; Gamer, M. T.; Roesky, P. W. *Organometallics,* **2005,** *24,* 2197.

15. Gribkov, D. V.; Hultzsch, K. C.; Hampel, F. *Chem. Eur. J.,* **2003**, *9*, 4796.

References for Chapter 3 begin on page 111

Chapter 4

Conclusion and Future Work

4.1 Conclusion

The characterization of paramagnetic organolanthanide species is heavily dependent on the growth of single crystals and X-ray crystallographic structure determination. In many cases, crystals are difficult to grow and if grown take a long period of time. In addition, catalytically-active complexes are often difficult to isolate, and the analysis of paramagnetic species in solution by NMR spectroscopy, is not informative, as evidenced in this thesis.

Investigations performed and presented in this MSc. thesis have shown that MALDI-TOF MS can be applied to the rapid screening of reactions of highly moisture-sensitive organolanthanide complexes. In Chapter 2, complexation reactions of lanthanide amide reagents with amine bis(phenol) ligands were assessed using MALDI-TOF MS. The technique confirmed in real-time the ligand coordination to the lanthanide metal centers. Although parent ion peaks were not observed, this could be attributed to difficulties in ionizing Ln^{3+} complexes by charge-transfer. The Ln^{3+} ions were in their highest stable oxidation state thereby resisting one electron-oxidation. However, peaks for lanthanide arene complexes formed *in situ* were seen. A mechanism for the ionization of the complexes in the spectrometer was postulated to have occurred via adduct formation. This mechanism was supported by the isotope distribution patterns, in which the

experimental and theoretical isotope patterns were in good agreement. In Chapter 3, hydroamination/cyclization reactions of 5-phenyl-4-pentyne-amine were attempted using various organolanthanide complexes. NMR spectroscopy did not provide any conclusive information due to paramagnetic nature of the organolanthanide complexes. The results obtained with MALDI-TOF MS gave some insight into the hydroamination reactions at room temperature. However, further experiments are needed before definite conclusions can be drawn. Although, the hydroamination product was not obtained, the MS results indicate that the aminoalkyne substrate may have coordinated to the $[O_2N_2]$-based lanthanide complexes. This observation may indicate that the complexes could be efficient precatalysts at slight elevated experimental temperature. Based on these results, it has been shown that MALDI-TOF MS possesses the potetial to be applied to many other paramagnetic non-moisture and moisture sensitive complexes, especially towards rapid screening of libraries of catalysts. The technique could also be valuable in studying many other lanthanide-centered reactions.

4.2 Future Work

Although arene adducts of lanthanide metals are observed and formed *in-situ* during the MS experiment as part of the ionization process, it remains to be seen whether arene adducts form within the spectrometer with other suitable metal centers such as Cr(0) which is in its lowest oxidation state but is known to form arene complexes e.g. $[Cr(\eta^6\text{-}C_6H_6)_2]$.

Furthermore, the arene complex formation can be investigated using tandem mass spectrometry (MS-MS); such an experiment would allow for detailed elucidation of the

References for Chapter 4 begin on page 118

arene adduct structure. This approach would also act to confirm the peak assignments and may allow many other reactions to be studied in this way.

4.2.1 Tandem MS-MS (MALDI-QTOF-MS/MS)

MALDI tandem mass spectrometry is an ion-desorption mass spectrometry technique designed for probing the structures of compounds. The technique has been used widely in the area of proteins analysis.[1-3] Tandem mass spectrometry analysis involves the dissociation of fragment ion of interest into small units, thus obtaining detailed compositional information of the fragment ion. The instrument consists of two quadrupoles Q1 (MS1), and Q2 followed by a reflecting TOF mass analyzer (MS2) as shown in **Figure 4.1**.[4] Q1 is a mass analyzer operated in radio frequency-only mode, which filters and selects only the particular precursor and/or fragment ion of interest. The ion e.g. arene complex ion is then accelerated to a certain voltage before entering the collision cell Q2, where it undergoes collision induced dissociation (CID) after the first few collisions with natural gas molecules (usually argon or nitrogen). The ensuing fragment ions are collected as daughter-ion spectrum by the TOF mass analyzer and their components ions are interpreted for structural elucidation. The most significant advantage of the method is the ability of detecting all species simultaneously and selecting *m/z* of the fragment ion with high resolution, thereby increasing selectivity and reducing signal-to-noise ratio.[5]

References for Chapter 4 begin on page 118

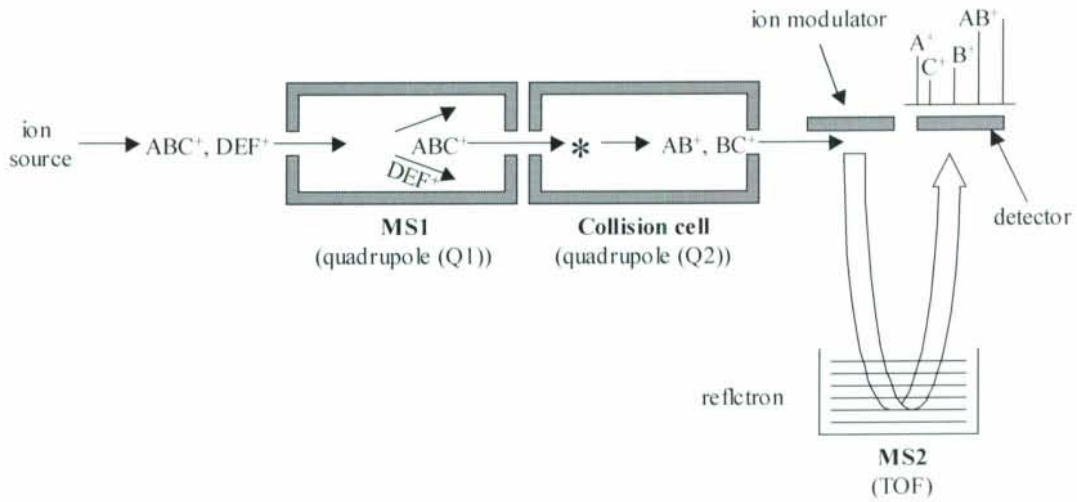

Figure 4.1 Schematic diagram of tandem Q-TOF mass spectrometer

4.2.2 Hydroamination Catalytic Reaction Scope

The results obtained for the intramolecular hydroamination/cyclization reaction of aminoalkyne revealed some coordination of the aminoalkyne substrate to the metal center. The trend of the coordination of the aminoalkyne substrate to the metal centers suggests that structural factors may have played a role in these observations. Kol *et al.*[6] reported that larger chelate ring size may result in different bond lengths and angles around the metal center, thereby affecting the reactivity. Although Kol's work is related to polymerization, it is necessary to understand the effect of this factor on hydroamination reactions. The pendant nitrogen donor may have brought about steric congestion hindering the substrate to coordinate to the metal center. Therefore, further experiments could be carried out to investigate the influence of the chelate ring size on the

References for Chapter 4 begin on page 118

hydroamination reactions. The investigation can be expanded to include variation of the chelate ring size of the [O_2NN'] ligand by removal of a methylene unit between the two nitrogen donors.

Since hydroamination of aminoalkynes is exothermic it might be expected that the hydroamination product would be observed at room temperature. In this study no hydroamination product was observed, however, coordination of the aminoalkyne substrate to the metal center is a promising result. Therefore, conducting the hydroamination reaction experiments at variable temperatures will be necessary. This will enable the investigation into the transference of the proton from the aminoalkyne substrate to the amide ligand. In addition to increasing the temperature, the reactivity over a longer time scale should also be performed in order see whether the catalytic cycle will proceed. The influence of metal loading on the catalytic activity will also have to be studied. Finally, the scope of catalytic hydroamination/cyclization reactions needs to be further investigated using a series of aminoalkyne substrates including bulky and nonbulky aminoalkynes. This will enable for the mechanistic study of the reaction and the determination of dependency of cyclization rate on the nature of the aminoalkyne substrate, the ligand and metal center. All these experiments will help determine whether the lanthanide amine bis(pheolate) complexes are active hydroamination precatalysts.

References for Chapter 4 begin on page 118

4.3 References:

1. Omaetxebarria, M. J.; Hagglund, P.; Elortza, F.; Hooper, N.; M. Arizmendi, J. M.; Jensen, O. N. *Anal. Chem.*, **2006**, *78*, 3335.
2. Gogichaeva, N. V.; Williams, T.; Alterman M. A. *J. Am. Soc. Mass Spectrom.*, **2007**, *18*, 279.
3. Shevchenko, A.; Loboda, A.; Shevchenko, A.; Ens, W.; Standing, K. G. *Anal. Chem.*, **2000,** *72*, 2132.
4. Henderson, W.; McIndoe, J. S. *Mass Spectrometry of Inorganic and Organometallic Compounds*; John Wiley & Sons Ltd: Chichester, 2005.
5. Chernushevich, I. V.; Loboda, A. V.; Thomson, B. A. *J. Mass Spectrom.*, **2001**, *36*, 849.
6. Tshuva, E. Y.; Goldberg, I.; Kol, M. *Organometallics*, **2001,** *20*, 3017.

References for Chapter 4 begin on page 118

Appendices

^{1}H NMR Spectra and MALDI-TOF Mass Spectra

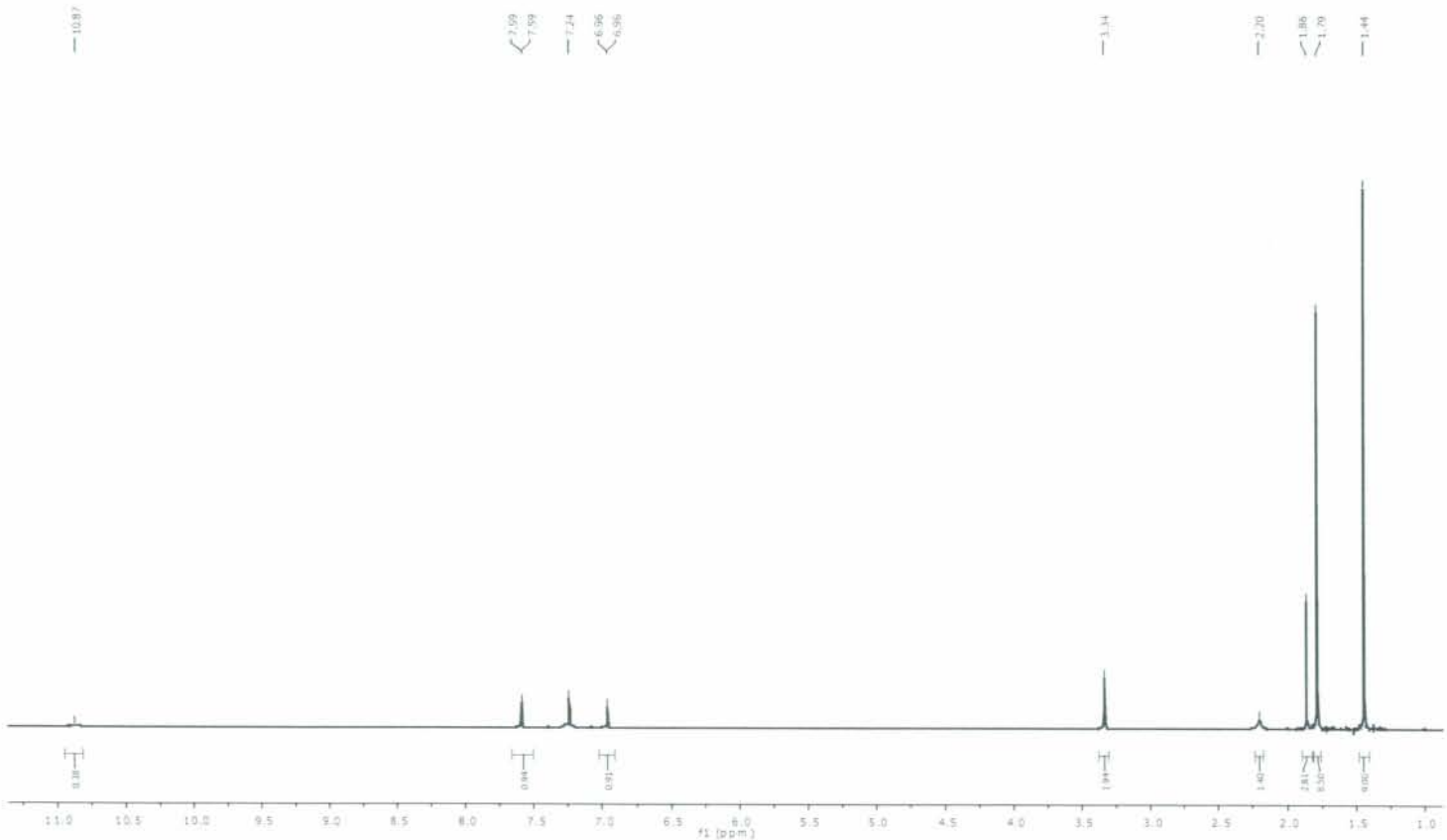

Appendix 2.1 ^{1}H NMR spectrum of $[O_2N_2{}^{t\text{-Bu}}]H_2$

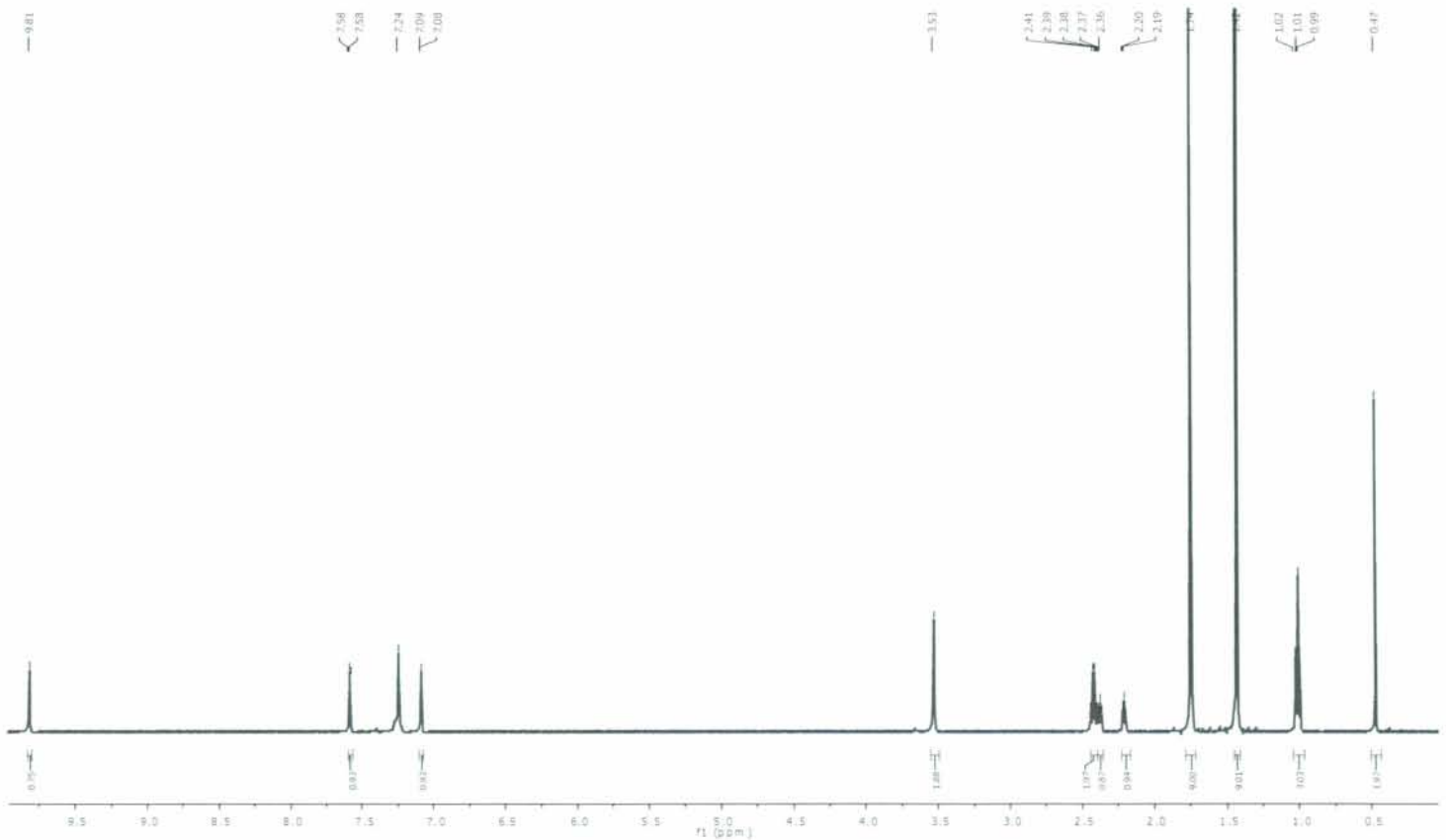

Appendix 2.2 ^{1}H NMR spectrum of $[O_2NN'^{t\text{-}Bu}]H_2$

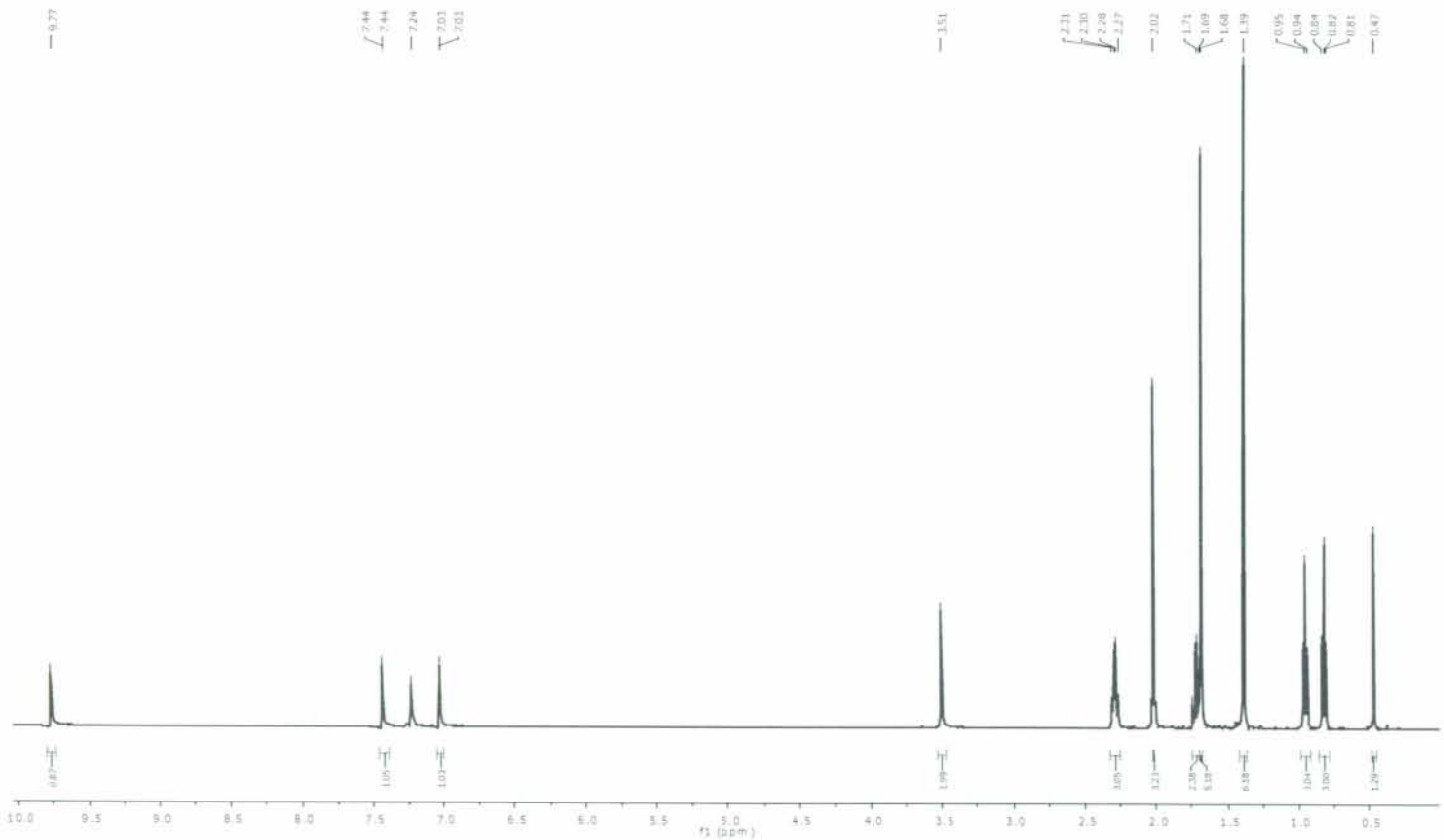

Appendix 2.3 ^{1}H NMR spectrum of $[O_2NN'^{t\text{-Am}}]H_2$

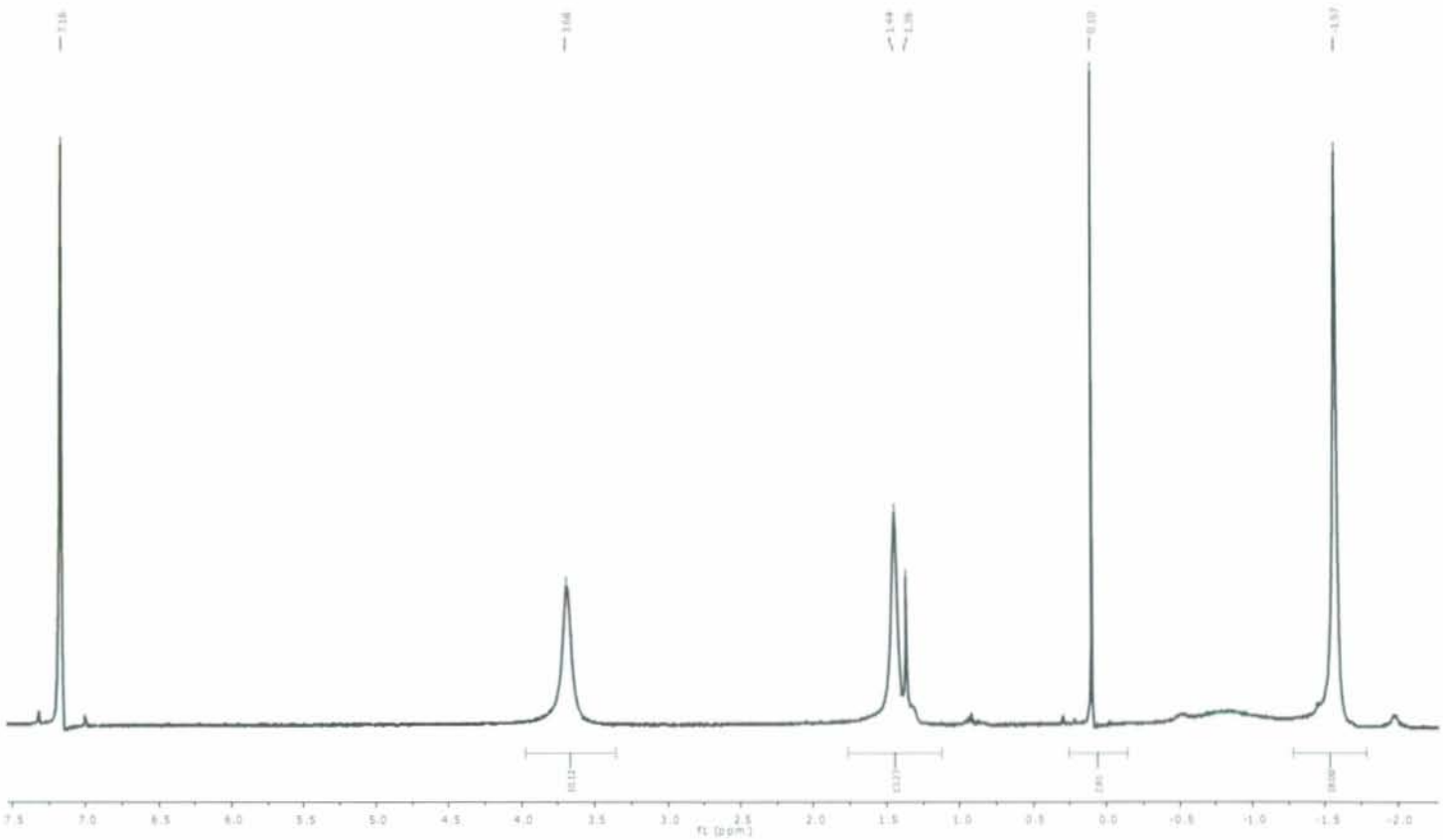

Appendix 2.4 ^{1}H NMR spectrum of $Sm\{N(SiMe_3)_2\}_3$

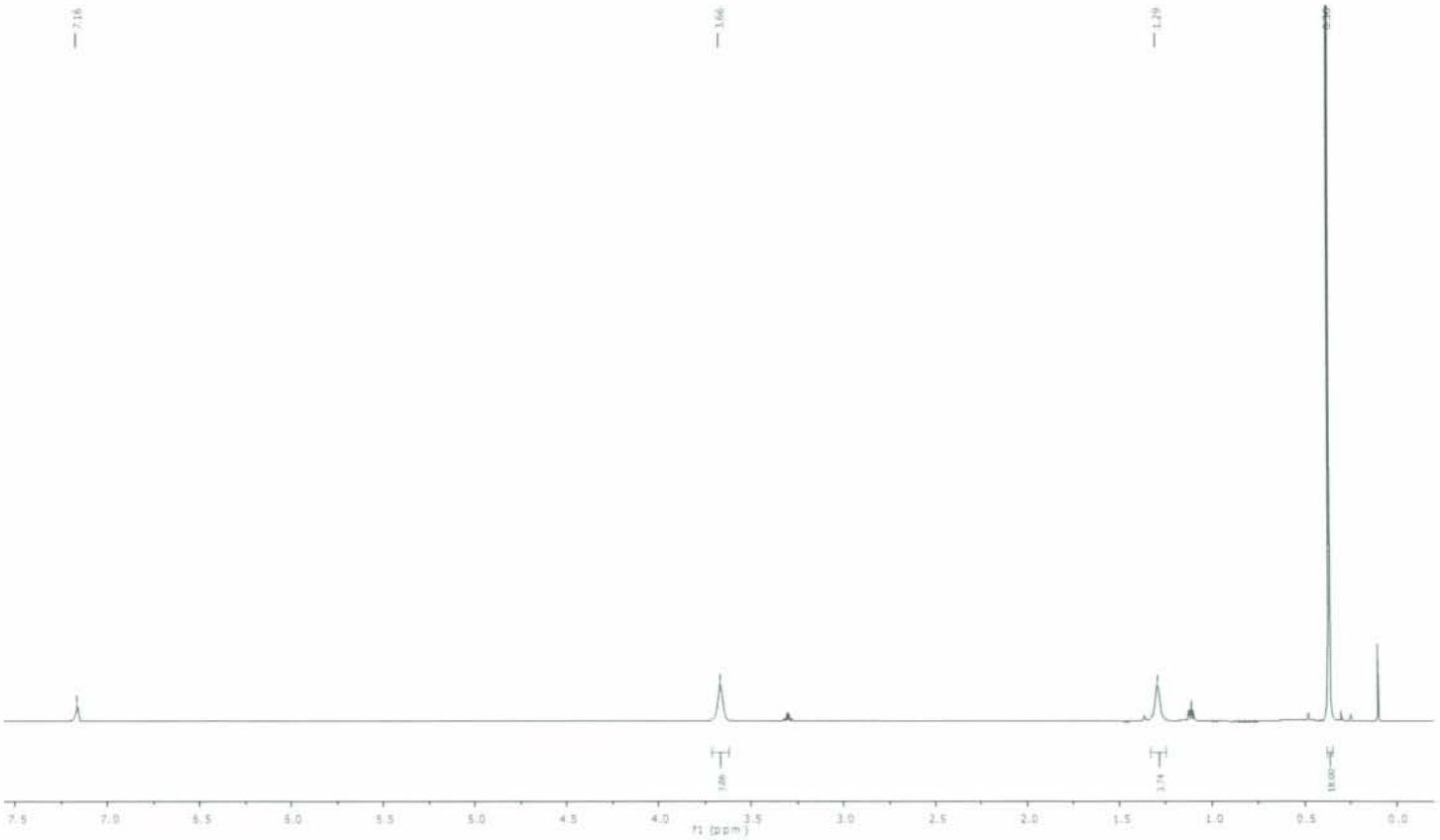

Appendix 2.5 ^{1}H NMR spectrum of La{N(SiMe$_3$)$_2$}$_3$

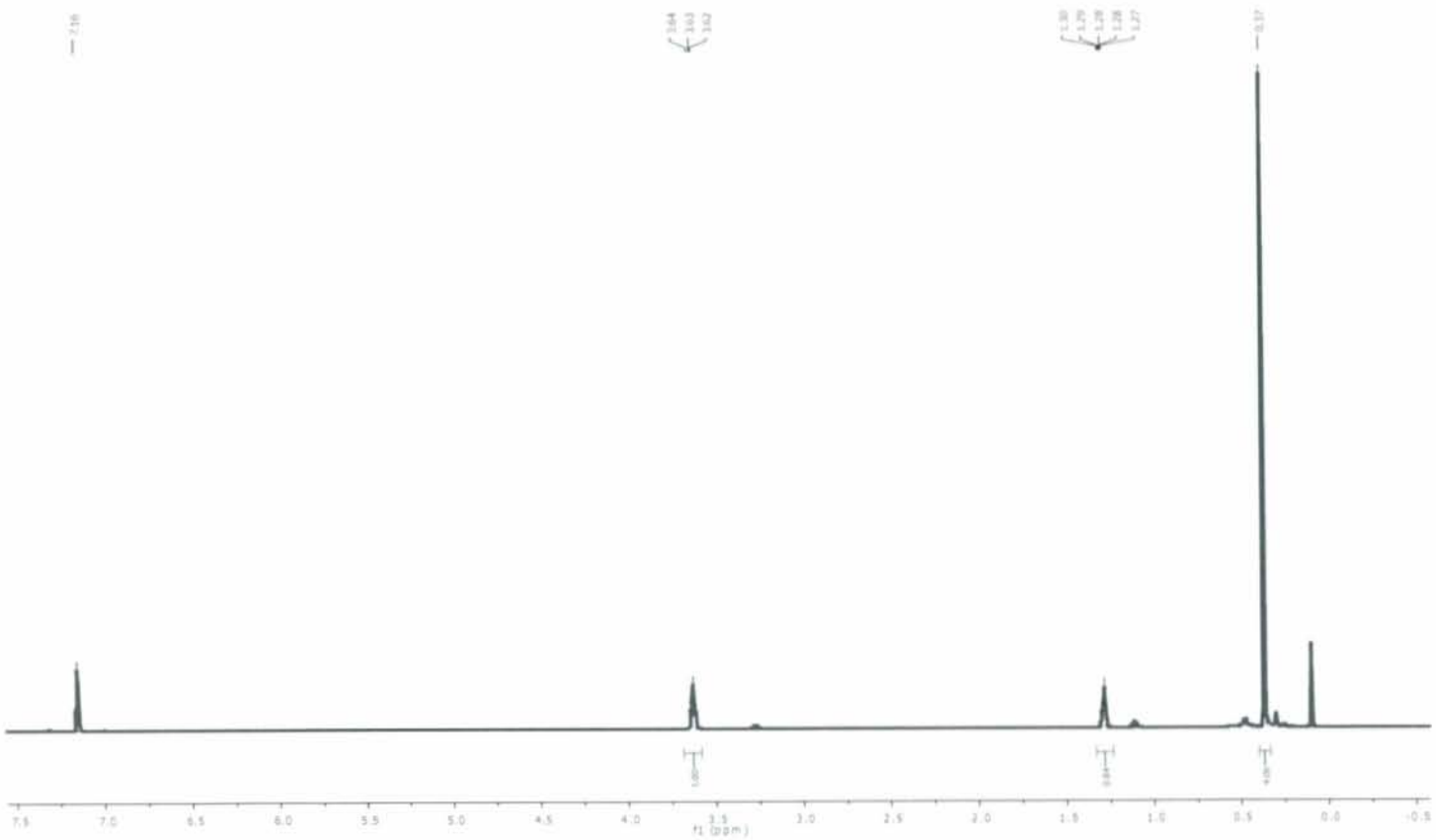

Appendix 2.6 ^{1}H NMR spectrum of $Y\{N(SiMe_3)_2\}_3$

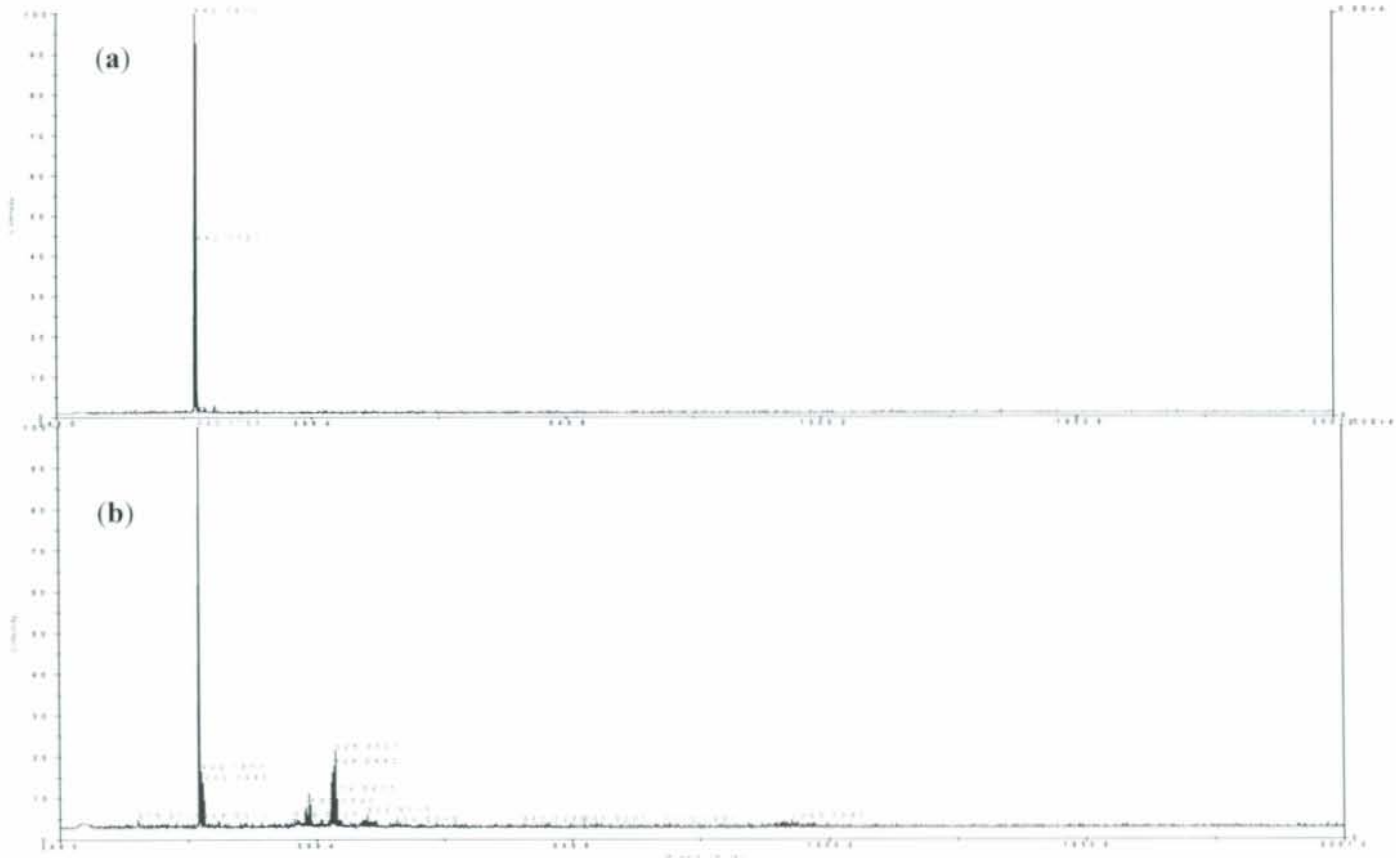

Appendix 2.7.1 MALDI-TOF MS spectra of (**a**) $[O_2N_2^{t\text{-Bu,Me}}]H_2$; (**b**) reaction mixture of $Sm\{N(SiMe_3)_2\}_3$ and $[O_2N_2^{t\text{-Bu,Me}}]H_2$

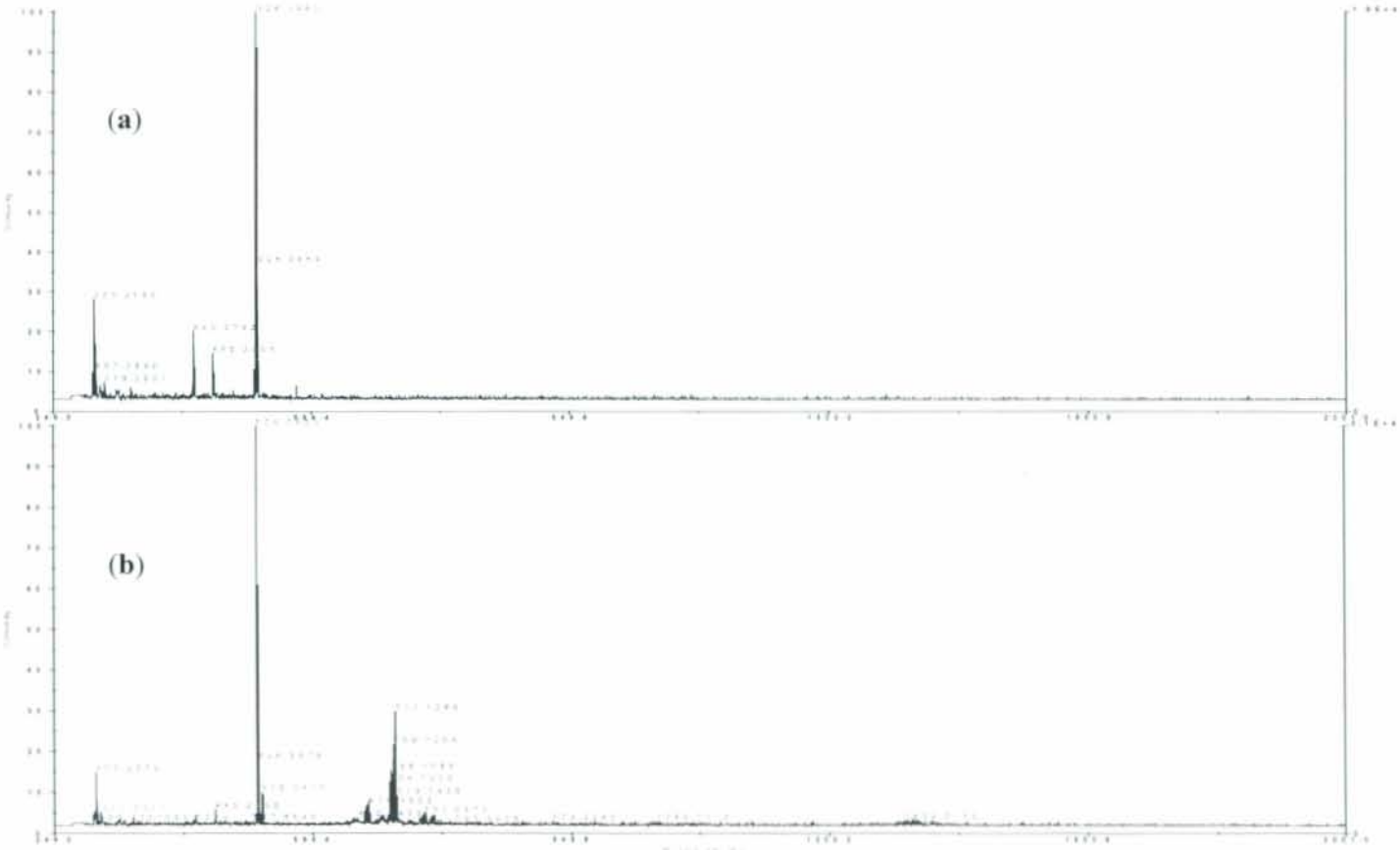

Appendix 2.7.2 MALDI-TOF MS spectra of (**a**) $[O_2N_2^{t\text{-}Bu}]H_2$; (**b**) reaction mixture of $Sm\{N(SiMe_3)_2\}_3$ and $[O_2N_2^{t\text{-}Bu}]H_2$

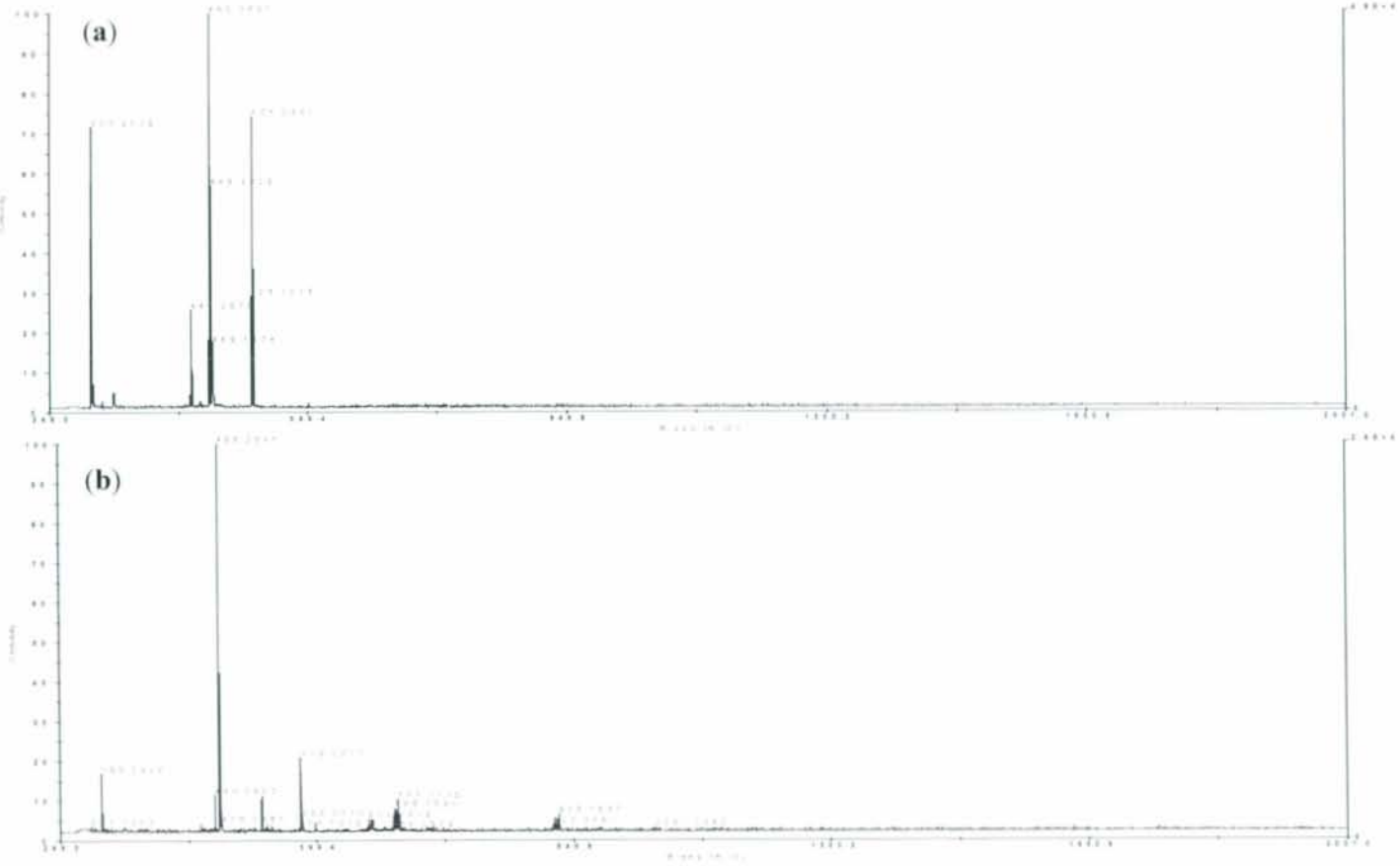

Appendix 2.7.3 MALDI-TOF MS spectra of (**a**) $[O_2NN'^{t\text{-}Bu}]H_2$; (**b**) reaction mixture of $Sm\{N(SiMe_3)_2\}_3$ and $[O_2NN'^{t\text{-}Bu}]H_2$

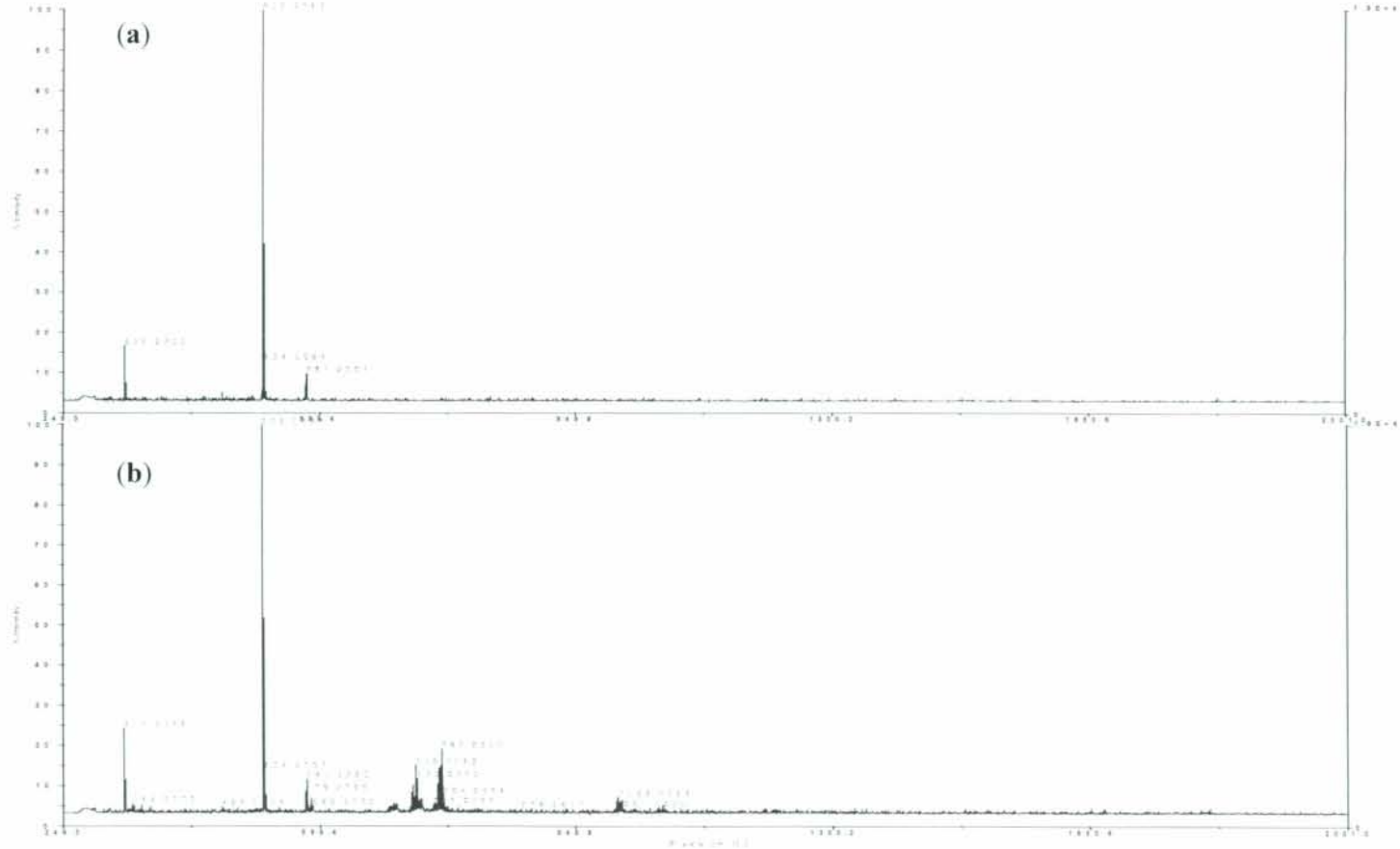

Appendix 2.7.4 MALDI-TOF MS spectra of (**a**) $[O_2NN^{t\text{-}Am}]H_2$; (**b**) reaction mixture of $Sm\{N(SiMe_3)_2\}_3$ and $[O_2NN^{t\text{-}Am}]H_2$

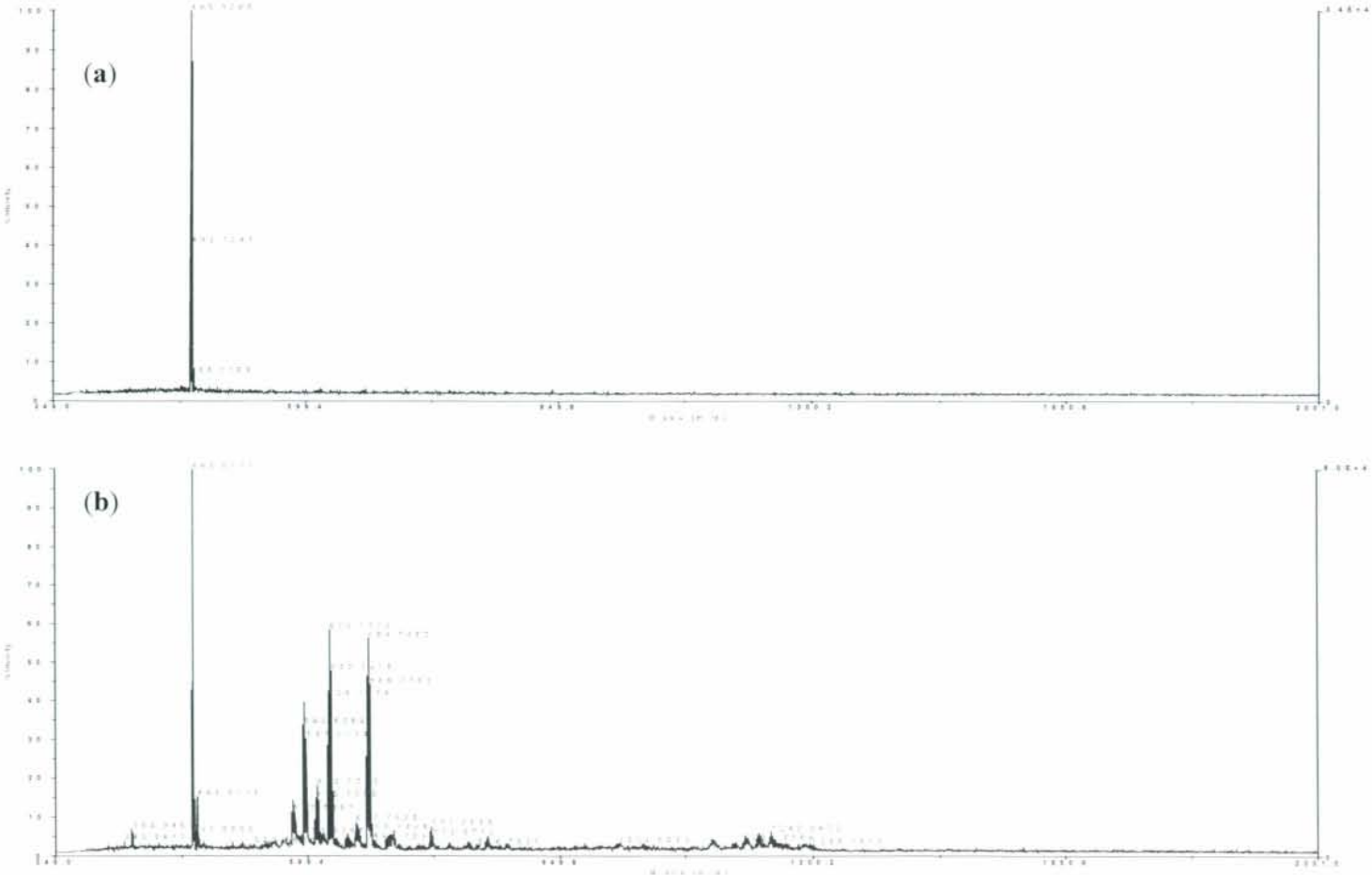

Appendix 2.7.5 MALDI-TOF MS spectra of (**a**) $[O_2N_2^{t\text{-Bu,Me}}]H_2$; (**b**) reaction mixture of $Gd\{N(SiMe_3)_2\}_3$ and $[O_2N_2^{t\text{-Bu,Me}}]H_2$

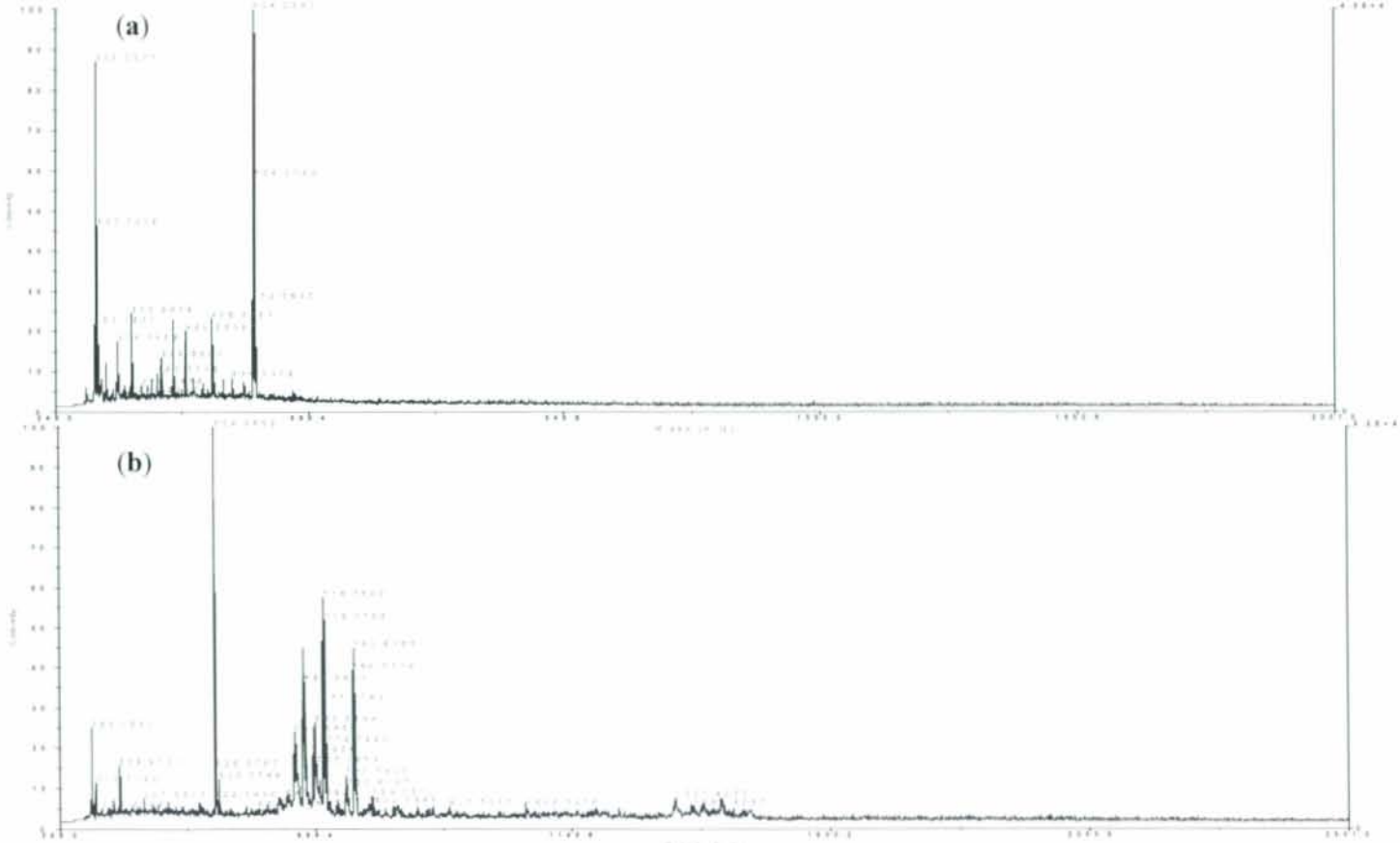

Appendix 2.7.6 MALDI-TOF MS spectra of (**a**) $[O_2N_2^{t\text{-}Bu}]H_2$; (**b**) reaction mixture of $Gd\{N(SiMe_3)_2\}_3$ and $[O_2N_2^{t\text{-}Bu}]H_2$

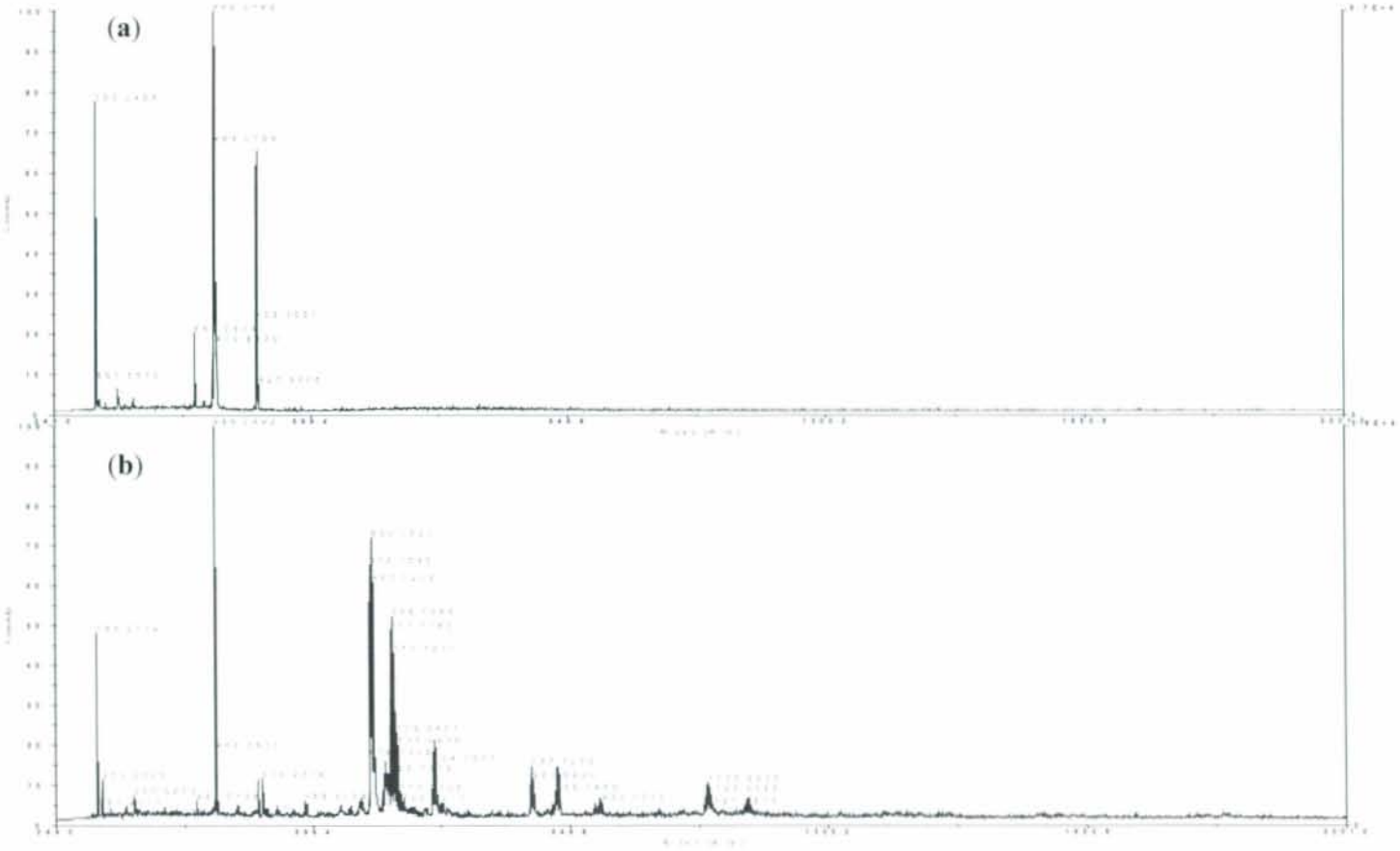

Appendix 2.7.7 MALDI-TOF MS spectra of (**a**) $[O_2NN'^{t\text{-}Bu}]H_2$; (**b**) reaction mixture of $Gd\{N(SiMe_3)_2\}_3$ and $[O_2NN'^{t\text{-}Bu}]H_2$

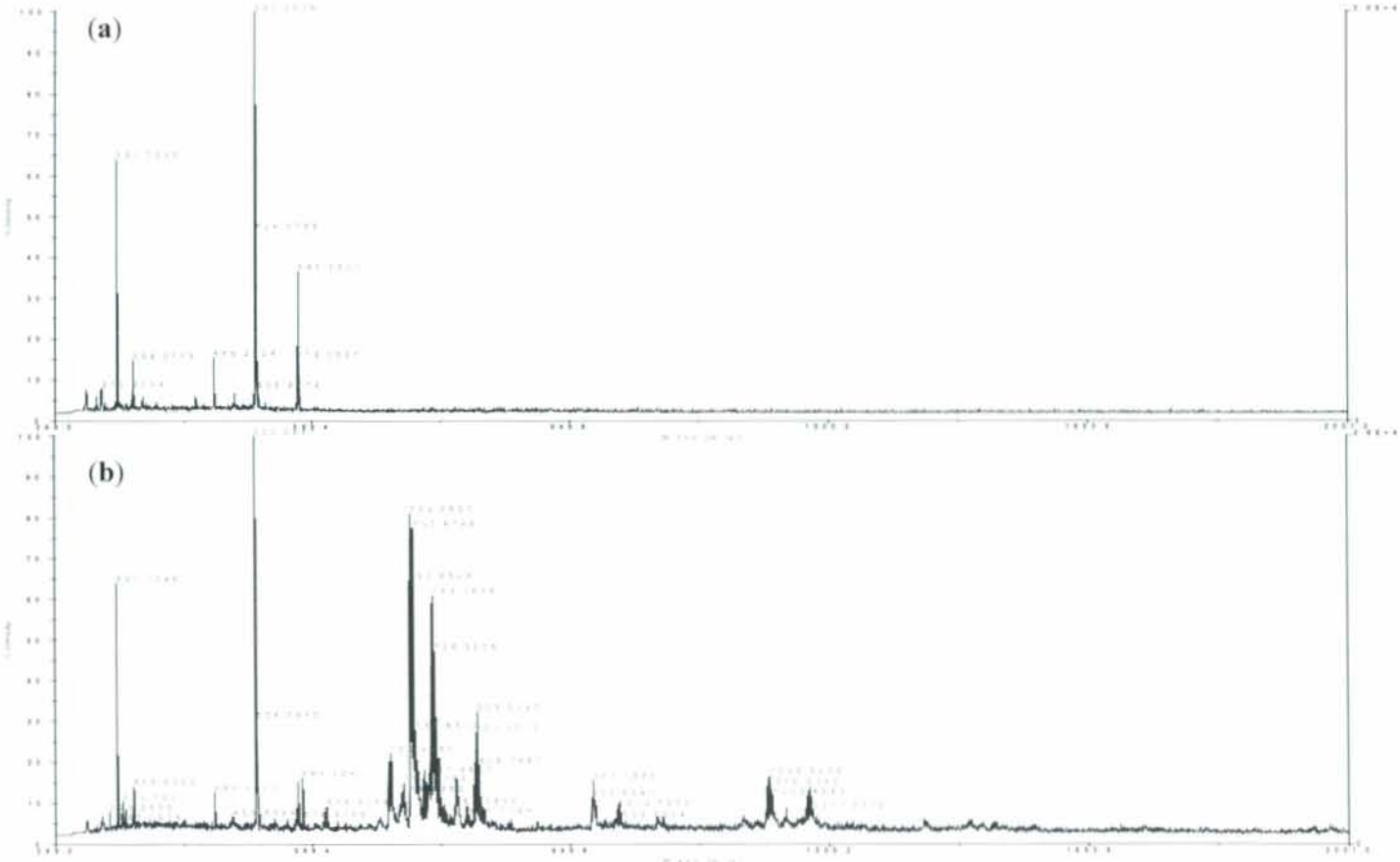

Appendix 2.7.8 MALDI-TOF MS spectra of (**a**) $[O_2NN'^{t\text{-}Am}]H_2$; (**b**) reaction mixture of $Gd\{N(SiMe_3)_2\}_3$ and $[O_2NN'^{t\text{-}Am}]H_2$

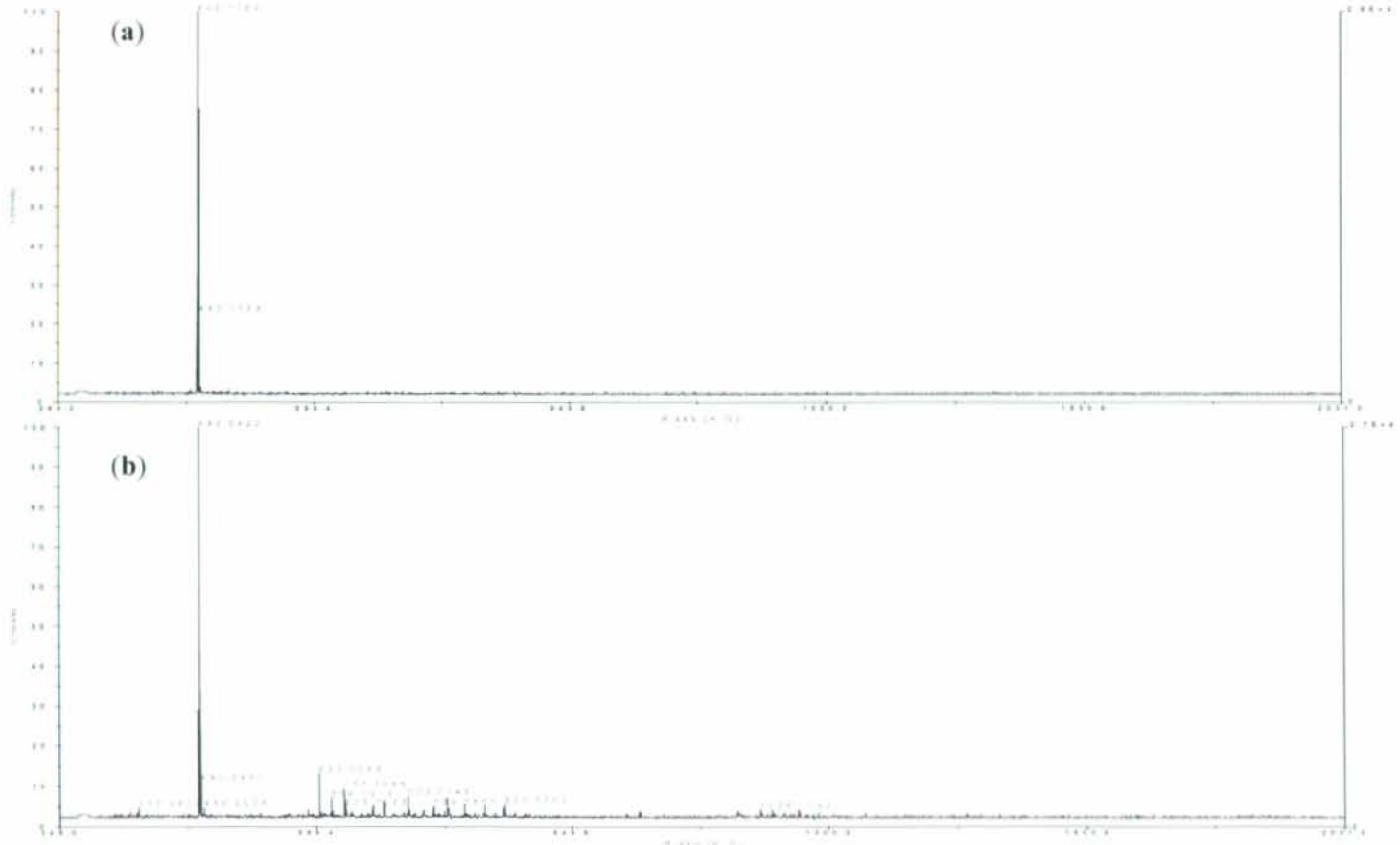

Appendix 2.7.9 MALDI-TOF MS spectra of (**a**) $[O_2N_2^{t\text{-Bu,Me}}]H_2$; (**b**) reaction mixture of $Ho\{N(SiMe_3)_2\}_3$ and $[O_2N_2^{t\text{-Bu,Me}}]H_2$

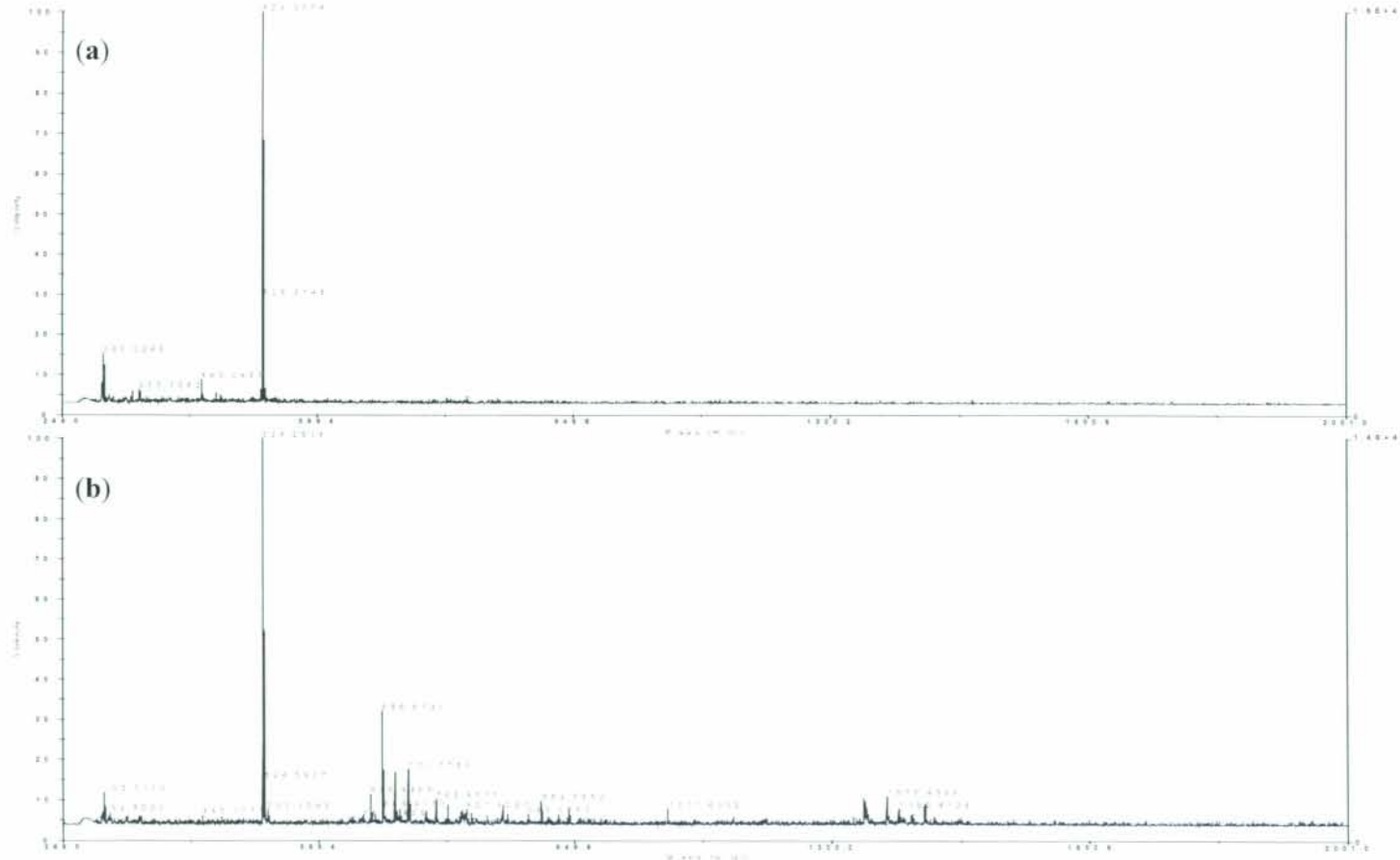

Appendix 2.7.10 MALDI-TOF MS spectra of (**a**) $[O_2N_2^{t\text{-Bu}}]H_2$; (**b**) reaction mixture of $Ho\{N(SiMe_3)_2\}_3$ and $[O_2N_2^{t\text{-Bu}}]H_2$

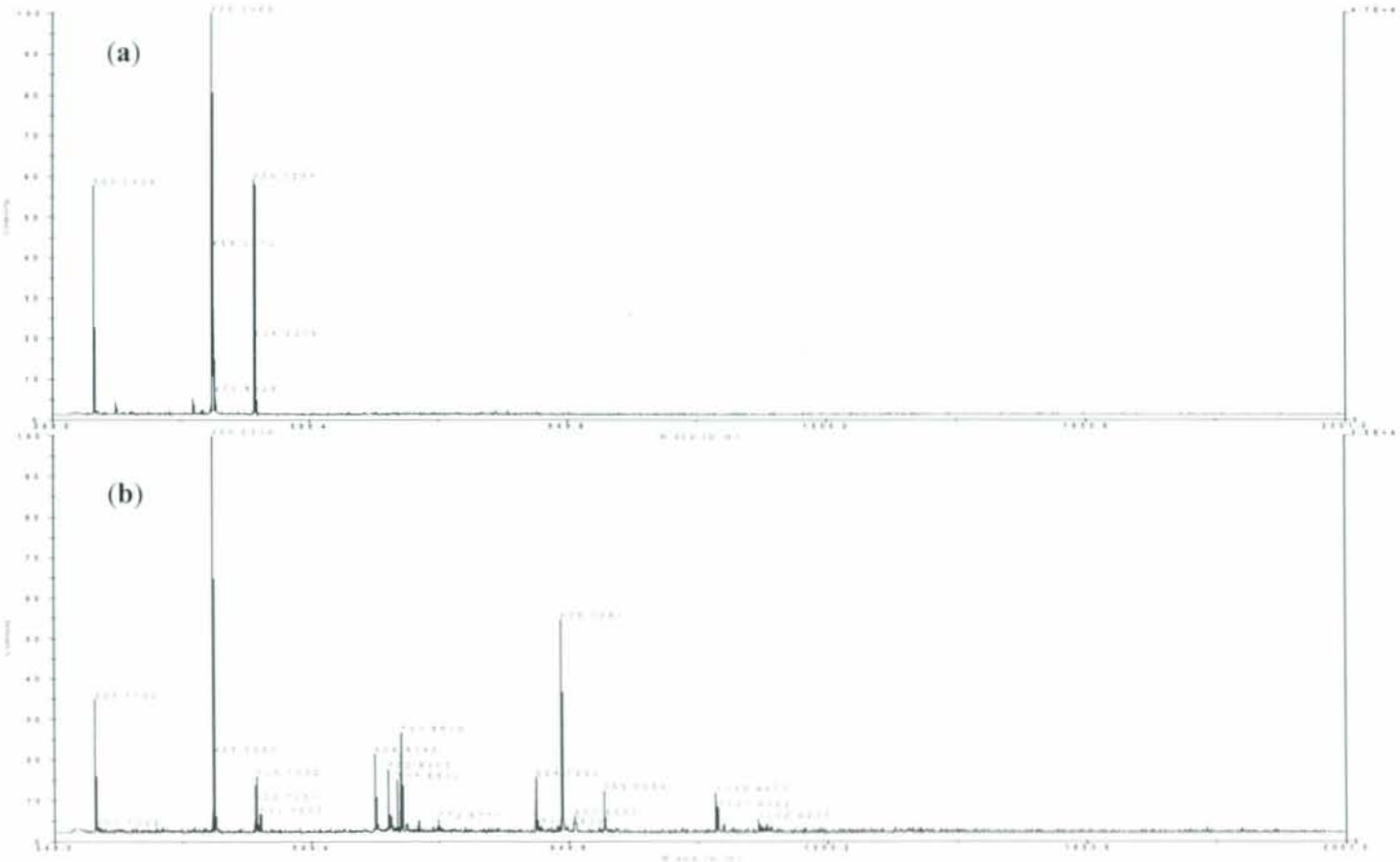

Appendix 2.7.11 MALDI-TOF MS spectra of (**a**) $[O_2NN'^{t\text{-Bu}}]H_2$; (**b**) reaction mixture of $Ho\{N(SiMe_3)_2\}_3$ and $[O_2NN'^{t\text{-Bu}}]H_2$

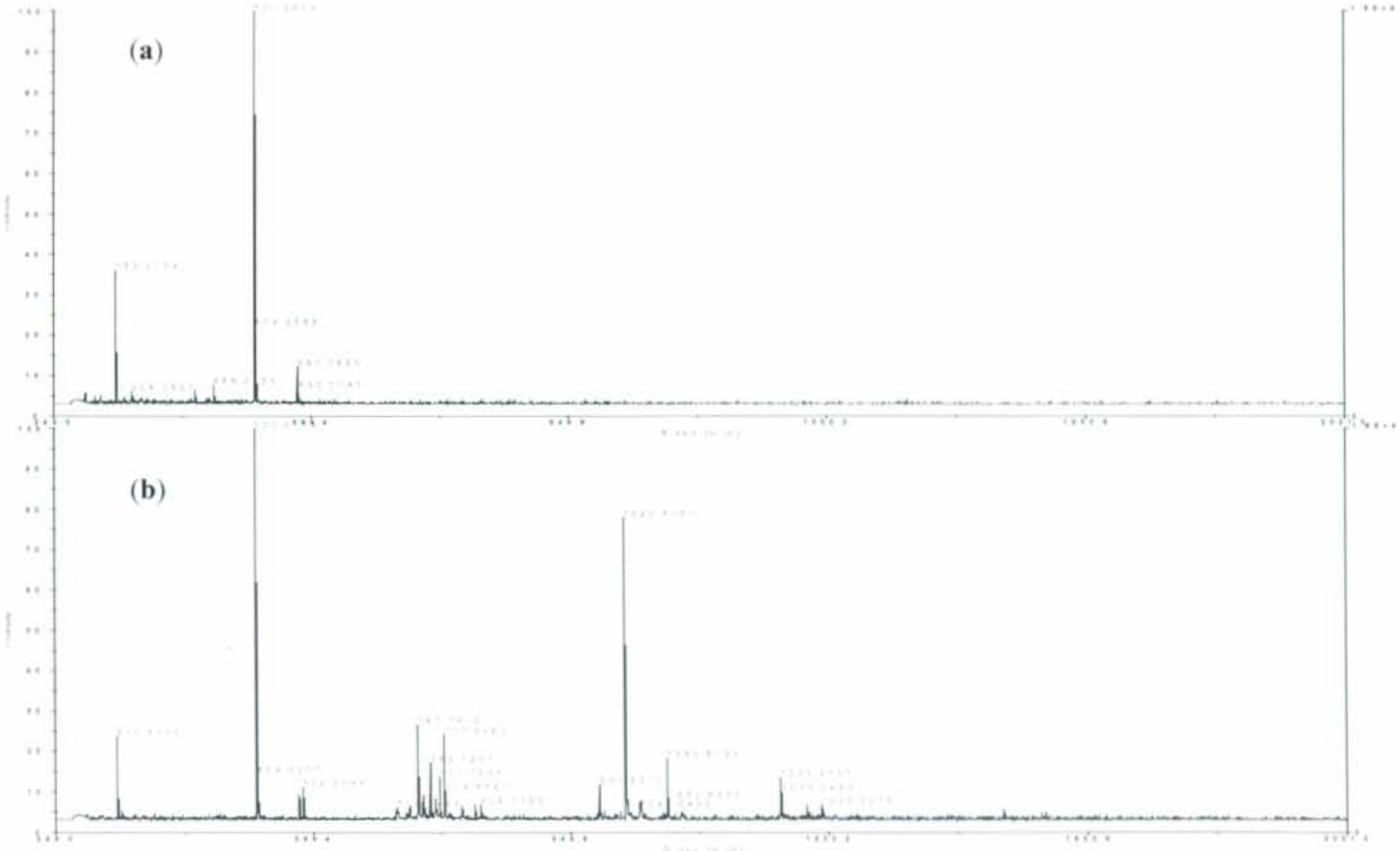

Appendix 2.7.12 MALDI-TOF MS spectra of (**a**) $[O_2NN'^{t\text{-}Am}]H_2$; (**b**) reaction mixture of $Ho\{N(SiMe_3)_2\}_3$ and $[O_2NN'^{t\text{-}Am}]H_2$

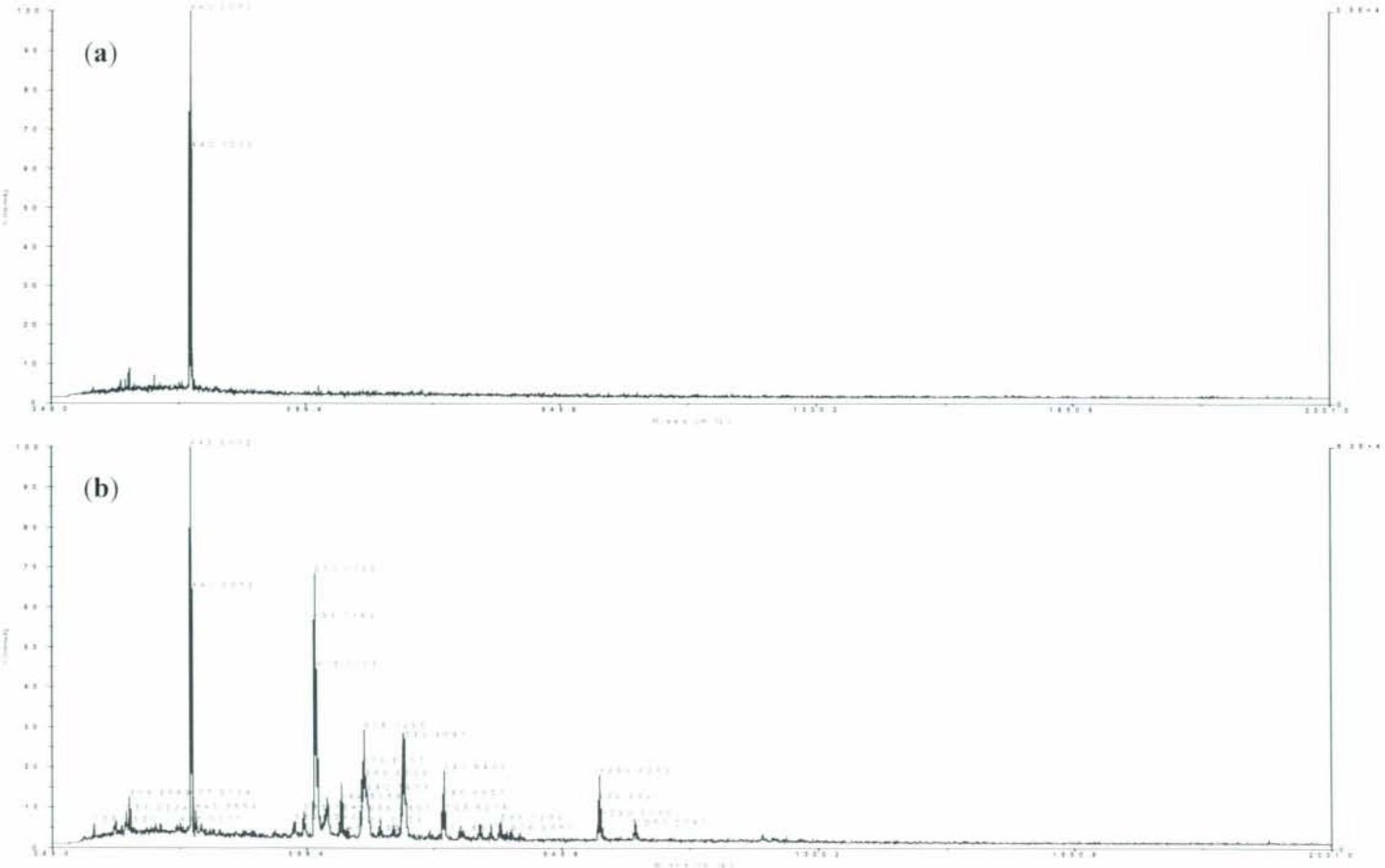

Appendix 2.7.13 MALDI-TOF MS spectra of (**a**) $[O_2N_2^{t\text{-Bu,Me}}]H_2$; (**b**) reaction mixture of $Yb\{N(SiMe_3)_2\}_3$ and $[O_2N_2^{t\text{-Bu,Me}}]H_2$

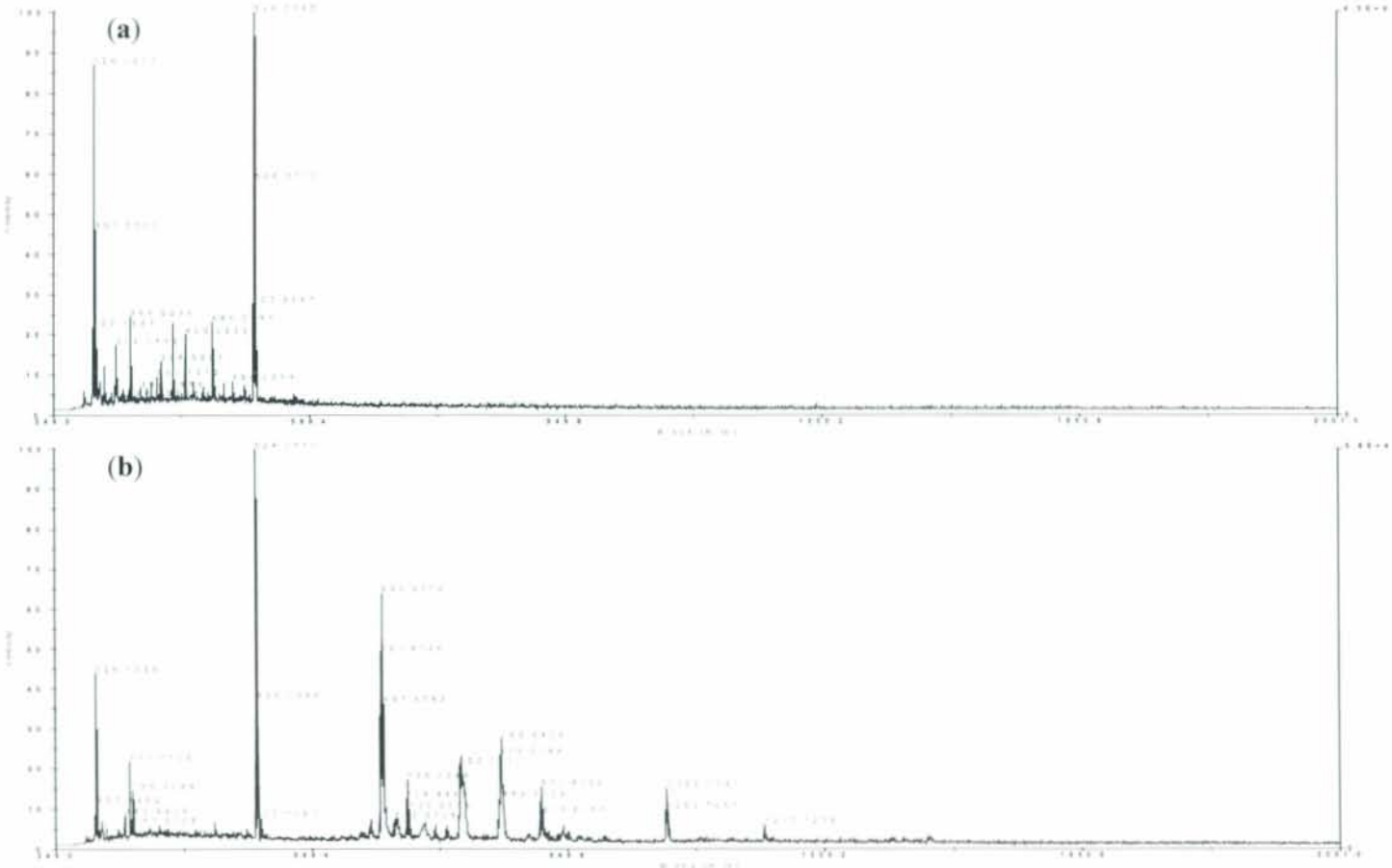

Appendix 2.7.14 MALDI-TOF MS spectra of (**a**) $[O_2N_2^{t\text{-}Bu}]H_2$; (**b**) reaction mixture of $Yb\{N(SiMe_3)_2\}_3$ and $[O_2N_2^{t\text{-}Bu}]H_2$

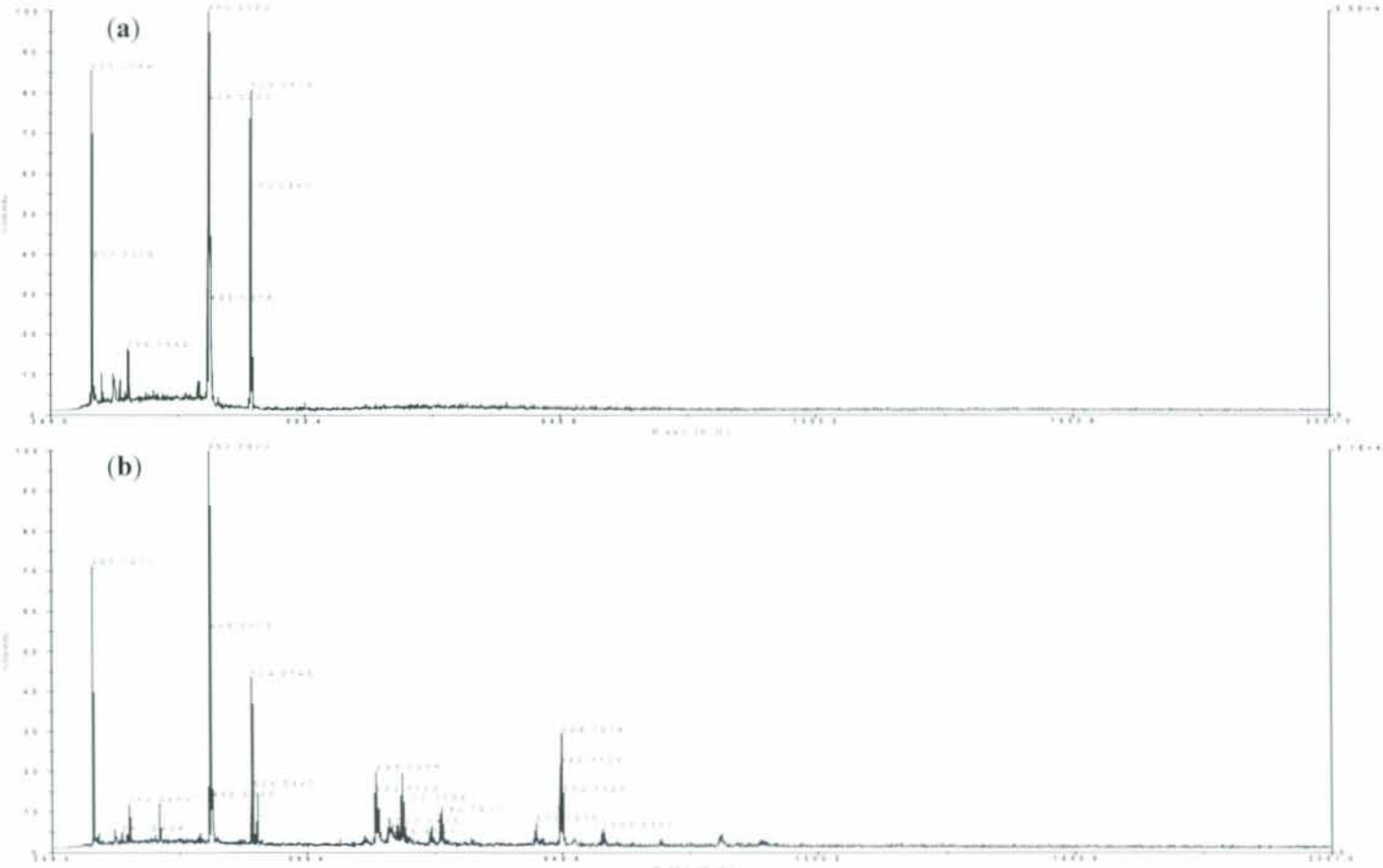

Appendix 2.7.15 MALDI-TOF MS spectra of (**a**) $[O_2NN'^{t\text{-}Bu}]H_2$; (**b**) reaction mixture of $Yb\{N(SiMe_3)_2\}_3$ and $[O_2NN'^{t\text{-}Bu}]H_2$

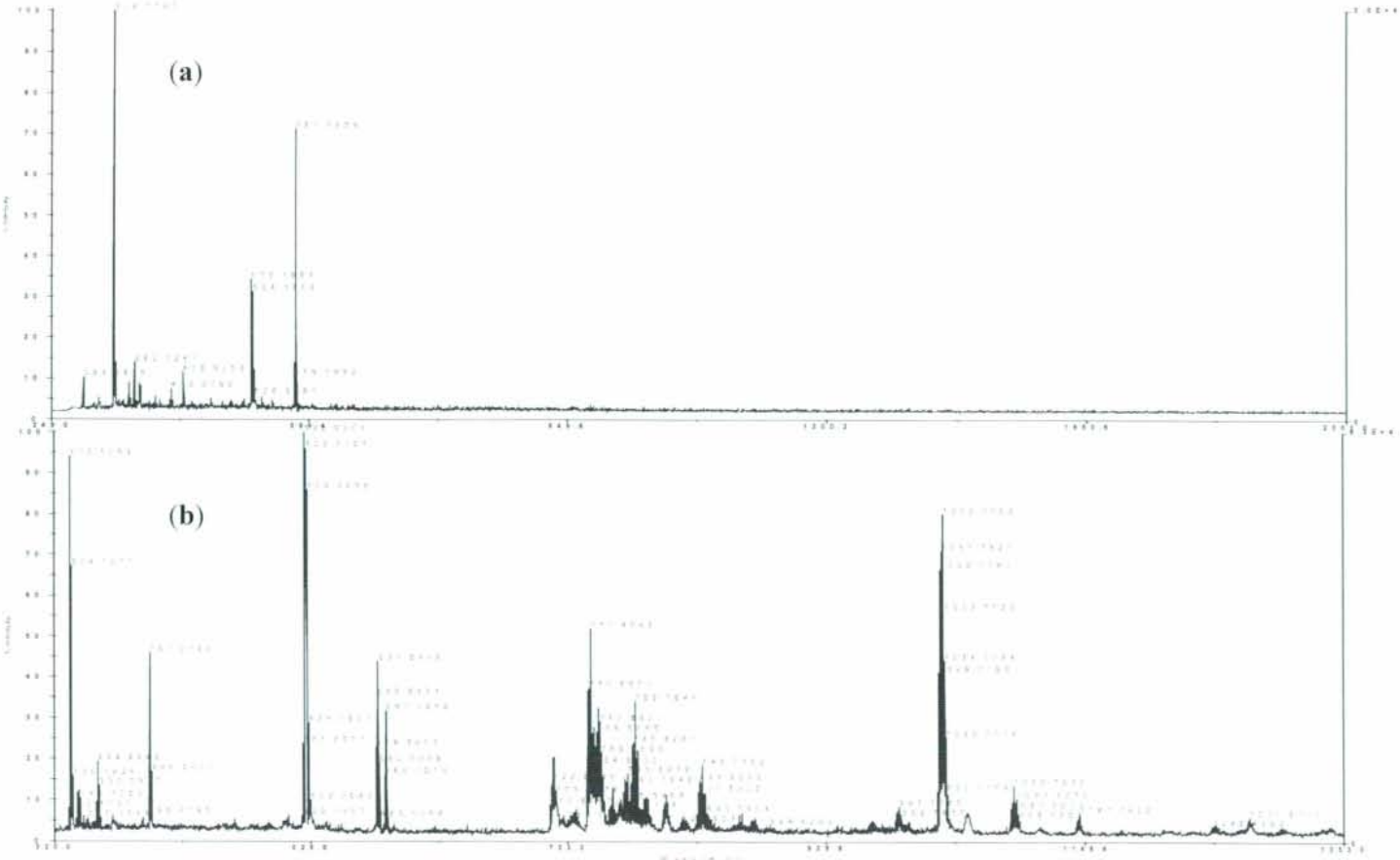

Appendix 2.7.16 MALDI-TOF MS spectra of (**a**) $[O_2NN'^{t\text{-}Am}]H_2$; (**b**) reaction mixture of $Yb\{N(SiMe_3)_2\}_3$ and $[O_2NN'^{t\text{-}Am}]H_2$

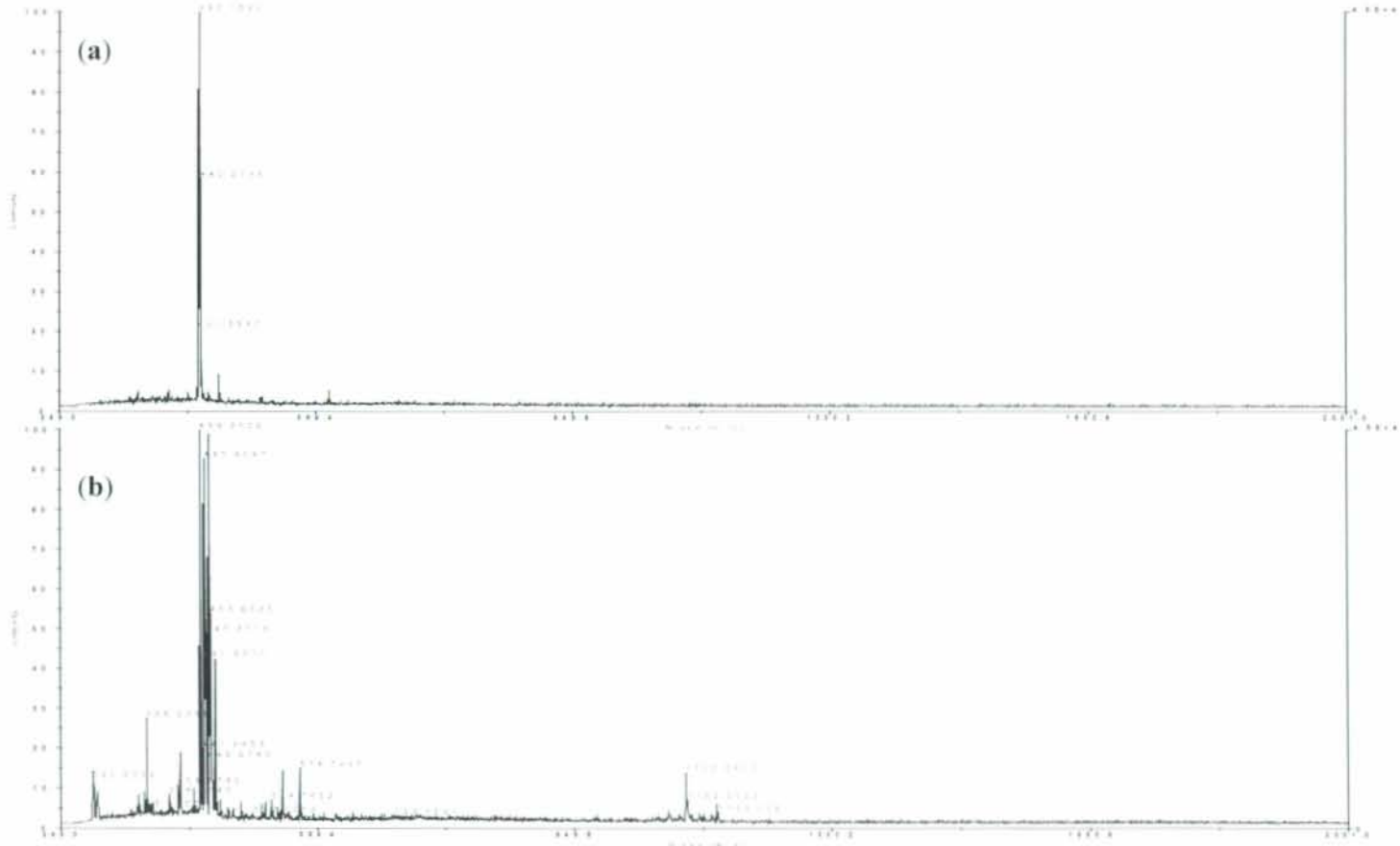

Appendix 2.7.17 MALDI-TOF MS spectra of (**a**) $[O_2N_2^{t\text{-Bu,Me}}]H_2$; (**b**) reaction mixture of $Y\{N(SiMe_3)_2\}_3$ and $[O_2N_2^{t\text{-Bu,Me}}]H_2$

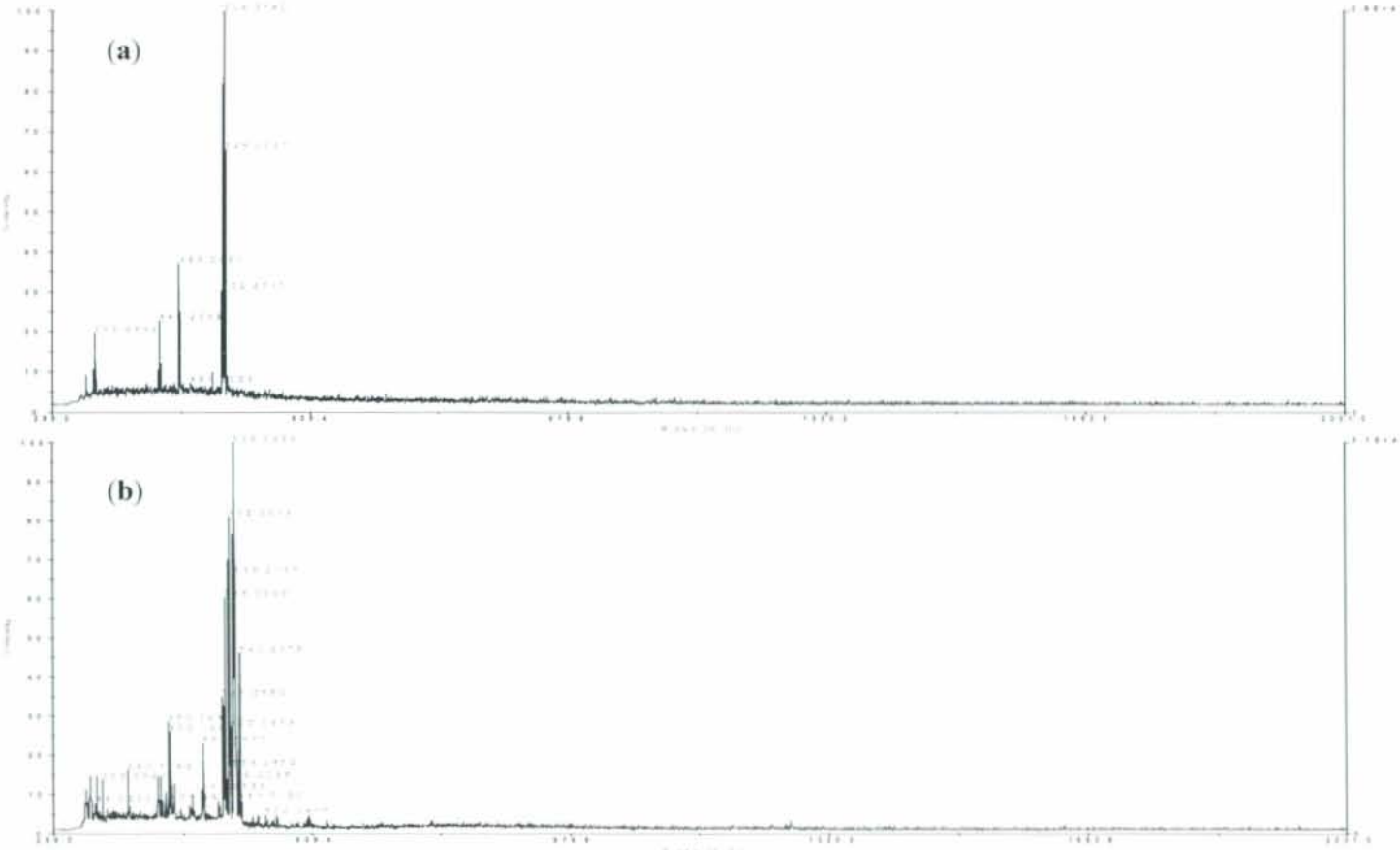

Appendix 2.7.18 MALDI-TOF MS spectra of (**a**) $[O_2N_2^{t\text{-}Bu}]H_2$; (**b**) reaction mixture of $Y\{N(SiMe_3)_2\}_3$ and $[O_2N_2^{t\text{-}Bu}]H_2$

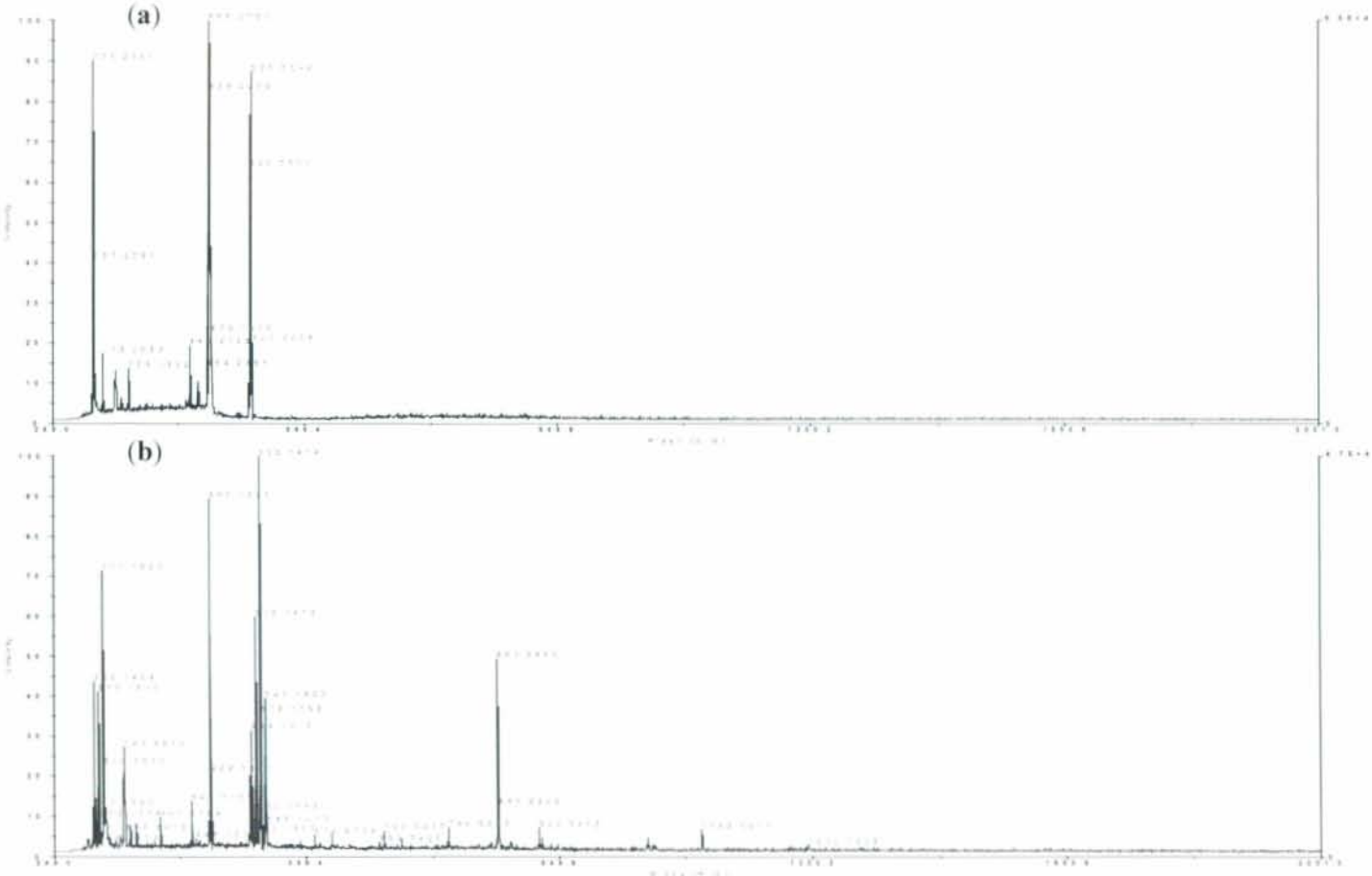

Appendix 2.7.19 MALDI-TOF MS spectra of (**a**) $[O_2NN'^{t\text{-}Bu}]H_2$; (**b**) reaction mixture of $Y\{N(SiMe_3)_2\}_3$ and $[O_2NN'^{t\text{-}Bu}]H_2$

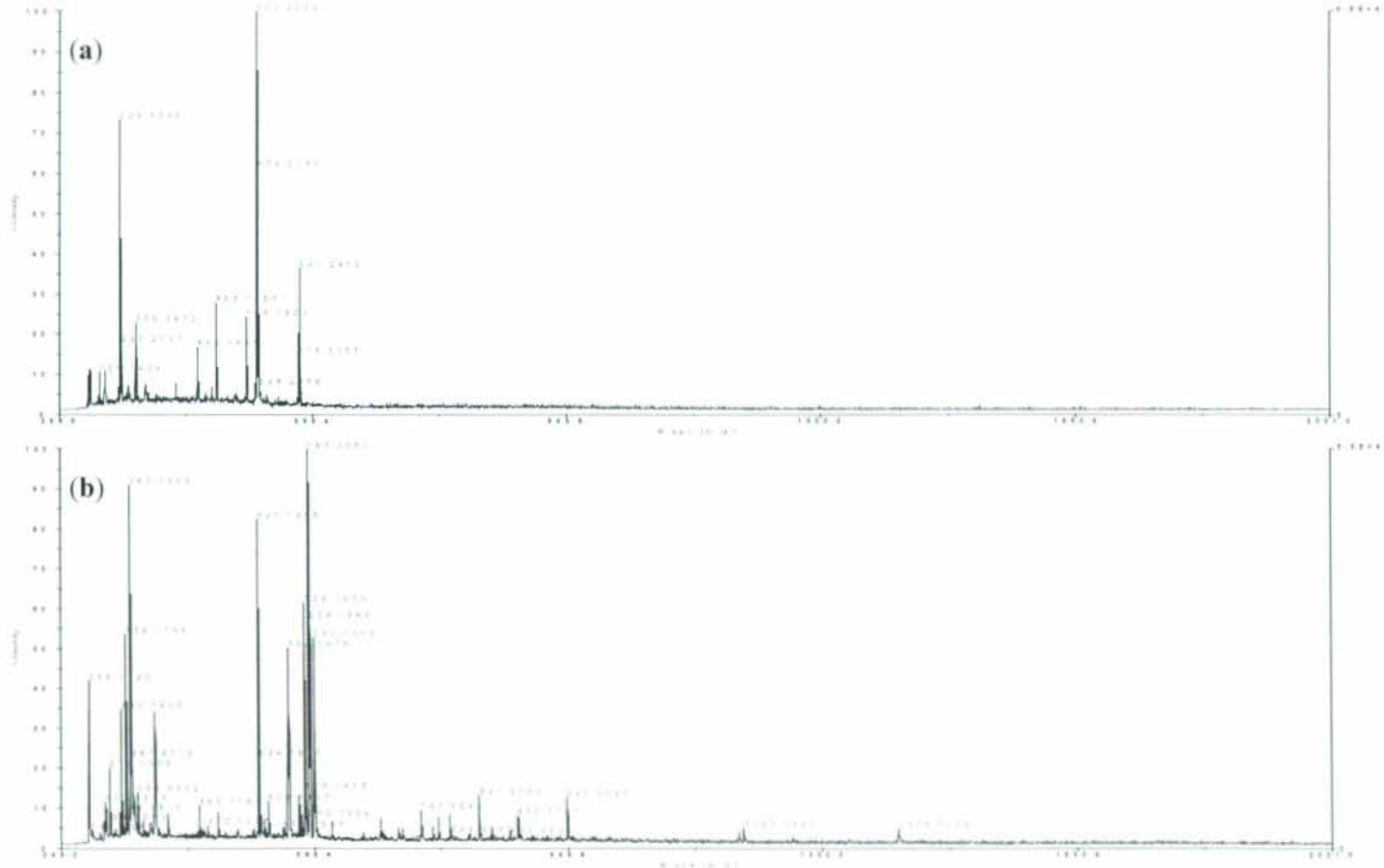

Appendix 2.7.20 MALDI-TOF MS spectra of (**a**) $[O_2NN^{tt\text{-}Am}]H_2$; (**b**) reaction mixture of $Y\{N(SiMe_3)_2\}_3$ and $[O_2NN^{tt\text{-}Am}]H_2$

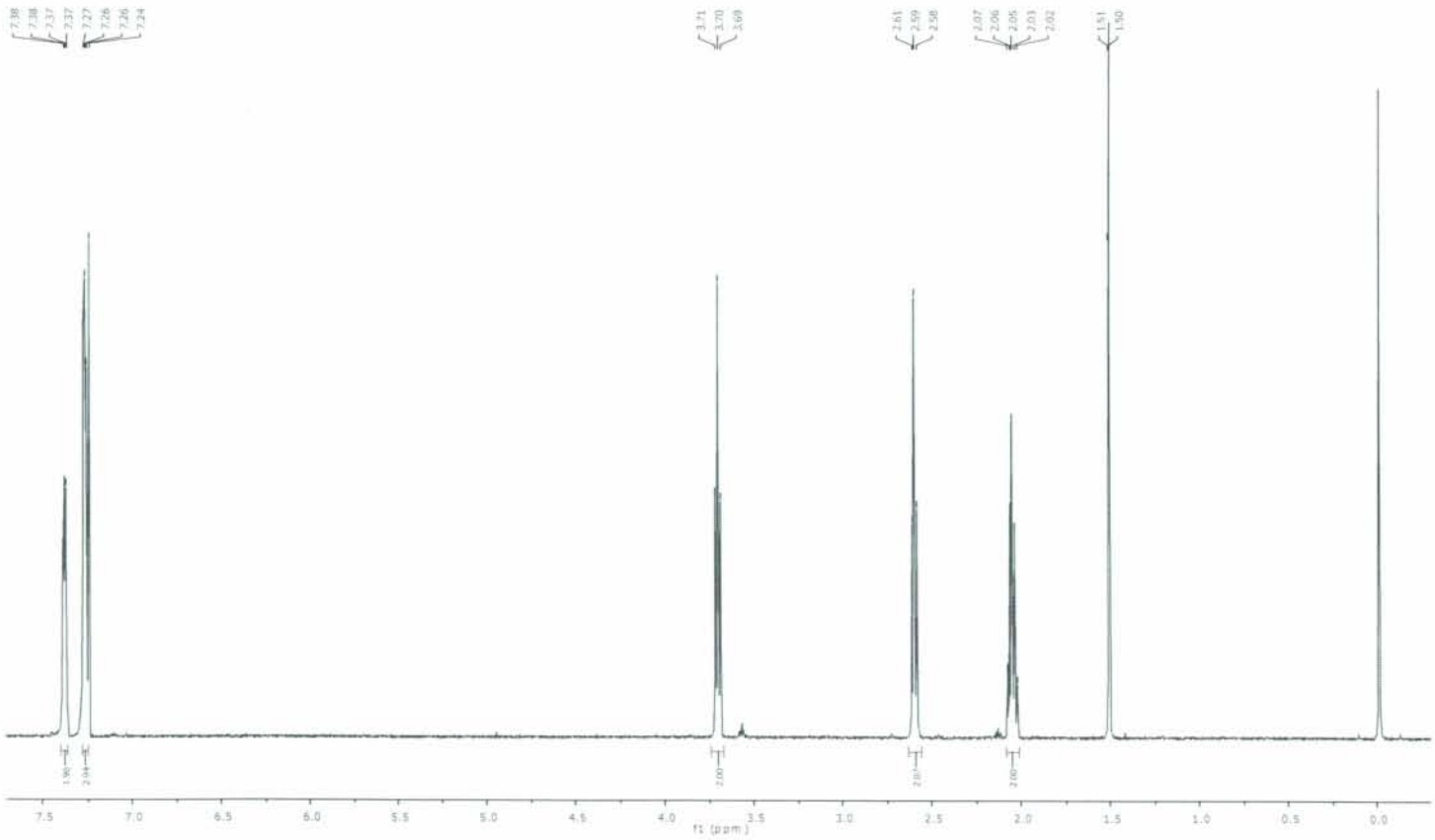

Appendix 3.1 ^{1}H NMR spectrum of 5-chloro-1-phenyl-1-pentyne

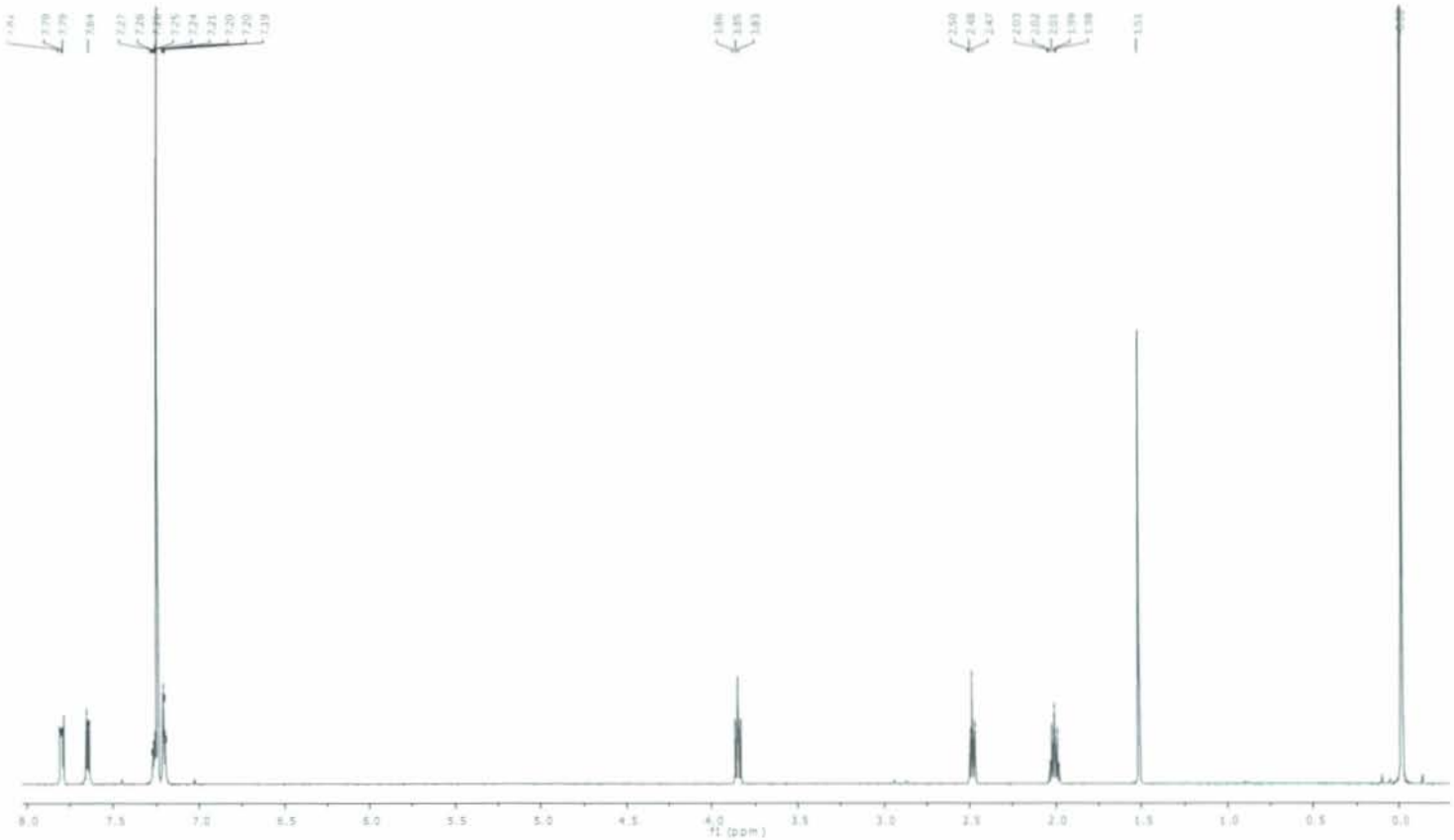

Appendix 3.2 ^{1}H NMR spectrum of N-(5-phenyl-4-pentylnyl)phthalimide

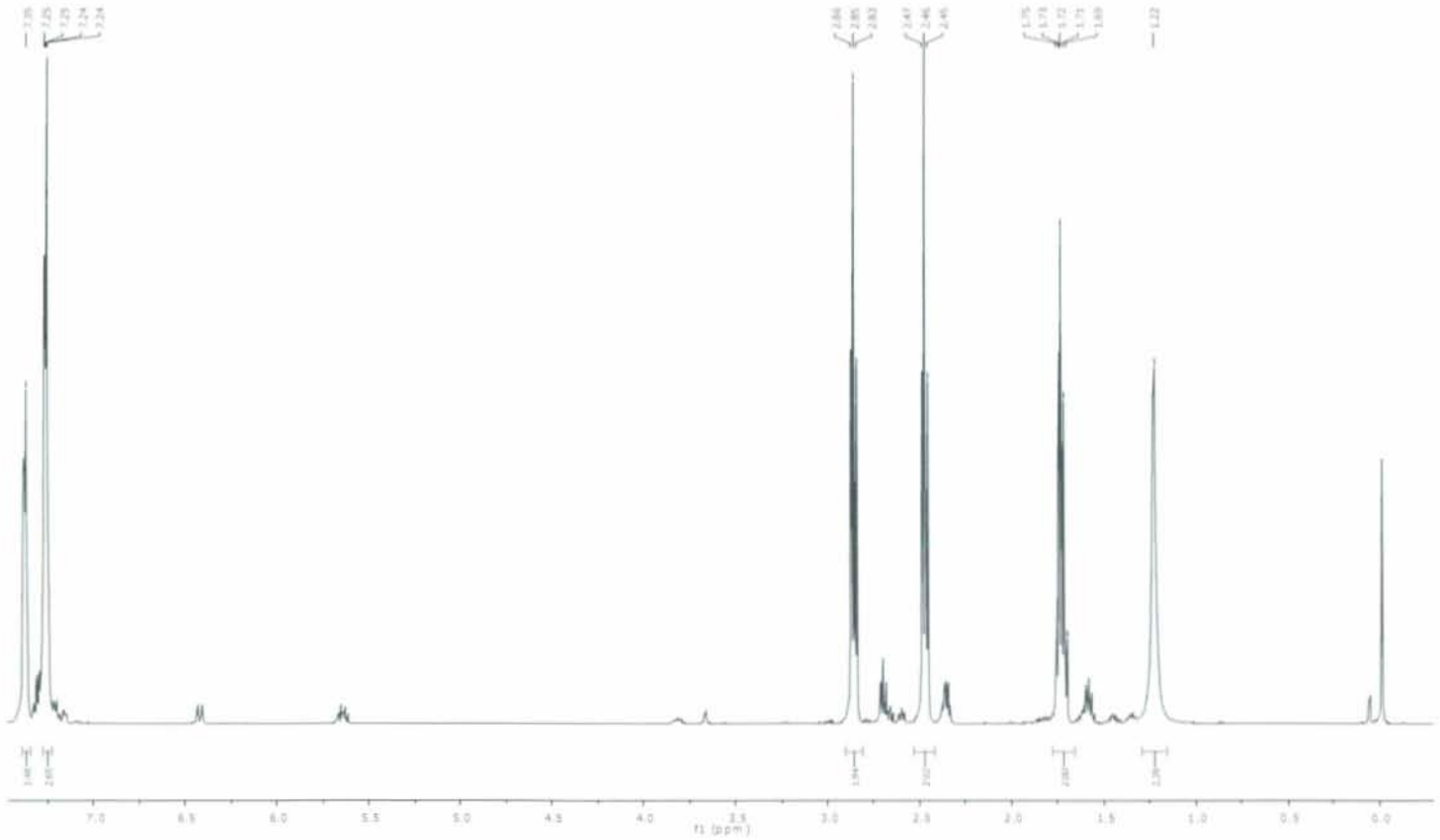

Appendix 3.3 ^{1}H NMR spectrum of 5-phenyl-4-pentyne-1-amine

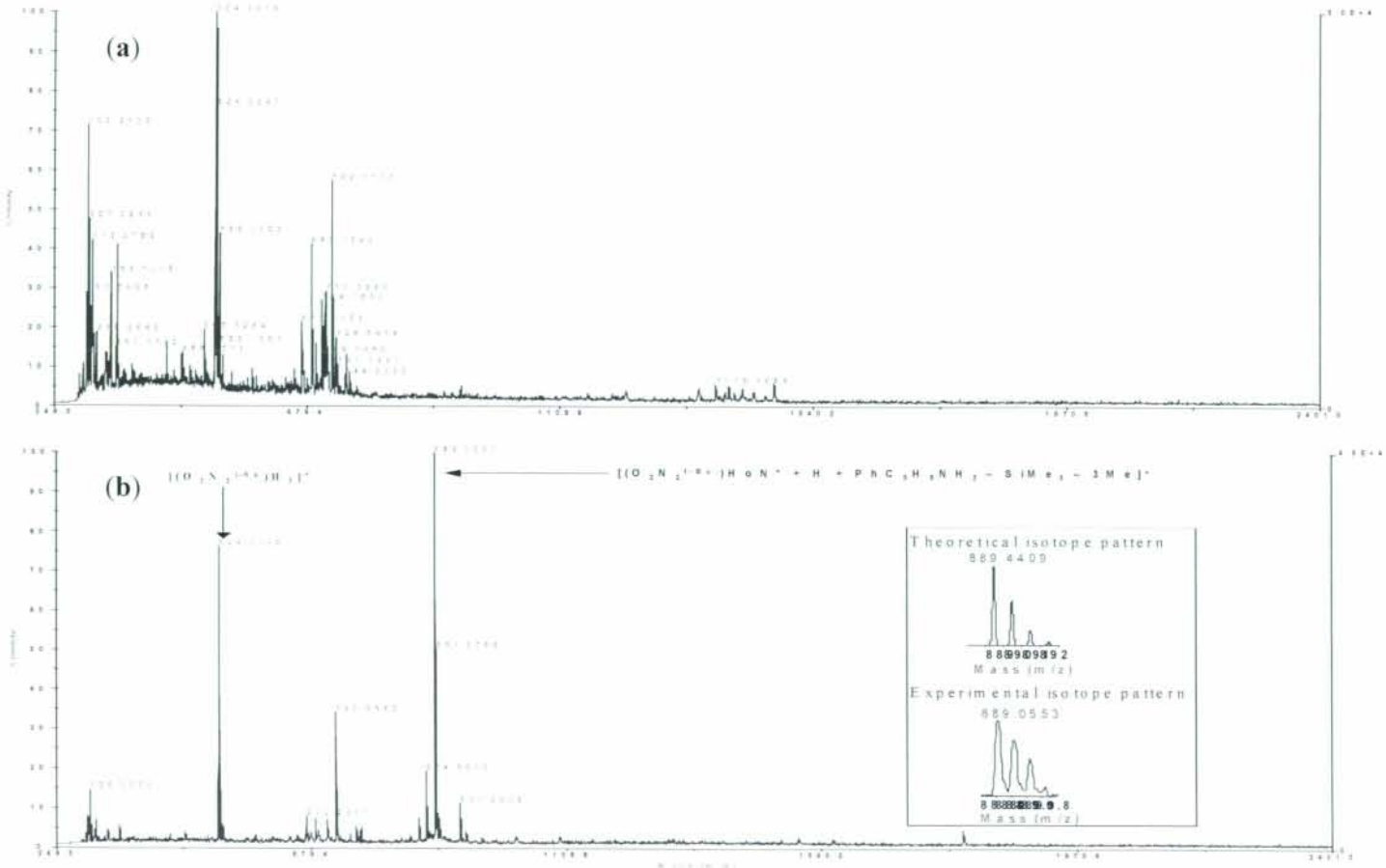

Appendix 3.4 MALDI-TOF mass spectra of (**a**) in situ generated $[O_2N_2^{t\text{-}Bu}]HoN(SiMe_3)_2$ (**2.14a$_{2.3}$**)

(**b**) hydroamination reaction of aminoalkyne substrate(**3.7**) with $[O_2N_2^{t\text{-}Bu}]HoN(SiMe_3)_2$ (**2.14a$_{2.3}$**)